Chapter 5
COMPUTER SIMULATION OF FIRE AND SMOKE SPREAD

The WPRI-TV video tape provided information to the investigation of the start and spread of the fire that was almost unprecedented in fire forensics. Supplemented with first person interviews and examination of the scene after the fact, a clear overall picture of the event emerged rather quickly. However, a number of important details could not be gleaned from the evidence, nor was it possible to examine the impact of the fire on the occupants. Both would have helped to understand the fire's effect on the evacuation process and to determine the relative importance of different contributors to the building failure.

Computer simulation has matured enough over the past five years to become credible when properly applied as a tool to help fill in critical details of the fire event, and to demonstrate the value of alternative building designs and fire safety measures. This chapter presents the results of numerical simulations and analyses of fire spread, smoke movement, tenability, and operation of fire protection systems that relate to the conditions in The Station on the night of Feb. 20, 2003.

The numerical models used in this investigation were the NIST Fire Dynamics Simulator (FDS) [1] and Smokeview [2]. The essential fire properties of the materials needed as input to FDS were generated from the small scale and real scale measurements described in Chapter 4. The following sections provide an overview of the models, describe how the testing was used to add credence to the simulations, and present the results of the full nightclub simulations.

5.1 NIST FIRE DYNAMICS SIMULATOR

The NIST Fire Dynamics Simulator is a computational fluid dynamics (CFD) model of fire-driven fluid flow. It solves numerically a form of the Navier-Stokes equations appropriate for low-speed, thermally driven flow with an emphasis on smoke and heat transport from fires [3]. Version 1 was publicly released in February 2000. The predictions performed here were made with the public pre-release version 4 of the model. Version 4 includes several new features, including multi-blocking, which were critical in performing the full night club simulations.

A CFD model requires that the room or building of interest be divided into small three-dimensional rectangular control volumes or computational cells. The CFD model computes the density, velocity, temperature, pressure and species concentration of the gas in each cell as it steps through time. Based on the laws of conservation of mass, momentum, species, and energy, the model tracks the generation and movement of fire gases. Radiative heat transfer is included in the model via the solution of the radiation transport equation for a non-scattering gray gas. All solid surfaces are assigned thermal boundary conditions, plus information about their burning behavior. Heat and mass transfer to and from solid surfaces is usually handled with empirical correlations. FDS utilizes material properties of the furnishings, walls, floors, and ceilings to compute fire growth and spread. A complete description of the FDS model is given in references [1,3].

Inputs required by FDS include the geometry of the structure, the computational cell size, the location of the ignition source, the energy release rate of the ignition source, thermal properties of walls, ceilings, floors, furnishings, and the size, location, and timing of door and window openings to the outside which critically influence fire growth and spread.

5.1.1 Geometry

FDS approximates the governing equations on a rectilinear grid. This three-dimensional grid represents the volume modeled by FDS. The grid is isolated from the surroundings, that is, all the smoke and heat generated by the fire stays within the grid and the air does not enter the grid. The user may, however, prescribe vents that allow smoke and heat to leave and air to enter the grid area. The user prescribes rectangular obstructions that are forced to conform to the underlying grid. Multi-blocking is a term used to describe the use of more than one rectangular grid or mesh in a calculation.

FDS predictions are sensitive to grid size; using a larger number of smaller cells will generally capture more features of the flow; however, the computation time increases more than linearly with the increase in number of grid cells. Computation times of one day on a fast computer are not uncommon but may increase to several months with a large number of grid cells. Therefore, it is important to use the smallest number of grid cells that still capture the important features of the fire. One way to reduce the number of grid cells is the use of multi-blocking. With multi-blocking, smaller grid cells that capture more detail are used near the fire and larger grid cells with less detail are used remote from the fire.

Building items such as walls, floors, windows, doors and furniture are described in FDS as rectilinear blocks. These blocks must have sides that are either horizontal or vertical and no sloped or curved surfaces are allowed. The blocks may be colored for identification and may be assigned material properties. The blocks may be entered into the simulation with exact measurements from the building. However FDS can only work with items that fall exactly on grid cell boundaries. FDS takes the input blocks and adjusts them to match the grid cell boundaries. As a result, items may either grow or shrink to match the grid. In most cases this does not have a major impact on the calculations, although it can result in walls with no thickness or walls with gaps at intersections. Usually these issues are resolved by adjusting the size of the blocks slightly to produce the desired geometry that matches the grid size.

5.1.2 Materials

When a wall, ceiling, floor, piece of furniture, or any other material is defined for use in the FDS model, it is given a set of physical and thermal properties that are used by the model. Some of these properties such as thermal diffusivity, thermal conductivity, density and thickness impact the heat transfer in the material. For materials that burn, additional parameters such as ignition temperature, heat of combustion, heat of vaporization and maximum burning rate are specified. The properties for the materials, to the extent they were available, were taken from standard references or fire experiments.

The combustion process is handled in two ways within FDS. In one version, the fuel gasification rate is related to the radiant heat flux imposed from the fire onto the material. The mass burning rates of these same materials are measured in a cone calorimeter (or similar) apparatus; hence, the importance of collecting these data as described in Chapter 4. An alternative way to handle the gasification of fuel in FDS is to base the fuel generation rate on a measured heat of vaporization and ignition temperature. Both versions utilize a mixture fraction combustion model, in which burning occurs in regions where the fuel and air are in stoichiometric proportion. The second approach was used in FDS to model both the mock-up experiments and the full nightclub fire.

The accuracy of either of these combustion models is related to the complexity of the fuel and the resolution of the numerical grid used during the simulation. A maximum burning rate is imposed to handle non-physical situations that can lead to excessive localized burning. To the extent that the heat release rates measured for the polyurethane foams by NIST and ATF differed, this had no effect on the

calculations presented in this chapter since the same ignition temperature, heat of vaporization, and maximum burning rate were used for simulations of the experimental mock-up and the full nightclub fires.

5.1.3 Vents

Vents in FDS are openings from the model to ambient conditions outside the computational domain. Vents allow smoke and heat to leave the grid area and air to enter. Vents may be either simple openings that allow natural flow to occur based on the buoyancy of the hot gases, or vents may use a specified or forced flow rate such as the flow from a fan.

5.1.4 Openings Within the Grid

The placement of blocks within the grid forms the structure of the building and its contents. The hydrodynamic calculations performed by FDS allow air, hot gases, smoke and flames to flow through the simulated building. Thermal radiation travels by line-of-sight and may be intercepted by obstacles within the grid.

Normal buildings may appear tightly constructed, but there are many small openings or leaks within a building that allow for the flow of air or combustion products. Since objects can only exist at grid boundaries, small leaks may be created by either using a very small grid size, or by representing many small leaks by fewer large leaks.

During the course of a fire, some items within the building may be consumed by the fire or otherwise change position. FDS does not have the capability to calculate burn-through or collapse but the user can remove items during the course of the calculations. Items that are removed can represent objects that fall or are destroyed by fire, or objects that are changed by people such as doors or windows that are opened.

5.1.5 Smokeview

Smokeview is a scientific visualization program that was developed to display the results of an FDS model computation [2]. Smokeview allows the viewing of FDS results in three-dimensional snapshots or animations. Smokeview can display contours of temperature, velocity and gas concentration in planar slices. It can also display properties with iso-surfaces that are three-dimensional versions of a constant value of the property. Iso-surfaces are most commonly used to provide a three-dimensional approximation of the flame surface where fuel and oxygen are present such that flames may exist.

5.2 FDS SIMULATIONS OF THE FULL-SCALE MOCK-UP

The primary objective of the mock-up experiments was to observe the primary mode of flame spread and smoke movement under fire conditions that were similar to what likely existed early in The Station fire on Feb. 20, 2003. Along with the video record, measurements of heat release rate, temperature, heat flux, oxygen volume fraction, and gas velocity were used as a basis to judge the capability of FDS in a complex fire environment. The secondary objective was to examine the impact of automatic fire sprinklers under experimental conditions, again to provide a basis of comparison with FDS.

5.2.1 Computational Domain, Grid Size, Initial Conditions, and Boundary Conditions

Selecting the appropriate grid size required balancing the need to resolve critical dimensions and physical phenomena, and the need to budget enough time to perform the hundreds of computer runs necessary to assess the importance of different variables on the outcome. FDS was run on a Linux cluster with eight 3.2 MHz processors. To complete the estimated 100 simulations needed of 300 seconds actual time for

the full nightclub fire in a six month window necessitated runs with a turn-around time of less than two days. Based upon the software needs and the hardware capabilities, this translated to a limit of about 2 million grid cells. The computational domain used to simulate the full nightclub measured about 22 m by 33 m by 4 m high, which led to a minimum grid size of about 145 mm.

Grid size sensitivity has been examined in several studies as noted by McGrattan [3]. For full-scale experiments involving a small compartment, 2.4 m (8 ft) by 3.6 m (12 ft) by 2.4 m (8 ft) high, with fires ranging from 55 kW to 110 kW, 100 mm grids were found to provide temperatures with 15% of the measured values. Based upon that work and the imposed time constraints, 100 mm was selected as the baseline grid size, with computational savings sought through multi-blocking and the physical evidence provided by the WPRI video and the real-scale mock-up experiments described in Chapter 4.

The choice of grid size influenced the selection of the appropriate values for the initial conditions, boundary conditions and material properties, including the size and energy of the ignition source, heat transfer at the boundaries, and burning properties of the fuel. With all other inputs kept constant, doubling the grid size did not lead to the fast growing fires seen in the video or mock-up experiments; halving the grid size led to a fire growth rate that was faster than the evidence (and a single run-time of 10 days). This implied that if the mock-up experiments were to be used to help inform the choice of parameters for the full nightclub, then the grid size should be the same, even though the mock-up required only 319,000 cells that were 100 mm on a side. Even so, about 17 hours was required to simulate 200 seconds of the mock-up experiments. While the simulations could not be shown to be grid size independent, the input parameters could be tuned to the 100 mm grid using the results of the mock-up experiments and then applied to the full nightclub simulation, with the WPRI video acting as a reality check.

For the real-scale mock-up, the platform area and the dance floor area to the west of the platform were located in a compartment that was 10.8 m east to west and 7.0 m north to south. The ceiling height over the dance floor was 3.8 m. The drummer's alcove, located to the east of the platform, was 3.1 m wide, 2.4 m deep, and 1.96 m high. The height of the drummer's alcove floor and ceiling relative to the dance floor were 0.74 m and 2.7 m respectively. The platform was 7.0 m wide and 2.4 m deep and 0.4 m high. Figures 5-1 shows the resulting FDS model in Smokeview based upon a 100 mm grid size. Refer to Fig. 4-16 through Fig. 4-17 for additional details on the mock-up design.

The exposed interior finish materials used in the experiment consisted of convoluted polyurethane foam, plywood paneling, gypsum board, and carpeting. In Fig. 5-1, the foam is shown as a dark gray surface, the paneling is depicted as the brown surface and the carpet is shown as a light blue surface. The remaining light gray surfaces are gypsum board. Foam, spruce, gypsum board and carpet material properties were used in conjunction with tabulated [1] and experimentally derived properties of polyurethane. The bottom of the domain was considered to be an inert, adiabatic solid.

The principal fuels in the mock-up were the convoluted polyurethane foam and plywood paneling. In the area of the platform and the drummer's alcove, the foam was installed over the plywood paneling. The complexity of this arrangement limited the extent to which the burning composite fuel could be modeled *a priori*. Therefore, several simplifications and assumptions were made in order to generate model results that were representative of the experimental data. The thickness of the convoluted polyurethane foam varied significantly as shown in Figure 5-3. Typical thickness variations ranged from 6 mm (0.24 in) valleys up to 30 mm (1.2 in) peaks in the "egg crate" configuration. Given that the thickness of two nested sheets was consistent at 36 mm (1.4 in), the foam was modeled as a uniform flat solid with an average thickness of 18 mm (0.7 in).

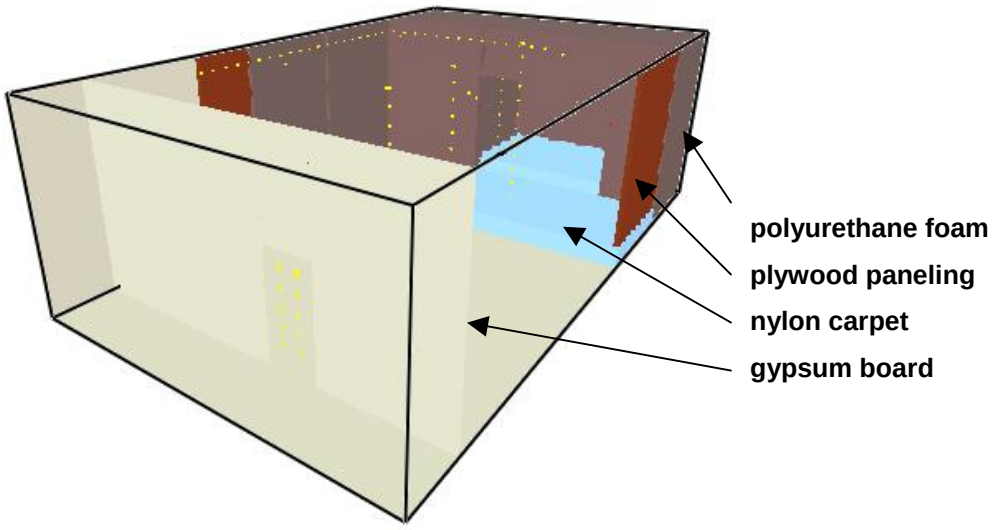

Figure 5-1. FDS model of mock-up in Smokeview

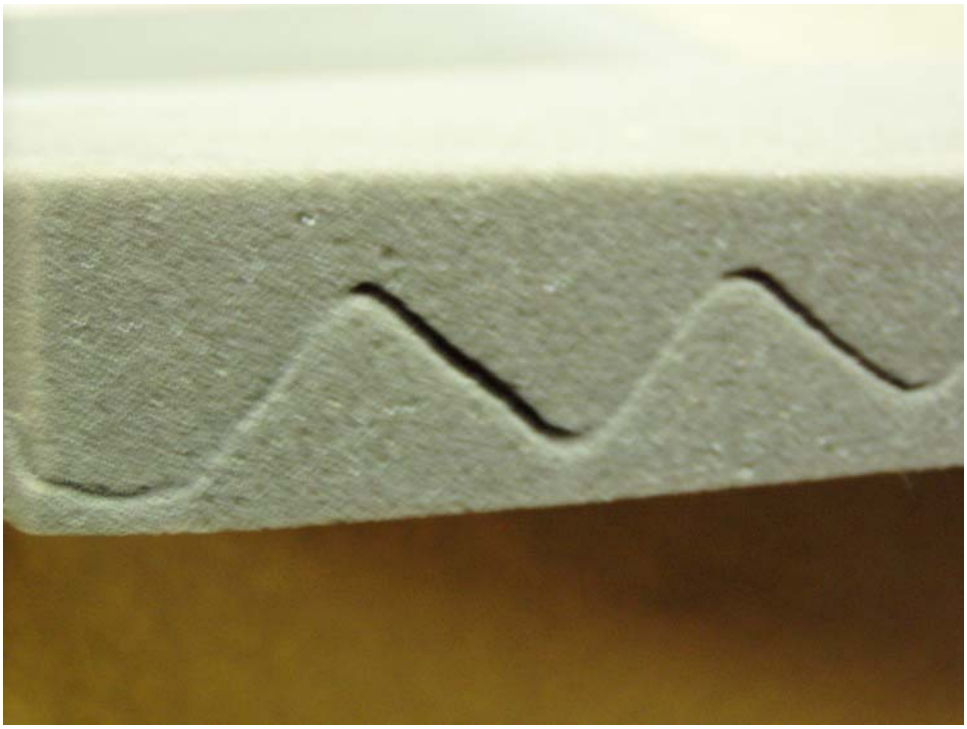

Figure 5-2. Photograph of the edge of two sheets of convoluted polyurethane foam.

Table 5-1. Polyurethane foam material properties used as FDS input.

Property	Value
Thermal Conductivity	0.034 W/m ºC
Specific Heat	1.4 kJ/kg ºC
Thickness	18 mm
Density	22 kg/m^3
Ignition Temperature	370 ºC
Heat of Vaporization	1350 kJ/kg
Maximum Burning Rate	0.008 kg/m^2 s

The other material properties used to describe the foam are given in Table 5-1. All of the foam material properties were derived from the experiments that were documented in Chapter 4, with the exception of the maximum burning rate. Given the complex nature of the foam over plywood composite, a series of simulations were conducted. The value of the maximum burning rate was varied from 0.004 to 0.028 kg/m^2 s. The maximum burning rate, which yielded the heat release rate results closest to the experimental results for the unsprinklered mock-up experiment was 0.008 kg/m^2 s.

The plywood paneling is based on the thermal properties of spruce [4] and is modeled as a charring material as described in [1]. The only modeled difference between the spruce material in the FDS database and the paneling is in the thickness of the material; 5 mm (0.2 in) was used to represent the paneling. The material properties of gypsum board and carpet were taken directly from the FDS 4 database with no changes [1].

Two 100 mm (4 in) wide by 200 mm (8 in) tall heat producing vents, simulating the heat feedback to the wall panels due to an ignition source, were located on the west side of the platform wall, at the north and south edge of the drummer's alcove. Two more heat inlet vents, 100 mm (4 in) square were located on the north and south walls of the drummer's alcove adjacent to the vents of the platform wall. The lower edge of the vents was located 1.50 m (5 ft) above the platform floor. The vents had a defined heat release rate per unit area of 1500 kW/m^2. These heat vents produced heat for the duration of the simulations.

The only opening within the grid of the model itself was the doorway in the west wall of the compartment, as shown in Figure 5-1. The doorway was 0.9 m (3.0 ft) wide and 2 m (6.6 ft) high. The computational grid extended outside the door 1.2 m to allow unrestricted flow into and out of the doorway.

Two simulations of the mock-up experiment are presented in the next section. The first simulation was unsprinklered. The second simulation examined the conditions resulting from the use of automatic fire sprinklers. The capability to model the sprinkler activation and the effects of suppression can not be done *a priori*. Several simulations were conducted by varying both the parameters that impacted the activation of the sprinklers and the parameters that impacted the suppression physics. The values which are presented in Table 5-2 provided the best fit to the data.

Three parameters are used in a lumped-mass model for the thermal element in the sprinkler: response time index (RTI), activation temperature, and conduction factor. This lumped mass sub-model is used to

Table 5-2. Sprinkler Properties Used as FDS Input

Property	Value
Sprinkler Type	Pendent
Operating Pressure	1.72 bar (25 psi)
K-factor	80 L/min/bar$^{1/2}$ (5.6 gpm/psi$^{1/2}$)
Response Time Index	16 m$^{1/2}$ s$^{1/2}$ (32.6 ft$^{1/2}$ s$^{1/2}$)
C-Factor	0
Activation Temperature	74 ºC (165 ºF)
Offset Distance	100 mm (3.9 in)
Size Distribution	Global Average
Median Volumetric Diameter	675 μm (0.03 in)
Minimum Spray Angle	75º
Maximum Spray Angle	105º
Speed	15 m/s (49 ft/s)

calculate the time of sprinkler activation. The values used represent a fast response sprinkler with an ordinary temperature classification. No conductive losses were considered.

The remaining sprinkler parameters describe how much water would be discharged, what the water droplet size distribution would be and the direction of the droplets discharge. The water flow rate is determined by the operating pressure and the discharge factor (or K-factor). As modeled, the water flow from each sprinkler was 94.6 L/min (28.0 gpm).

The water droplet size distribution is based on a median droplet diameter to which a size distribution is applied. A median droplet diameter of 675 μm (0.03 in) was used with the FDS default parameters of the Rosin-Rammler/log-normal distribution (γ= 2.4).

The droplets were distributed uniformly in the conical spray pattern emanating from the sprinkler deflector. The spray pattern is defined by the minimum and maximum spray angles. Relative to a sphere that is centered on the sprinkler, with a radius equal to the offset distance, the spray pattern ranged from 75º north of the south pole to 15º above the equator. Further discussion of the sprinkler properties are provided in section 5.2.3.

5.2.2 FDS Full-scale mock-up Simulation, Non-Sprinklered Results

The results of the non-sprinklered simulation are compared with the video record of the experiment, and the measurements of temperature, oxygen volume fraction, heat flux, heat release rate and gas velocity. Visual comparisons of the experiment and simulation are shown in Figures 5-2 through 5-11. Quantitative comparisons between the experimental data and the model predictions are given in Figures 5-12 through 5-18.

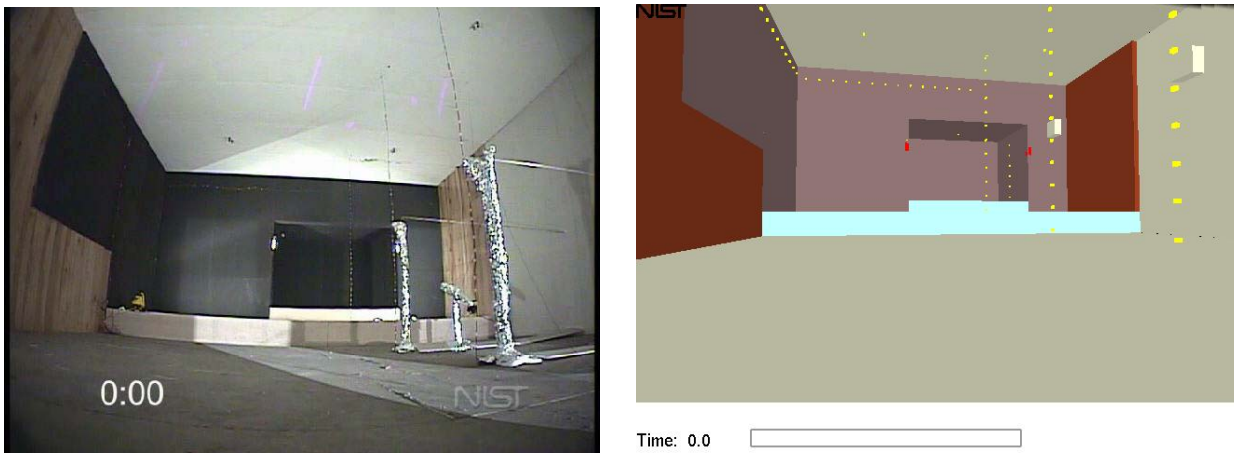

Figure 5-2. Ignition at the corners of the drummer's alcove, t = 0 s.

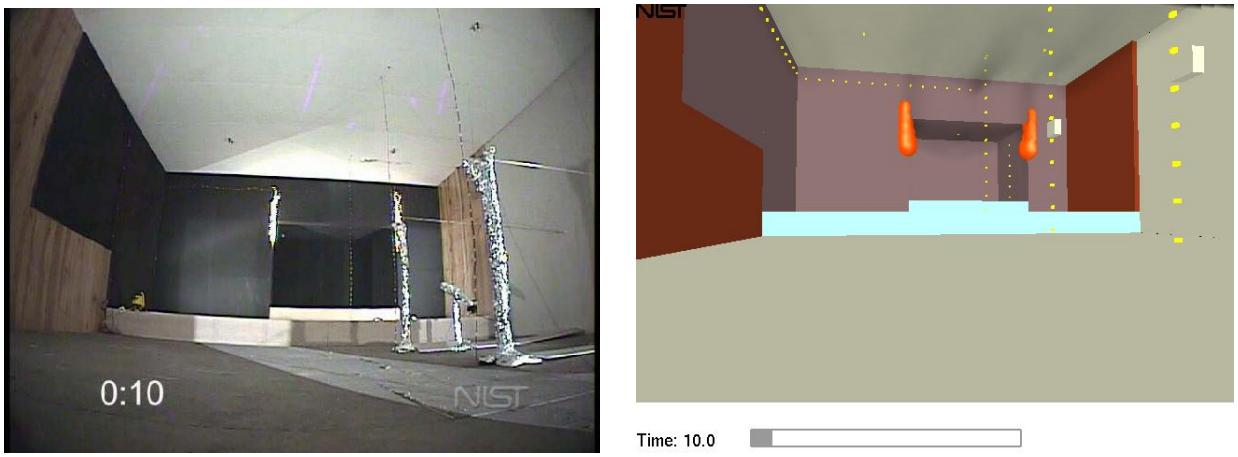

Figure 5-3. Flames spreading toward ceiling, t = 10 s after ignition.

(i) Visual Comparisons

Figures 5-2 through 5-11 are composed of pairs of images. The still frames, captured from video tape, appear on the left. The images on the right are rendered from Smokeview. Both images represent the same time after ignition. The pairs of images begin at ignition, or t = 0 seconds, and continue at 10 second intervals until 90 seconds after ignition, when most of the visibility from the video is lost.

Figure 5-2 shows the experiment and the simulation at the time of ignition. The video frame on the left shows the foam covered walls, the wood paneling, and the carpeted platform. Gypsum board covered the ceiling, floor and the remaining wall areas which were not covered with wood paneling or foam. Some of the instrumentation can be seen in the foreground of the video frame. In the image from the simulation, on the right, the comparable interior finishes can be seen. The instrumentation in the right figures is represented by colored dots. The thermocouples appear as yellow dots in evenly spaced arrays. The light gray blocks represent the locations of the heat flux sensors and the gas sampling locations, which were installed at approximately 1.5 m (5 ft) above the floor.

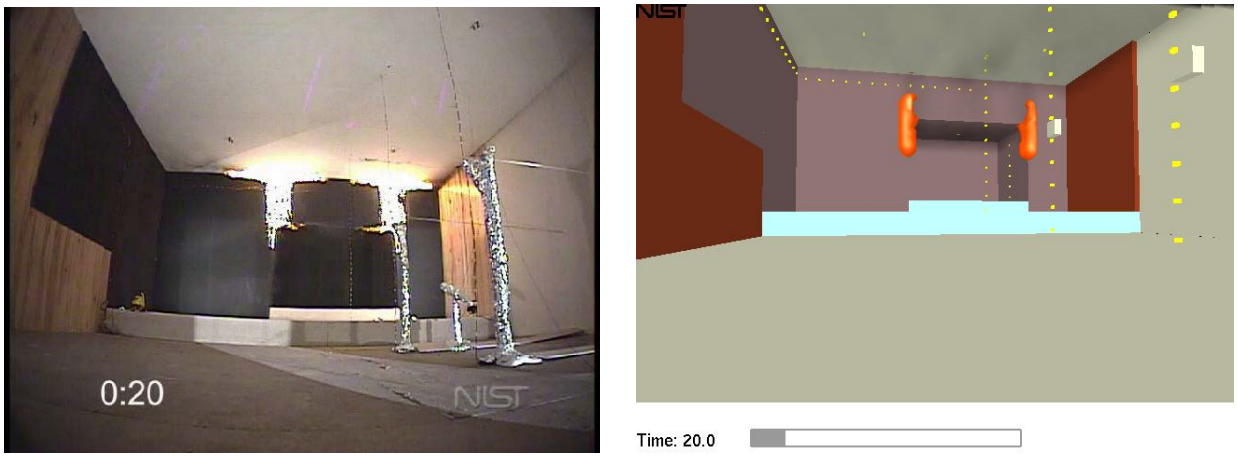

Figure 5-4. Flames impinging on ceiling, t = 20 s after ignition.

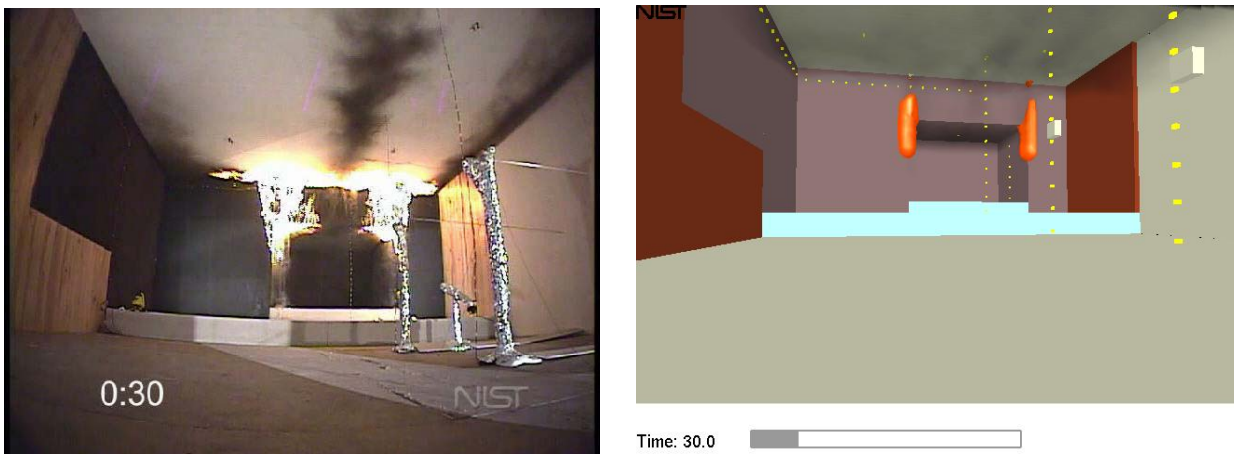

Figure 5-5. Visible smoke spreading across ceiling, t = 30 s, after ignition.

Figure 5-3 compares the fire development at 10 seconds after ignition. A flame is shown on both corners where the platform wall intersects with the drummer's alcove. In the case of FDS, the area that appears to be involved with flames is based on the stoichiometric mixture fraction, where there is the ideal mixture of fuel and oxygen for a robust flame to exist. The heat release rate per unit volume represented by the simulated flames is 285.5 kW/m^3. The flames in the simulation appear wider due to the grid resolution, which is 100 mm (4 in) throughout the room.

The video frame to the left in Figure 5-4 shows flames 20 seconds after ignition growing vertically and impinging on the ceiling. The simulated flames on the right, however, have not yet reached the ceiling. As noted above, the simulated flame is constrained to grow in 100 mm (4 in) increments, both vertically and laterally. This may account for the wider flame and the accompanying redistribution of energy which would reduce the propensity for rapid vertical flame spread. Light smoke can be seen in both images along the ceiling of the alcove, with light wisps of smoke along the ceiling above the platform.

Figure 5-5 shows an increased amount of smoke flow across the ceiling at 30 seconds after ignition. The actual fire continues to grow at a faster rate than the simulated flames. In the video frame on the left the flames

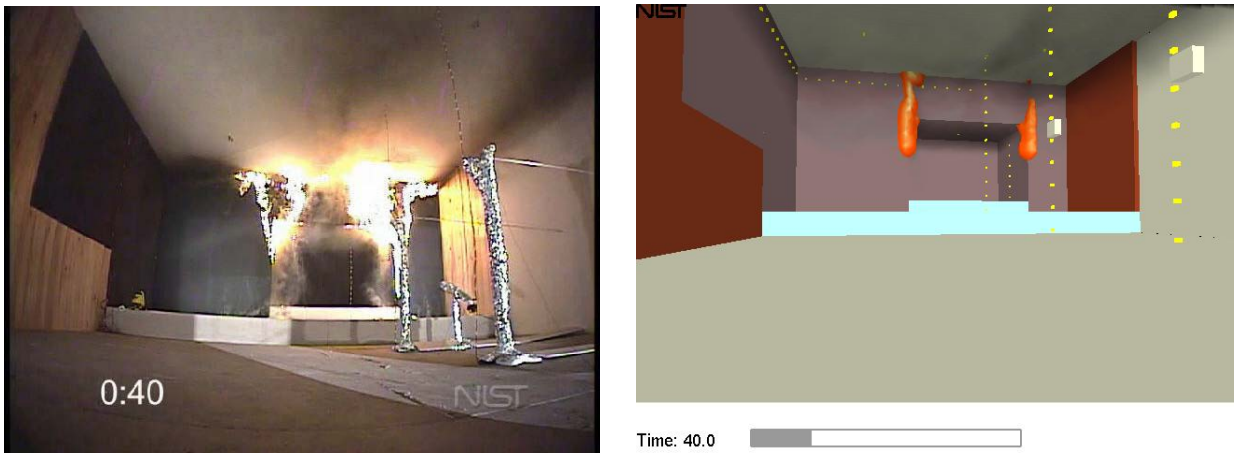

Figure 5-6. Flames continue to spread into alcove, t = 40 s, after ignition.

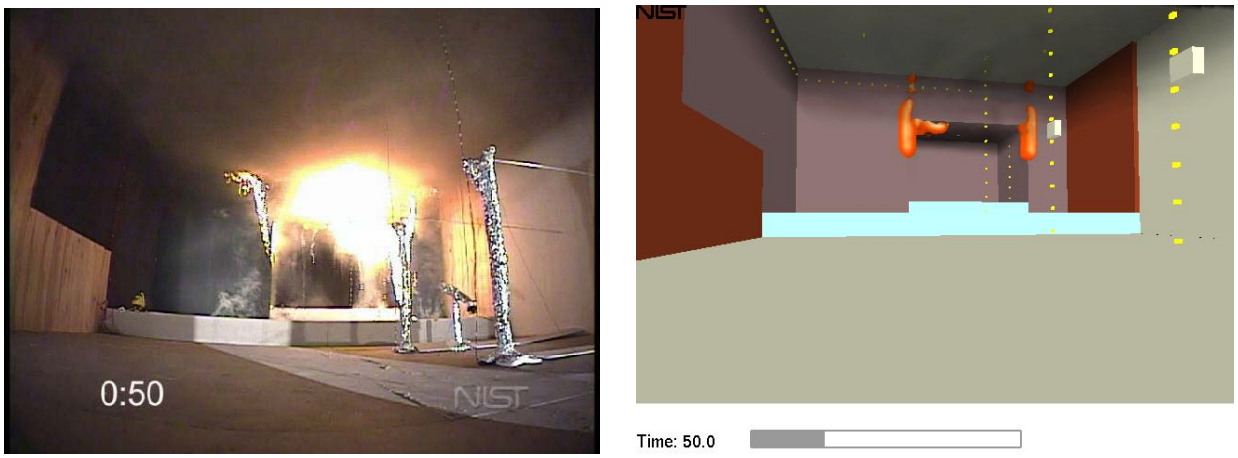

Figure 5-7. Ceiling of alcove fully involved in fire, t = 50 s, after ignition.

have formed twin V-patterns on each side of the alcove and the flames are spreading across the alcove ceiling. Notice the light smoke that is coming up from the carpeting below the two fire plumes. This is the result of foam melting and the burning foam droplets falling to the floor. This mode of flame spread is not accounted for within the FDS model. At 40 seconds after ignition, the video frame in Figure 5-6 shows areas of the foam on the platform wall have burned out (note the dark area directly above the point of ignition on the left side of the alcove). The actual flame fronts have continued to spread and into the alcove, where fire is visible on portions of the side walls and the ceiling of the alcove. The flames simulated with FDS have also grown, although at a slower rate. Both of the simulated flames have impinged on the ceiling.

Figure 5-7, has images captured at 50 s after ignition. In the experiment, it appears that the entire ceiling of the alcove is burning, as well as the area of the platform wall above the opening to the alcove. There is also more smoke from drop-down of the burning foam onto the carpet, both in the alcove and on the platform. In the simulation, the flames have moved into the alcove and are spreading across the ceiling. In both images, the smoke or hot gas layer has developed across the ceiling of the enclosure.

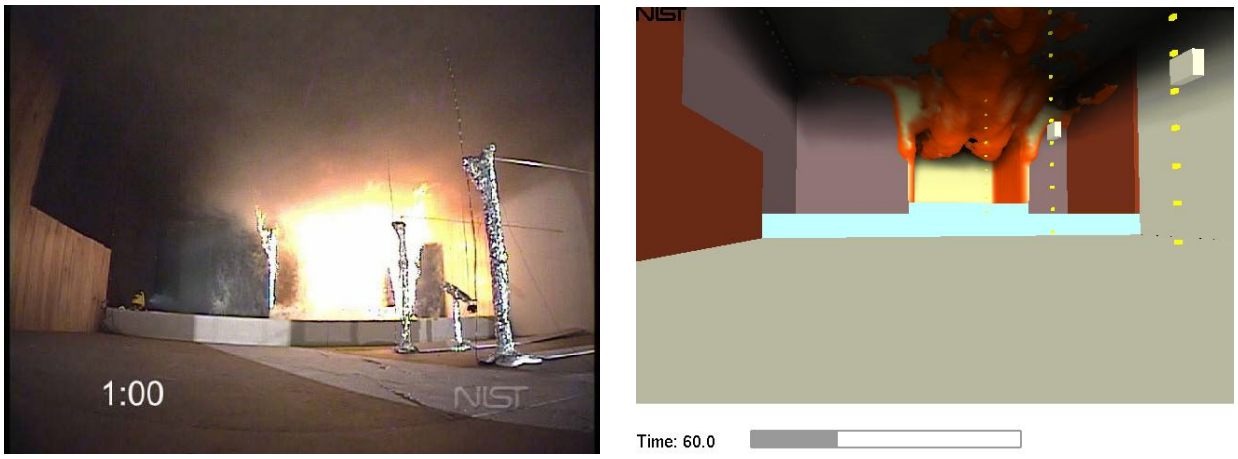

Figure 5-8. Flashover has occurred in alcove area, t = 60 s, after ignition.

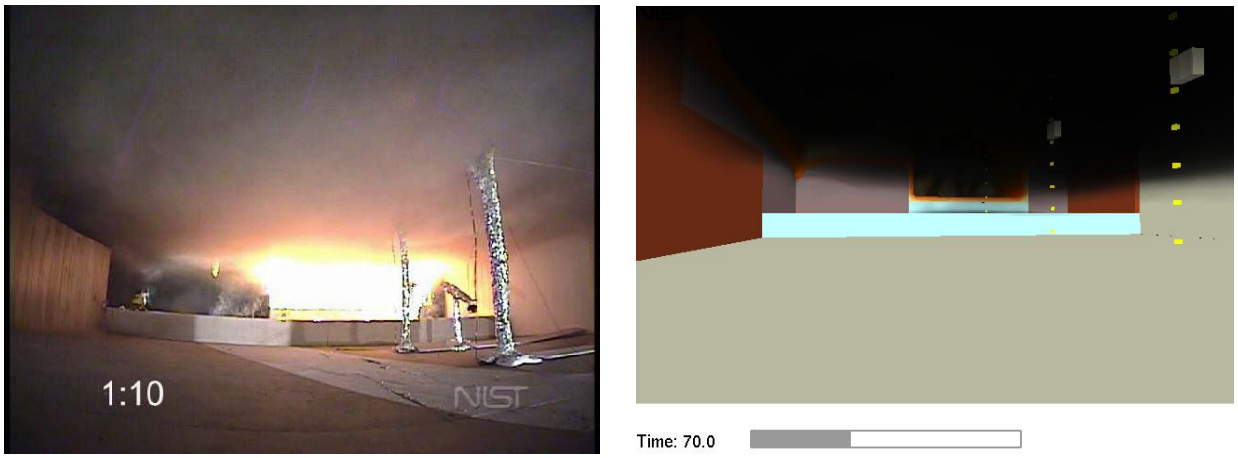

Figure 5-9. Smoke layer has dropped to 1.5 m above floor, t = 70 s after ignition.

In Figure 5-8, the ceiling and the walls of the alcove have become fully involved with fire in both of the images. At 60 seconds after ignition, flashover has already occurred in the experiment and flashover is about to occur in the simulation. In both cases, flames are extending out of the alcove across the ceiling and the smoke layer has become thicker and darker.

The images in Figure 5-9 show a significant increase in the amount of the smoke in the enclosure. The smoke layer has descended to within 1.5 m (5 ft) of the floor. The flames have spread along the wall behind the platform and can be seen at the lower edge of the smoke layer in both the video frame and the image from the simulation. The smoke in the experiment appears lighter in color than it actually is due to light that is being reflected from floor level halogen lights that were used to improve the visibility for the video cameras.

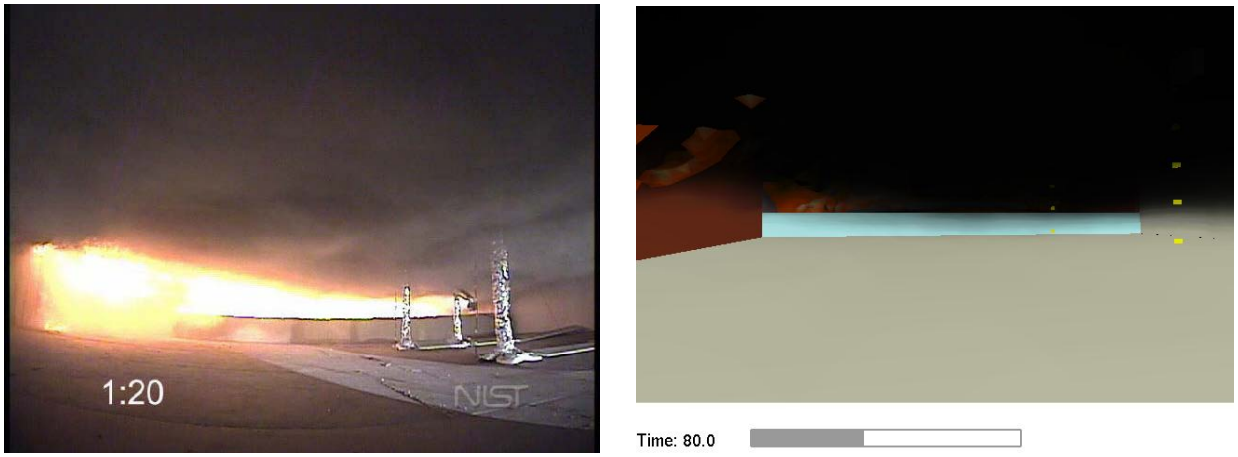

Figure 5-10. Fire continues to spread, t = 80s after ignition.

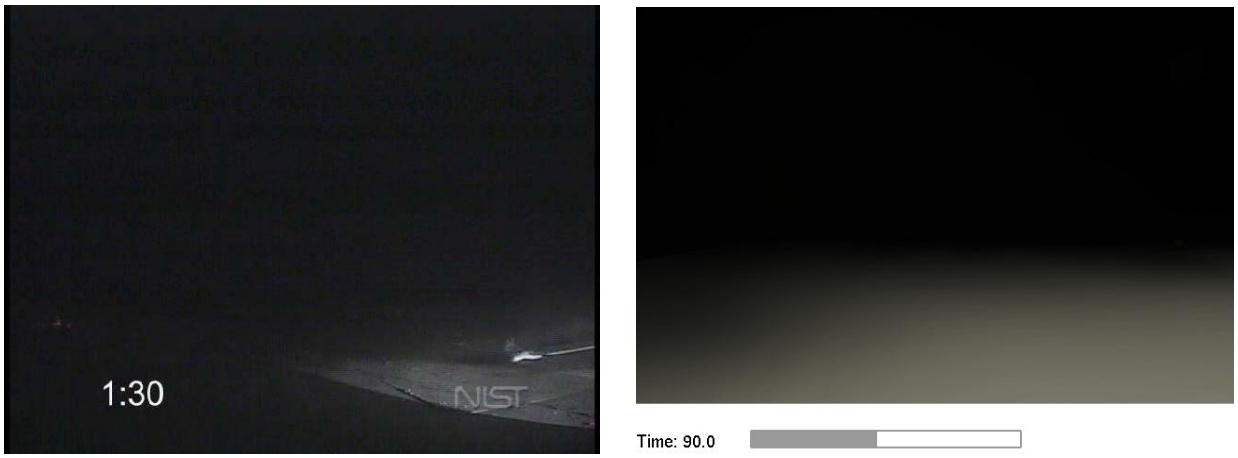

Figure 5-11. Visibility lost, t = 90 s after ignition.

The fire continues to grow in both the experiment and the simulation as shown in Figure 5-10. The smoke layer has continued to descend. The interface height of the smoke layer is approximately 0.75 m (2.5 ft) above the floor at 80 s after ignition for both the experiment and the simulation. Both images also show the flame extension on the left wall of the enclosure. The upper portion of the left wall near the platform had foam installed over the paneling.

The last set of images, Figure 5-11 demonstrate that most of the visibility in the enclosure has been lost due to smoke filling. A small layer of clear area can be seen near the floor in both the experiment and the simulation. This is due to fresh air being drawn into the fire enclosure through the open doorway.

The image pairs show that the simulation is not exact with respect to time, in reproducing the development and growth of the fire, especially during the initial growth stages of the fire. Based on the images during the first 40 seconds of the fire FDS appears to lag behind in fire growth by approximately 10 to 20 seconds. As the fire reaches the transition point of flashover, the simulation has reduced the time

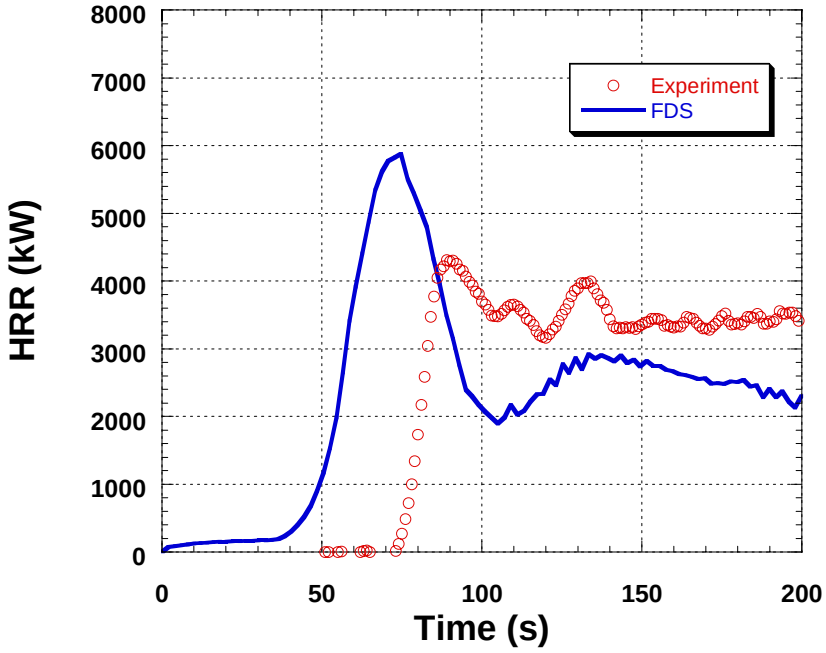

Figure 5-12. Power generated in experiment as measured outside of doorway, compared to FDS simulation of heat release rate from fire within compartment.

lag significantly. Post-flashover, the appearance of the fire progression and the smoke development for both the experiment and the simulation are more closely synchronized with each other.

(ii) Numerical Comparison

In this section, measurements of power generated, temperature, heat flux, oxygen volume fraction, and gas velocity from the full-scale mock-up experiments described in Chapter 4 are compared with the values generated by the FDS simulation.

The heat release rate of the fire is the source for the energy transfer which occurs throughout the fire environment. It is critical in fire protection engineering for assessing the development of a hazard due to a fire within a building. In addition, the heat release rate is a function of oxygen depletion. Therefore, differences in the heat release rate comparison also impact the comparison of the temperature, heat flux, oxygen, and velocity measurements.

Figure 5-12 compares the measured thermal power leaving the door of the experiment (based upon oxygen consumption) to the heat release rate from the fire within the compartment as predicted by FDS. For fires burning in the open under the laboratory hood, the thermal power measured by the oxygen depletion calorimeter is equal to the heat release rate from the fire. However, for a fire within an enclosure, the effluent from the room is a mixed average of the upper layer gases, and does not represent the instantaneous heat release rate of the fire. This means that a direct comparison between the experimental measurements and the numerical predictions cannot be made because the oxygen depletion calorimeter does not respond to a fire within an enclosure until the combustion products have had time to exit the door and become entrained into the hood. The heat release rate predicted by FDS in Fig. 5-12 represents the instantaneous heat release throughout the room. The heat release rate reaches a peak of

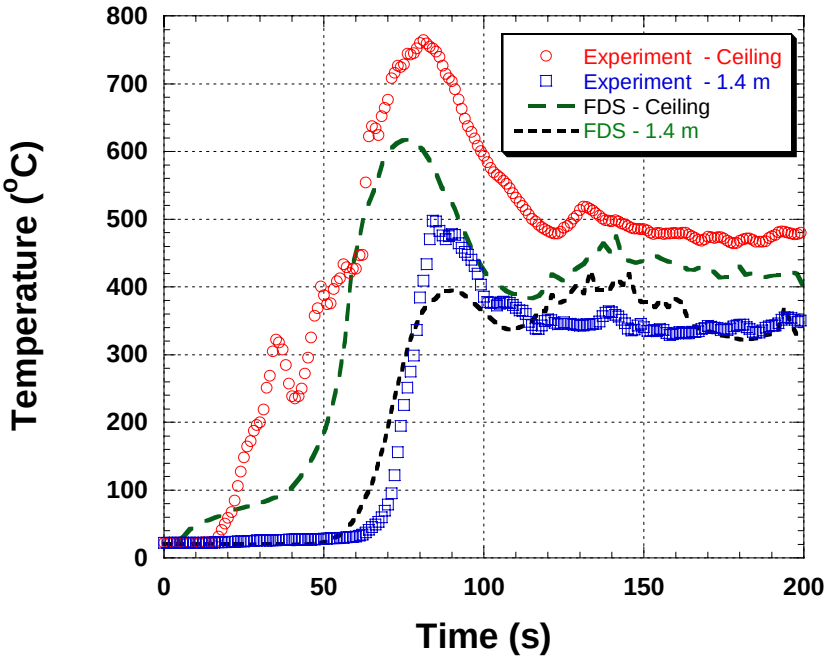

Figure 5-13. Temperature comparison between the un-sprinklered fire experiment and the FDS simulation at Station C.

approximately 6 MW about 70 seconds into the simulation, 20 seconds prior to the peak in thermal power measured in the oxygen depletion calorimeter. Both curves approach 3000 kW ± 300 kW approximately 150 seconds into the fire, again consistent with a ventilation limited condition. The heat release rates diverge at longer times as the model consumes the remaining interior finish fuels while the physical fire continues to burn at a reduced rate into the wood supporting the platform and walls. When the areas under the heat release rate curves were integrated, the resulting energies were found to agree within 10 %.

Figure 5-13 is a comparison of the temperatures predicted and measured 25 mm below the ceiling and 1.4 m above the floor at the thermocouple array located at Station C (4.25 m east of the door opening or 1.7 m from the platform). The FDS output has been smoothed by applying a Stineman function (a geometric weight applied to the current point ±10 % of the data range). The temperature data show reasonable agreement with the predictions, including an overshoot followed by a leveling off as the fire reaches a ventilation limit. The temperatures near the ceiling increase faster in the test; conversely, the lower level temperatures increase at a slower rate in the test.

Note that, unlike the heat release rate, the temperature measurements respond to the local environment within a second; hence, the experimental temperatures and FDS predictions can be compared directly. Initially, the experimental measurements near the ceiling increase more rapidly than predicted. This is probably due to the strong transverse temperature gradients associated with the ceiling jets created early in the fire (see Fig. 5-5), where small differences in position between the experiment and simulation can have a large change in temperature. The peak temperatures for the experiment and the simulation occur within 5 seconds of each other.

Figure 5-14 is a comparison of the temperatures predicted and measured 25 mm below the ceiling and 1.4 m above the floor at the thermocouple array located at Station D (2.35 m east of the door opening). Similar to the previous figure, the temperature data show reasonable agreement with the predictions. The

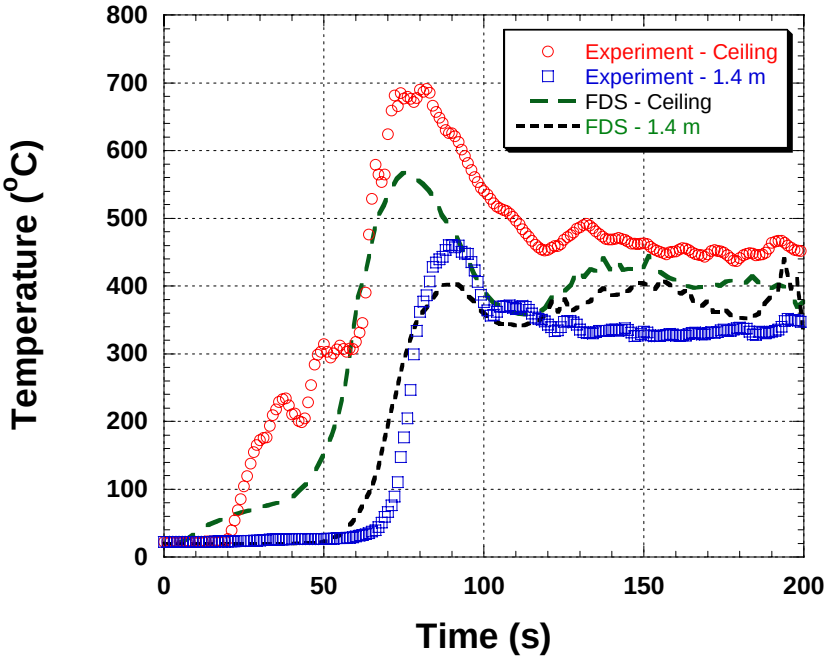

Figure 5-14. Temperature comparison between the un-sprinklered fire experiment and the FDS simulation at Station D.

trends are also similar and both of the measured temperatures and the predictions exhibit a reduction in peak temperatures relative to the values from Station C which is located approximately 2 m closer to the platform.

Figures 5-15 and 5-16 present the heat flux measurements taken at Stations C and D respectively. There were three total heat flux sensors at each position: one installed at ceiling level with the sensor aimed at the floor; and two sensors installed at approximately 1.5 m (5 ft) above the floor with one aimed at the ceiling and the other aimed toward the platform end of the enclosure. In both cases, the predictions follow the trends of the measured heat flux. Better agreement in terms of magnitude occurs at the ceiling level. The predicted heat fluxes 1.5 m above the floor are low by almost 50 % when compared with three out of four measurements.

Figures 5-17 and 5-18 represent the oxygen volume fraction comparisons between the measurements at Stations C and D and the predicted values from FDS. The measurements and the predictions were positioned at 1.5 m (5 ft) above the floor. The oxygen levels predicted by FDS dropped sooner but slightly less rapidly than the experimental measurements; both reached the same low value of about 2 %, confirming that the fire was close to ventilation-limited at this point.

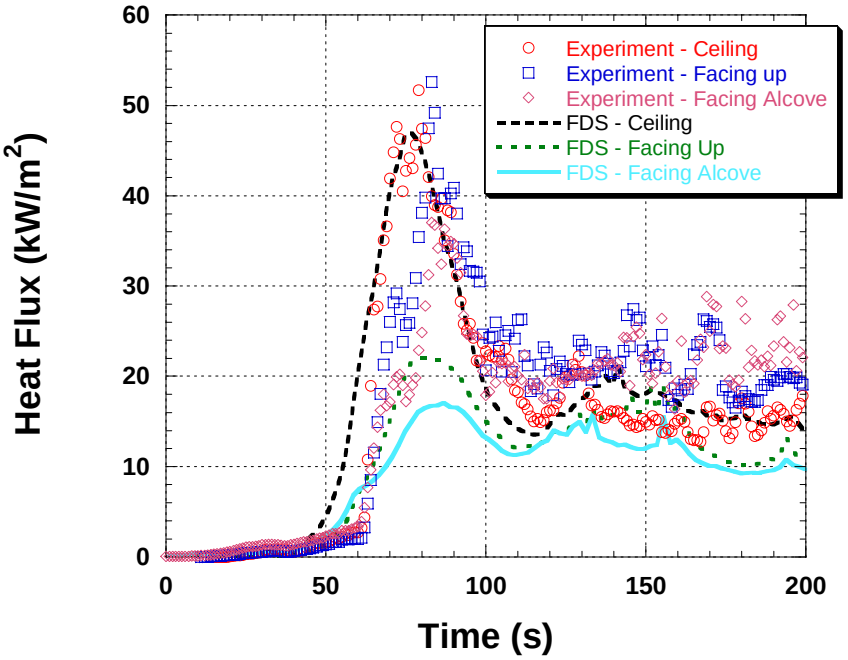

Figure 5-15. Heat flux comparison between the un-sprinklered fire experiment and the FDS simulation at Station C

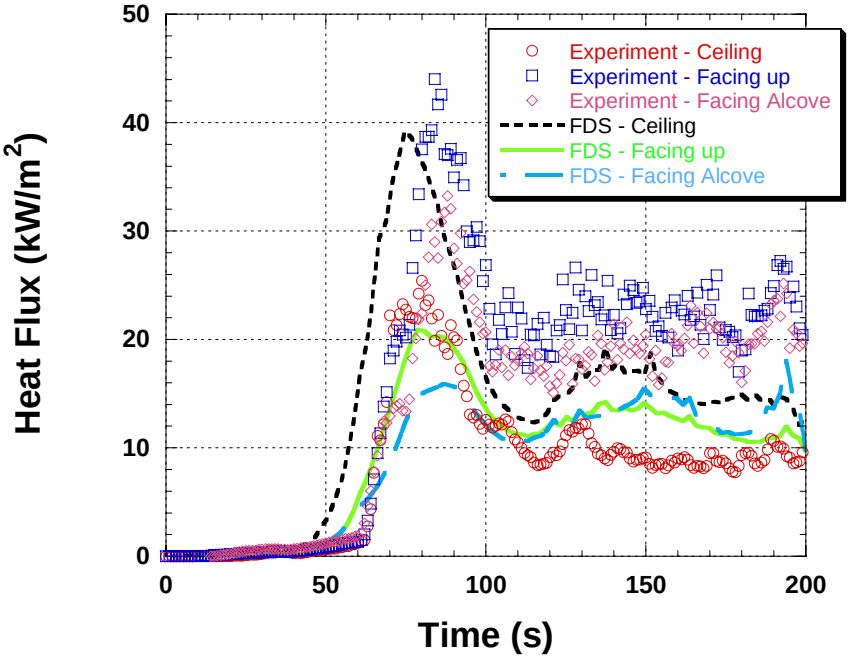

Figure 5-16. Heat flux comparison between the un-sprinklered fire experiment and the FDS simulation at Station D.

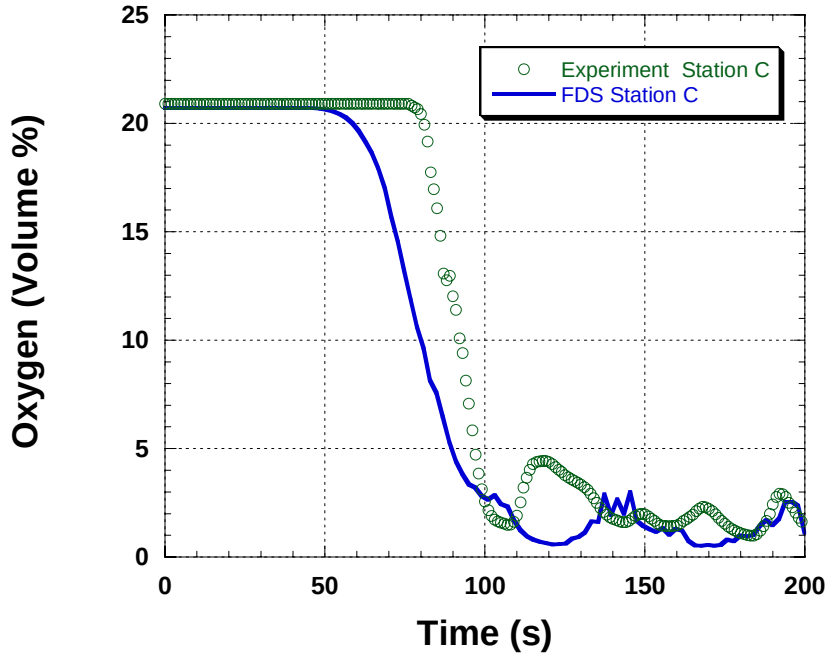

Figure 5-17. Oxygen volume fraction comparison between the un-sprinklered fire experiment and the FDS model at approximately 1.5 m above the floor at Station C.

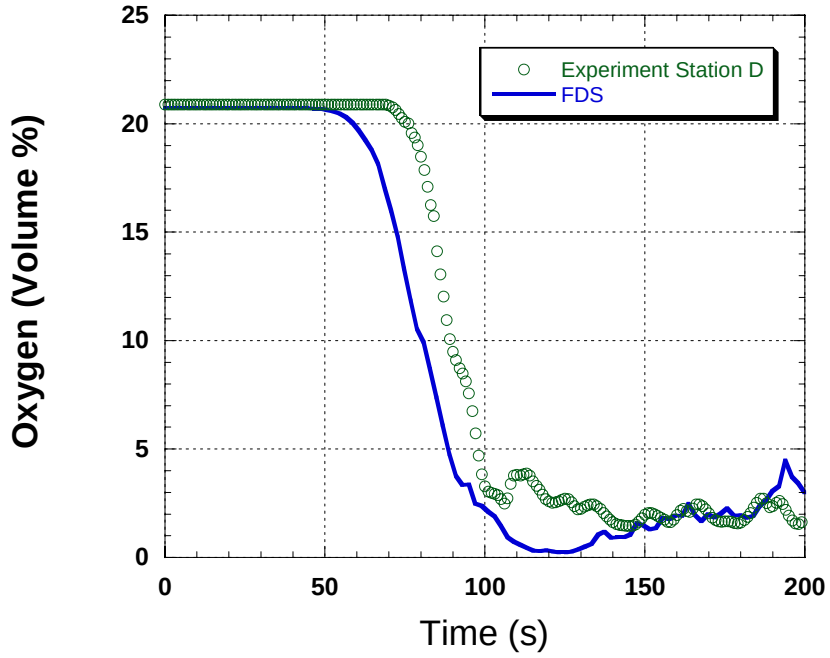

Figure 5-18. Oxygen volume fraction comparison between the un-sprinklered fire experiment and the FDS model at approximately 1.5 m above the floor at Station D.

Table 5.3 Time to reach tenability criteria at Location C, or maximum deviation obtained, in sprinklered and unsprinklered simulations, compared to experimental measurements

	Temperature > 120 °C	Heat Flux > 2.5 kW/m^2	Oxygen < 12 %
Unsprinklered			
Experiment	76 seconds	61 seconds	87 seconds
FDS	72 seconds	57 seconds	80 seconds
Sprinklered			
Experiment	< 24 °C	< 0.32 kW/m^2	> 20.6 %
FDS	< 22 °C	<0.15 kW/m^2	> 18.8 %

(iii) Tenability

Tenability limits based upon the work of Purser [5] were discussed in section 4.6.8. The time predicted by FDS to reach the limits of temperature, heat flux, and oxygen are summarized in the top portion of Table 5.3. The agreement between the simulation and experimental measurements at Location C is within 8 %, with both methods indicating the heat flux criteria is exceeded first, around one minute into the fire.

5.2.3 FDS Full-scale mock-up Simulation, Sprinklered Results

The results of the sprinklered simulation are compared with the video record of the experiment, and the measurements of temperature and oxygen volume fraction. Visual comparisons of the experiment and simulation are shown in Figures 5-19 through 5-27. Quantitative comparisons between the experimental data and the model predictions are given in Figures 5-28 through 5-32. Given the limited growth of the fire during the experiment, the oxygen depletion calorimeter did not register a significant rate of heat release.

The comparison of the sprinkler activation times from the sprinklered mock-up experiment and the FDS simulation of that experiment are given in Table 5-4. In FDS, the activation time of the first sprinkler was the result of adjusting the RTI in the simulation until the times were similar. The RTI which provided the best match, 16 m$^{1/2}$ s$^{1/2}$ (32.6 ft$^{1/2}$ s$^{1/2}$), was used as the RTI for the remaining sprinklers in both the mock-up and the full night club simulation. The order of sprinkler activation, and the number of sprinklers activated, were the same in the simulation and the experiment. The times to activation differed by no more than 6 seconds.

(i) Visual Comparisons

Figures 5-19 and 5-27 are composed of pairs of images. The still frames, captured from the video tape of the experiment, appear on the left. The images on the right are rendered from Smokeview. Both images represent the same time after ignition. The pairs of images begin at ignition or t = 0 seconds and continue at 10 second intervals until 60 seconds after ignition, when most of the fire in the experiment had been suppressed. Additional sets of images are included at 25 seconds after ignition to show the initial sprinkler just after activation and at 90 seconds to demonstrate the lack of significant fire spread after sprinkler activation. Figures 5-19 through 5-21 show a very similar progression in fire growth as the unsprinklered case for both the experiment and the FDS simulation between ignition and 20 seconds after

Table 5-4. Comparison of sprinkler activation times.

Sprinkler Location	Sprinkler Activation Times (seconds)	
	Experimental	Fire Dynamic Simulator
Southeast	24	23
Northeast	29	35
Alcove	30	36
Southwest	Did Not Activate	Did Not Activate
Northwest	Did Not Activate	Did Not Activate

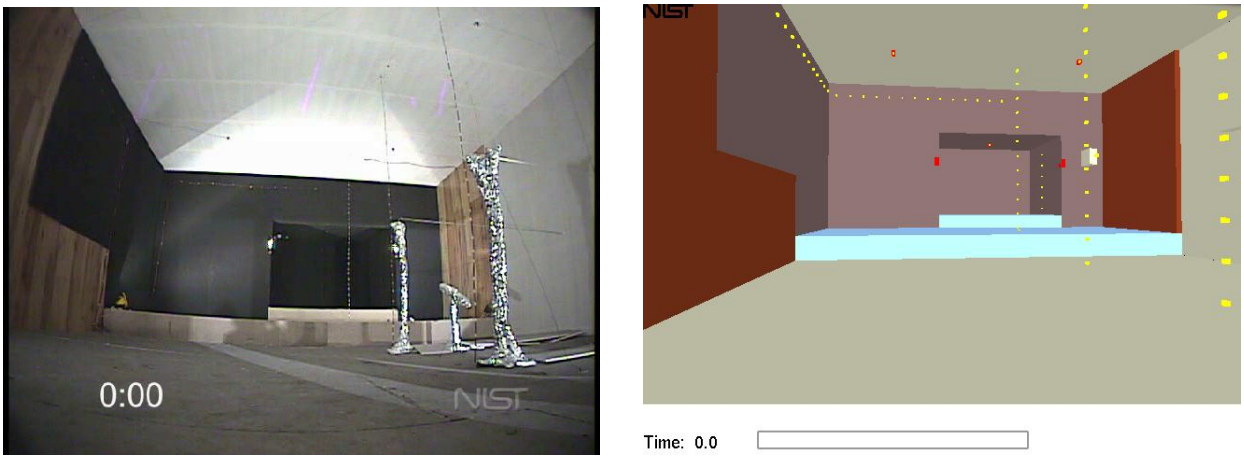

Figure 5-19. Ignition at the corners of the alcove, t = 0 seconds.

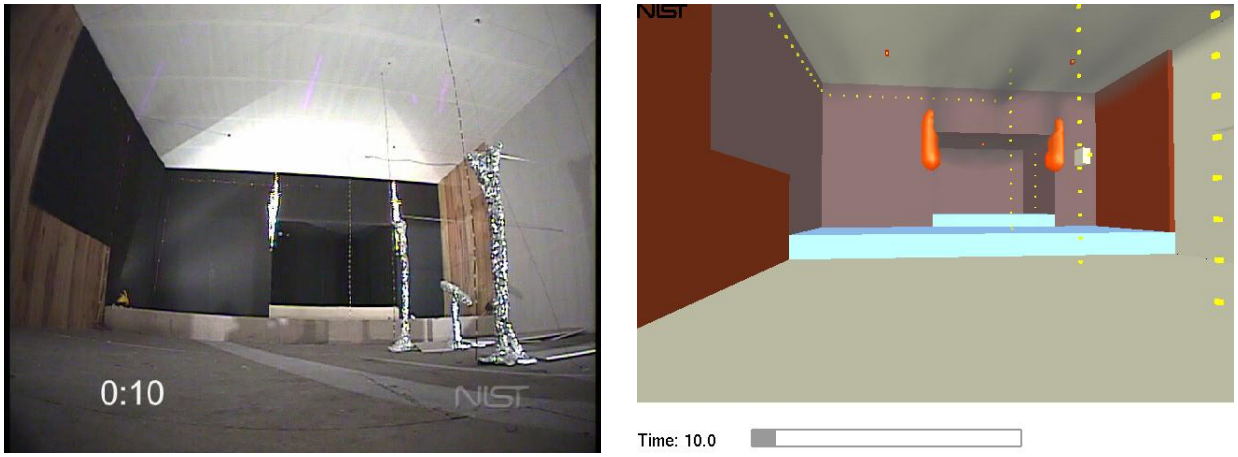

Figure 5-20. Flames spreading toward ceiling, t = 10 seconds after ignition.

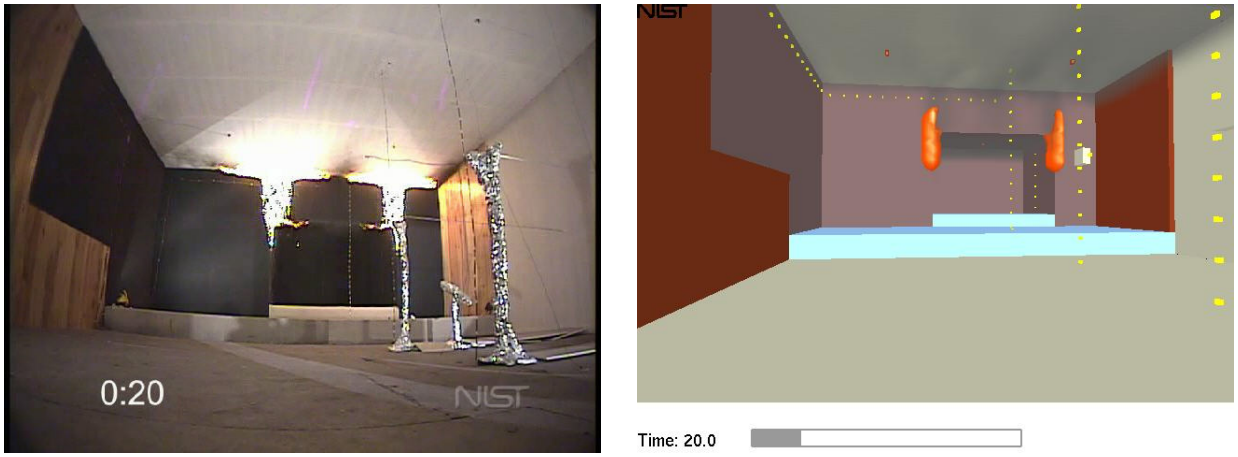

Figure 5-21. Flames impinging on ceiling, t = 20 seconds after ignition.

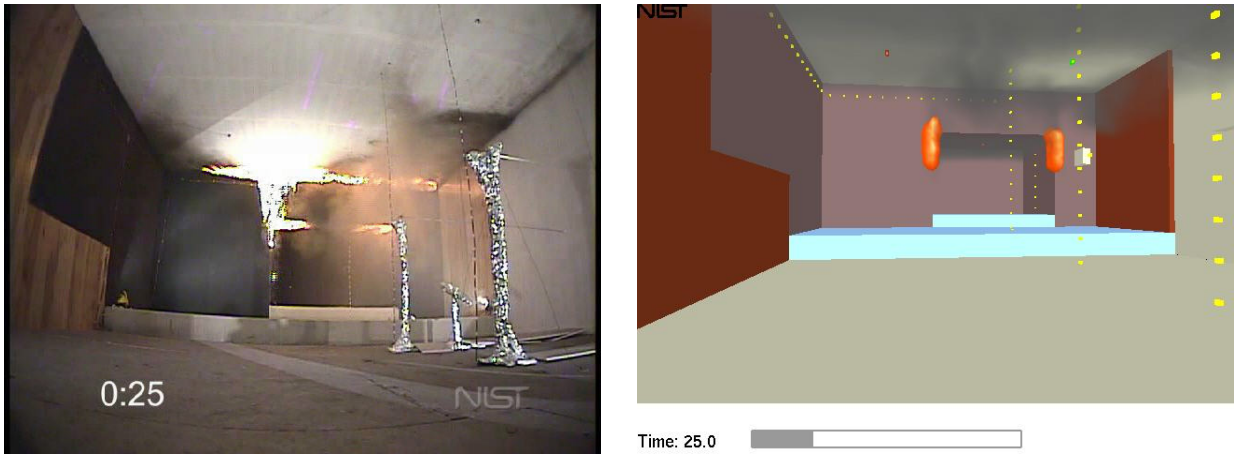

Figure 5-22. Initial sprinkler operating, t = 25 seconds after ignition.

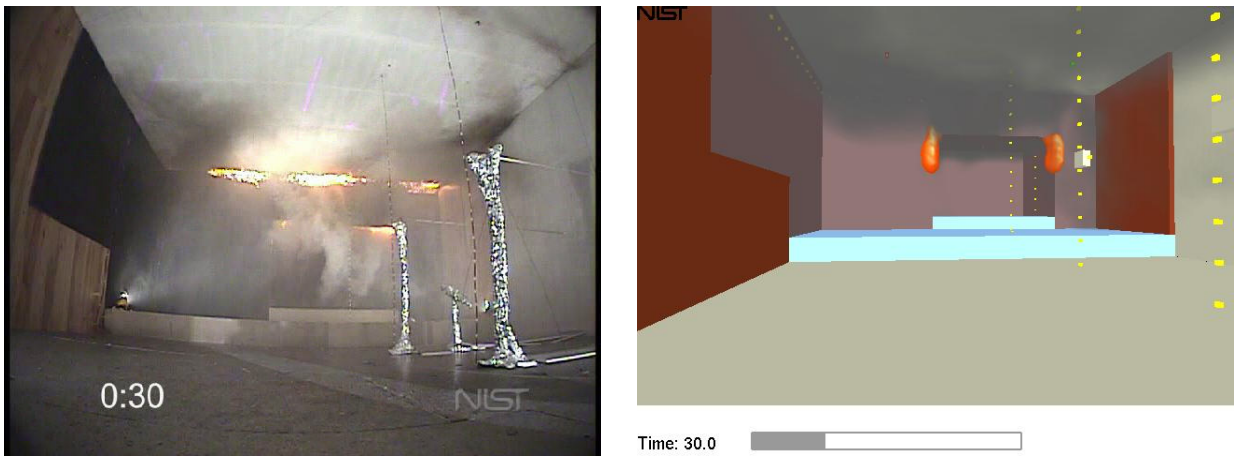

Figure 5-23. Third sprinkler operating in experiment, t = 30 seconds after ignition.

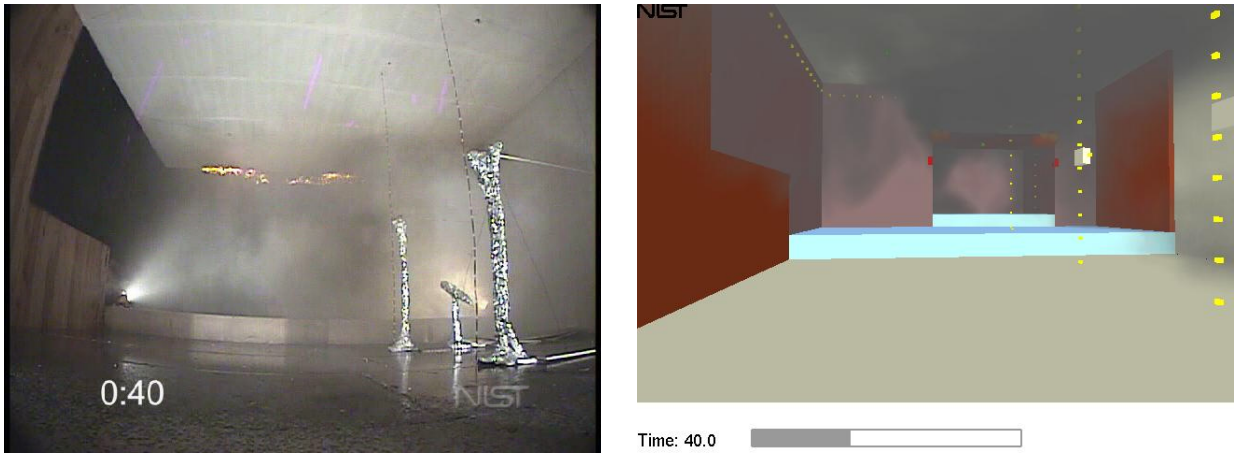

Figure 5-24. Suppression with three sprinklers operating in each case, t = 40 seconds after ignition.

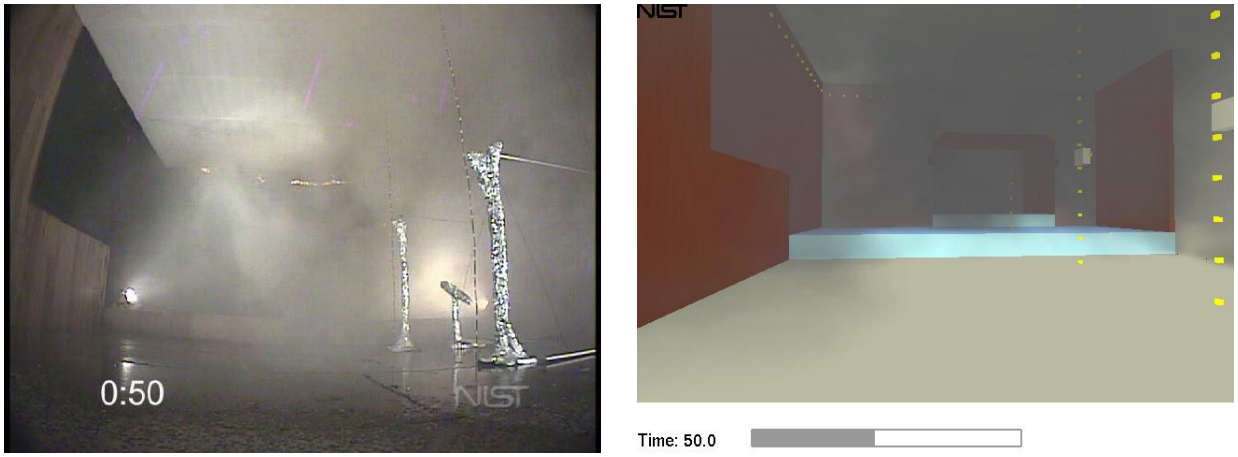

Figure 5-25. Fire suppression continues in both the experiment and the simulation, t = 50 seconds after ignition.

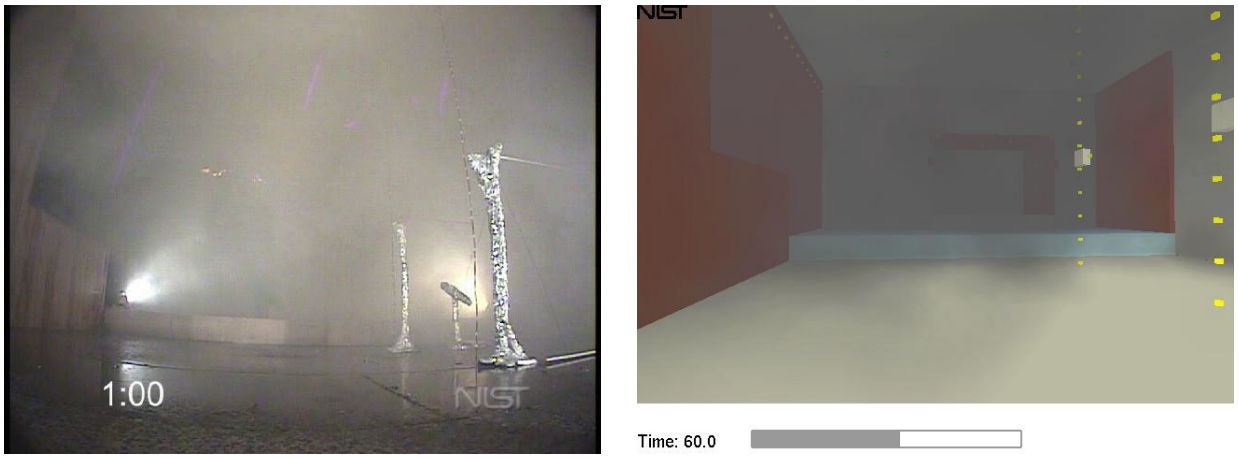

Figure 5-26. Fire controlled in both cases, t = 60 seconds after ignition.

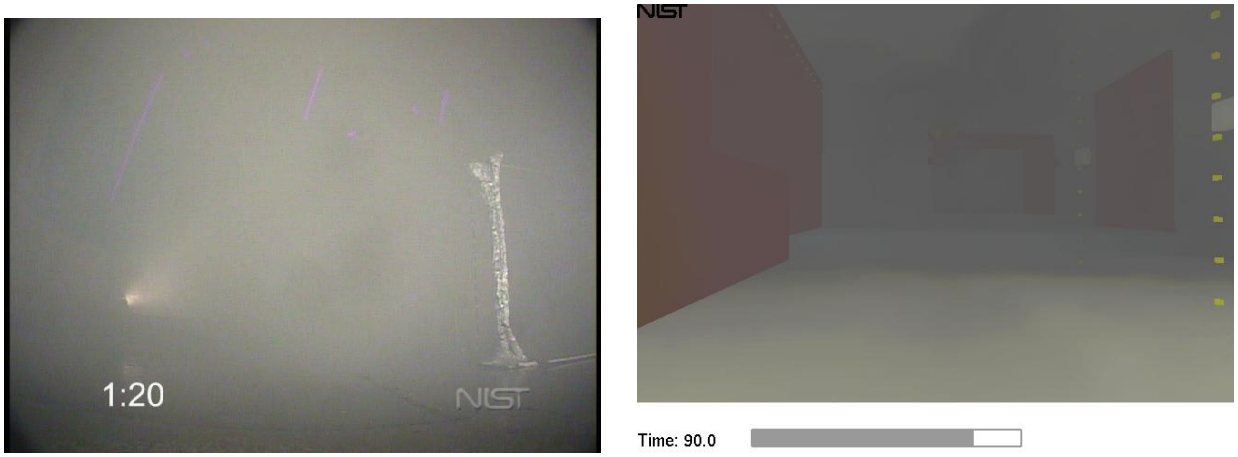

Figure 5-27. Fire controlled in both cases, t = 90 seconds after ignition.

ignition. Figure 5-22 was captured at 25 seconds after ignition, approximately 1 second after the first sprinkler activated in both the experiment and the simulation. With the experiment, the impact of the sprinkler can be seen as the fire on the right side of the platform wall is suppressed. In FDS the flame height on the right side of the alcove can be seen to be reduced.

By 30 seconds (see Fig. 5-23) the effect of both of the sprinklers above the platform operating as well as the sprinkler in the alcove is apparent. Burning continues at the intersection of the platform wall and the ceiling. This area is above where the water spray is hitting the wall. Also notice the flames on the ceiling of the alcove. This area is shielded from the water spray of the two sprinklers. The smoke being pushed out of the alcove is due to the activation of the sprinkler on the ceiling of the alcove. In the simulation, only one sprinkler is operating at this time. The fire growth on the right side of the alcove has been limited by the single sprinkler.

By 40 seconds after ignition, three sprinklers in the experiment and in the simulation have activated. The video frame in Figure 5-24 shows that the fire in the alcove has been suppressed and that the burning above the water line on the platform wall continues. With three sprinklers operating in FDS, the water spray is significantly reducing the visible flames. The flames on the platform wall have been suppressed. However, there are still flames visible at the intersections of the alcove ceiling and the alcove walls on both sides of the alcove. These areas are shielded from the water spray of the sprinklers over the platform and they are above the water impact line from the sprinkler in the alcove.

Figures 5-25 through 5-27 show continued fire suppression for both the experiment and the simulation. In both cases some flames exist in the ceiling area of the alcove. But clearly the rate of fire growth and the resulting hazard development has been reduced significantly when compared with the unsprinklered case.

Both the experiment and the computer model demonstrate that the sprinklers would prevent flashover and considerably mitigate the hazard from the fire. However, the degree to which the fire is controlled is different between the experiment and the model, since the simulation has more flame spread along the edges of the alcove ceiling after activation of the sprinklers.

(ii) Numerical Comparison

In this section, measurements of heat release rate, temperature, heat flux, and oxygen volume fraction from the full-scale mock-up sprinklered experiments conducted in Section 4 are compared with values generated by the FDS simulation.

Figure 5-28 shows the FDS predicted heat release rate for the sprinklered enclosure. The experiment failed to produce enough combustion gases for the oxygen depletion calorimeter to measure a heat release rate. This was due to the rapid sprinkler activation, the effective fire suppression and the large volume of the enclosure. This graph demonstrates that in the simulation the fire grew after the activation of the third sprinkler (all were operating by 36 seconds). The decrease in HRR at approximately 140 is when the shielded (dry) foam on the alcove ceiling burns itself out.

The comparison of the temperatures at Stations C and D are shown in Figures 5-29 and 5-30. In both cases FDS under predicts the temperatures near the ceiling. The FDS predictions in these two graphs have not been smoothed in order to show that the peak values near the ceiling are very close to the sprinkler activation temperature of 74 ºC. Typically the temperature of the fire gases surrounding a sprinkler at the time of activation are approximately twice the listed temperature.

Due to the continued burning of foam on the ceiling of the alcove prior to complete extinguishment,, the temperature in the simulated enclosure increases over the experimental temperatures. However, at the 1.4 m level above the floor the temperature never exceeds 35 ºC (95 ºF). This is well within the temperature tenability range.

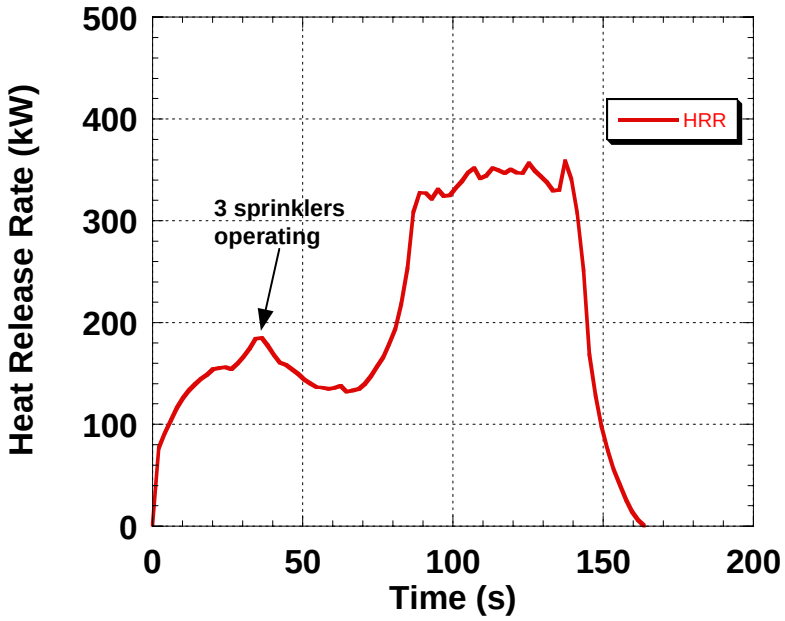

Figure 5-28. FDS predicted heat release rate for the sprinklered case.

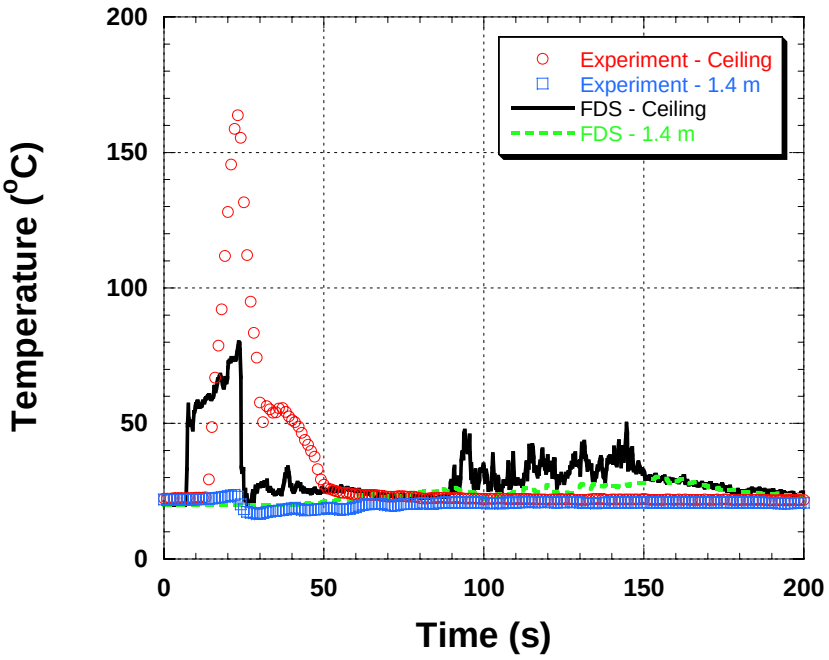

Figure 5-29. Temperature comparison between the sprinklered fire experiment and the FDS simulation at Station C.

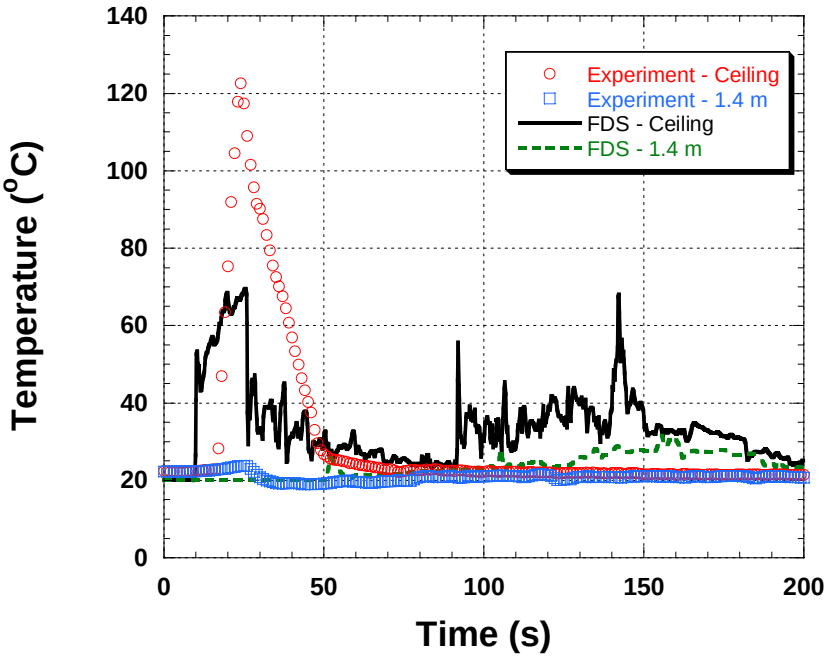

Figure 5-30. Temperature comparison between the sprinklered fire experiment and the FDS simulation at Station D.

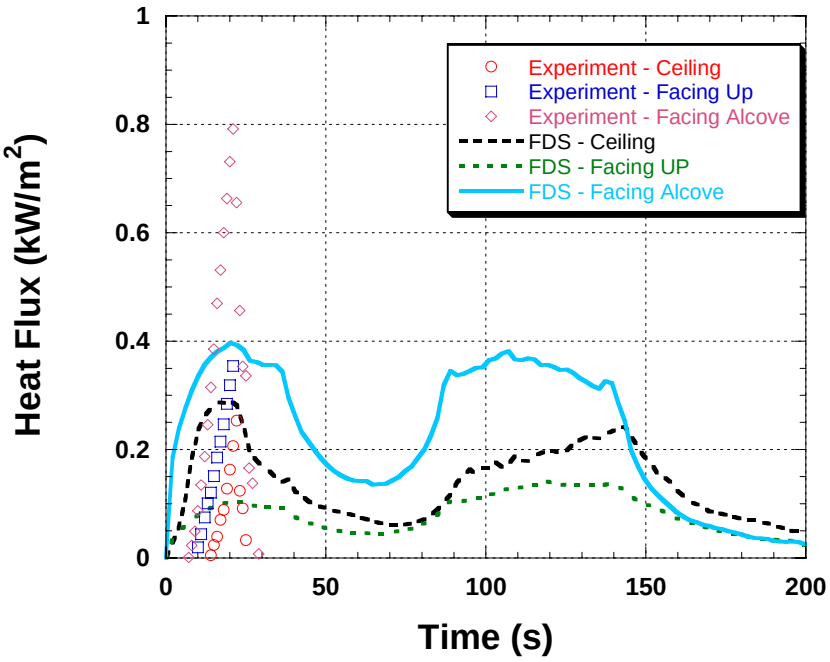

Figure 5-31. Heat flux comparison between the sprinklered fire experiment and the FDS simulation at Station C.

The comparison of the measured heat flux with the calculated heat flux is shown in Figures 5-31 and 5-32. Due to the limited fire growth and significant cooling by the water all of the heat flux values are less than 1 kW/m^2. One notable difference between the experiment and the simulation is after the sprinklers activate in the experiment, the measured heat flux goes to zero, while in the simulation small values heat flux energy continue to be shown.

Figure 5-33 exhibits the comparison of the measured and predicted oxygen concentrations at Station C. The measured oxygen concentration shows only a slight decrease during the 200 seconds, while the simulation shows a decrease of approximately 2 percent. This may be due to the continued burning of the foam along the ceiling of the alcove that is taking place in the simulation of the experiment.

(iii) Full-scale mock-up comparison - Summary

The visual and numerical comparisons demonstrate that the effects of an automatic fire sprinkler system on a fire can be successfully modeled by FDS and visualized with Smokeview. Both the experiment and simulation demonstrate that the sprinklers would prevent flashover and considerably mitigate the hazard from the fire in the test enclosure. However, the degree to which the fire is controlled is different between the experiment and the model, since the simulation has more flame spread along the edges of the alcove ceiling after activation of the sprinklers.

The temperature, heat flux, and the oxygen volume fraction comparisons show reasonable agreement between the experiments and the model in terms of both trends and range. Again some differences were caused by the increased burning after the start of suppression in the shielded areas, but that phenomena has been documented in other experiments as well [6]. Tenability limits were predicted never to be exceeded using FDS, consistent with what was observed in the full-scale mock-up experiments. The lower portion of Table 5.3 compares the extreme values of heat flux, temperature, and oxygen volume fraction predicted in the simulation to the measured values.

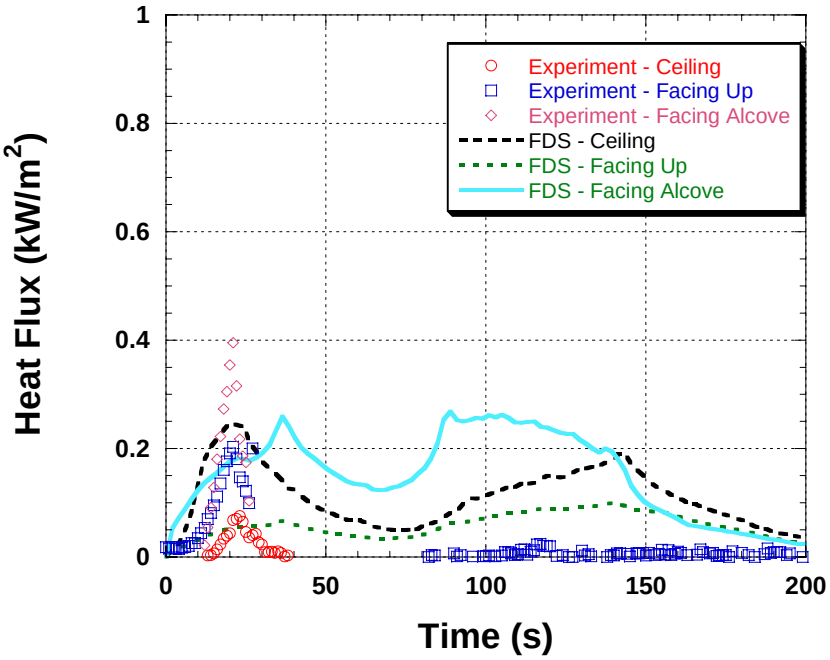

Figure 5-32. Heat flux comparison between the sprinklered fire experiment and the FDS simulation at Station D.

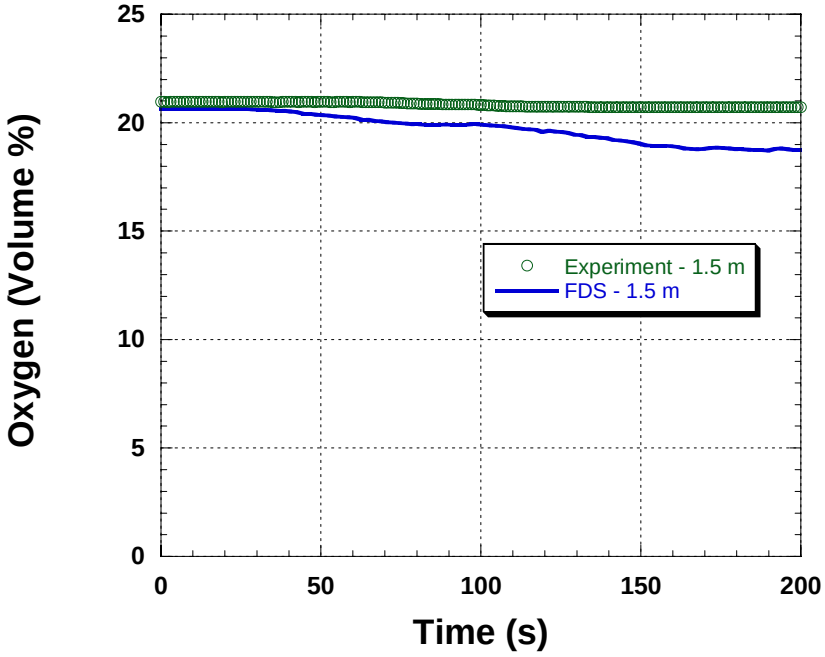

Figure 33. Oxygen volume fraction comparison between the sprinklered fire experiment and the FDS simulation at approximately 1.5 m above the floor at Station C.

5.3 FDS INCIDENT SIMULATION

5.3.1 Computational Domain and Materials

The computational domain used for the incident simulation consisted of eight adjoining rectangular meshes. Figure 5-34 shows an isometric view and Figures 5-35 and 5-36 show two different external views of the building. Each mesh was 4.1 m (13.5 ft) wide and the lengths varied from 10.8 m (35.4 ft) to 21.6 m (70.9 ft) based on the size of the structure and vent location. Each computational (or grid) cell was 100 mm (3.9 in) on a side. The input geometry for the Station night club including all wall, door and window sizes and locations was modeled based on the documentation provided in Chapter 2. Figure 5-37 is a plan view, Figures 5-38 shows the grid spacing used for the foam on the platform, and Figure 5-39 is a view looking toward the horseshoe bar and side exit from the center of the nightclub.

The interior finishes of the structure were simplified and modeled as five different materials: foam, wood, ceiling tile, gypsum board and carpet. The foam was prescribed with a wood backing due to the fact that the foam burns away leaving the wood paneling behind. Typically, FDS accounts for the burning of a single material; thus, the model was modified to allow the wood behind the foam to burn once the foam had burned away. The actual structure was lined with multiple types of wood such as paneling, wafer boards and bead board. In the simulation, all of these woods were prescribed with a single set of material properties. The ceiling tile, gypsum board and nylon carpet properties were based upon a combination of the cone calorimeter tests described in Chapter 4 and the FDS materials database. The view of the platform area seen in Figure 5-40 contains foam (grey), wood (brown and black), gypsum board (tan) and ceiling tile (tan).

The only difference in the material properties used in the simulation of the full night club vs the mock-up is the thickness of the foam and the paneling. Based on materials observed in the field, the foam recovered from the night club was thicker than the foam used in the mock-up; a value of 30 mm (1.2 in) was chosen. The paneling that remained in the night club was installed in two layers. Therefore the thickness of the paneling for the incident simulation was doubled relative to the mock-up. The ceiling tile, gypsum board, and carpet used the same values as the FDS database, which were the same values used in the mock-up simulation.

Table 5-4. Simulation Material Properties

Material	Thickness (m)	Ignition Temperature (^oC)	Heat of Vaporization (kJ/kg)	Thermal Conductivity (W/m K)	Density (kg/m^3)
Foam	0.03	370	1350	0.034	22.0
Paneling	0.01	360	500	0.13-0.29	450
Ceiling Tile	0.016	NA	NA	0.0611	NA
Gypsum Board	0.013	400	NA	0.48	NA
Carpet	NA	280	3000	NA	NA

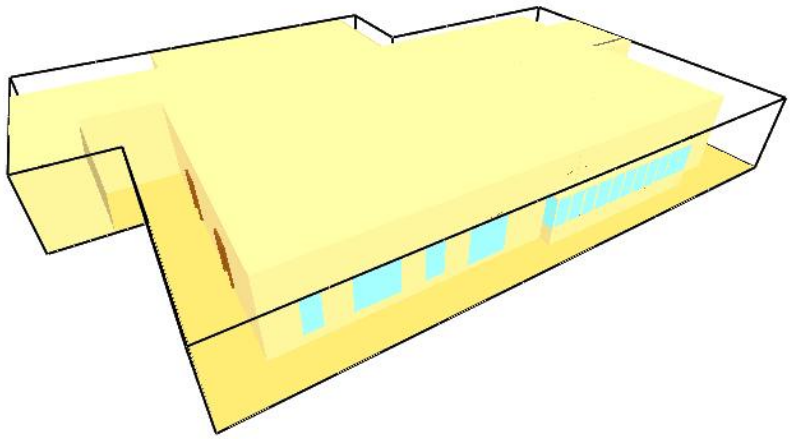

Figure 5-34. FDS computational domain of full nightclub

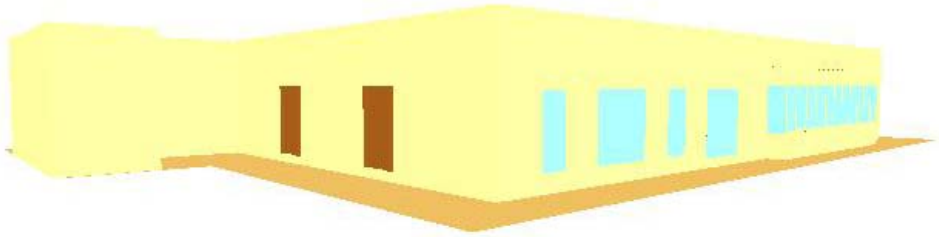

Figure 5-35. External view of nightclub from northeast corner

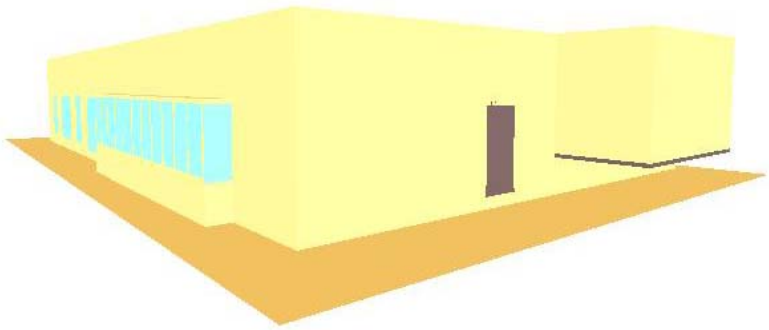

Figure 5-36. External view of nightclub from northwest corner

Figure 5-37. View from above with structure sliced 2.5 m above floor

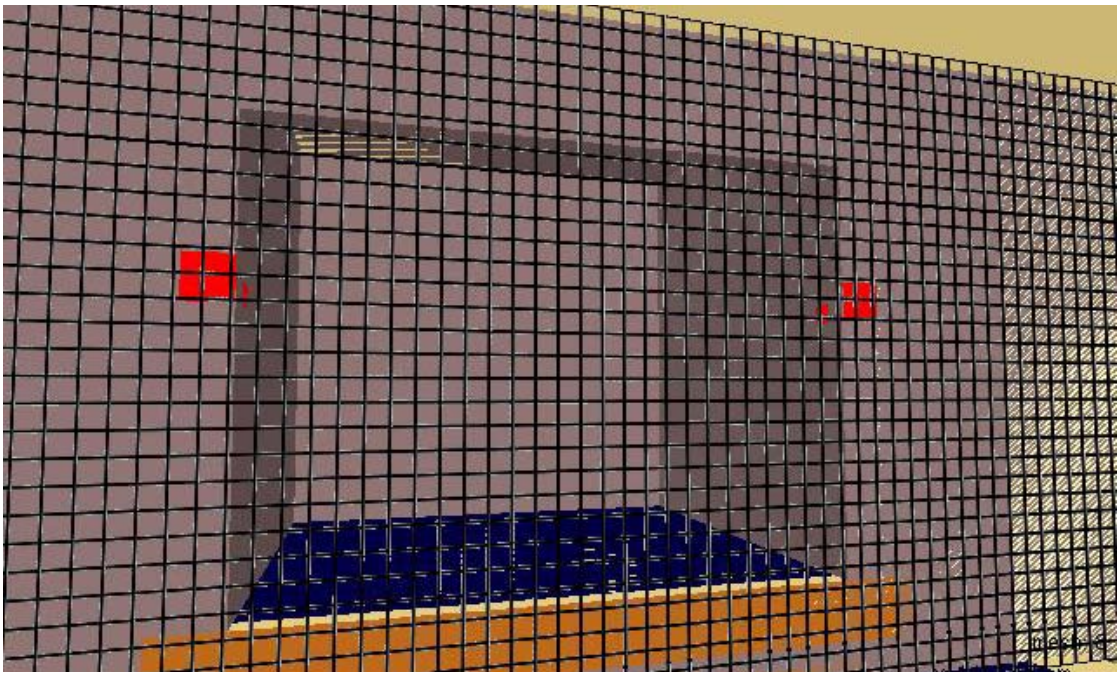

Figure 5-38. Numerical grid used for foam covered walls on platform. Red squares represent the points of ignition

Figure 5-39. View from center of nightclub toward horseshoe bar, with side exit and front windows in background

Figure 5-40. View of platform and dance floor showing different materials

5.3.2 Vents and Openings

All four sides and the top of the computational domain were modeled as open to the environment outside of the domain to allow air to enter and combustion products to exit. The outside temperature was assumed to be the same as the initial temperature inside, and the wind was assumed to be calm[1]. The bottom of the domain was considered to be an inert, adiabatic solid. Four heat producing vents were modeled: two 200 mm (7.8 in) square vents on the front corner of the alcove, and two 100 mm (3.9 in) square vents located 100 mm (3.9 in) back from the corner, into the alcove. All of the heat producing vents were 1.24 m (4 ft) above the floor of the alcove. The vents have an energy flux of 1500 kW/m^2 and emit energy for 35 seconds beginning at t = 0 seconds.

The structure's doors and windows were opened during the simulation based on estimations from the WPRI video. The first door to open was the door adjacent to the platform. This door was observed opening in the video 29 seconds after ignition. The front double door was assumed to open shortly after the stage door at 30 seconds. This time was selected due to the crowd beginning to notice the fire and to move toward the front door. The side door near the main bar was opened at 45 seconds and the side door in the kitchen was opened at 60 seconds. These times were estimated by the crowd movement seen in the video and the remoteness of the doorways from the stage area.

At 78 seconds, the lower portion of one of the bay windows was removed. This appeared to occur as the cameraman passes by on his way to the rear of the structure. Portions of the windows located on the front of the structure, left of the main entrance were removed at 80 seconds. This included the lower half of each of the matching windows next to the large window in the center, the entire large window in the center, all of the thin window to its left and the lower half of the thin window to its right. Finally, more sections of the bay window, surrounding the portion that was removed at 78 seconds, were removed between 100 and 130 seconds. The side bay window facing the main entrance was seen open in the WPRI video and the three other windows between the side window and the lower portion of the window were removed at 78 seconds based on the sounds heard in the video. Vent opening times are summarized in Table 5-5 and visualized in Figure 5-41.

Table 5-5. Time of Openings for FDS Simulation

Location of Opening	Time of Opening (s)
Stage Door	29
Front Double Door	30
Side Door (near main bar)	45
Side Door (kitchen)	60
Front Bay Window (lower portion)	78
Front Windows	80
Left Side Bay Window	100
Three Bay Windows	110, 120, 130

[1] The temperatures recorded at T.F. Green Airport that night were in the high 20s (^{o}F) and the winds were light.

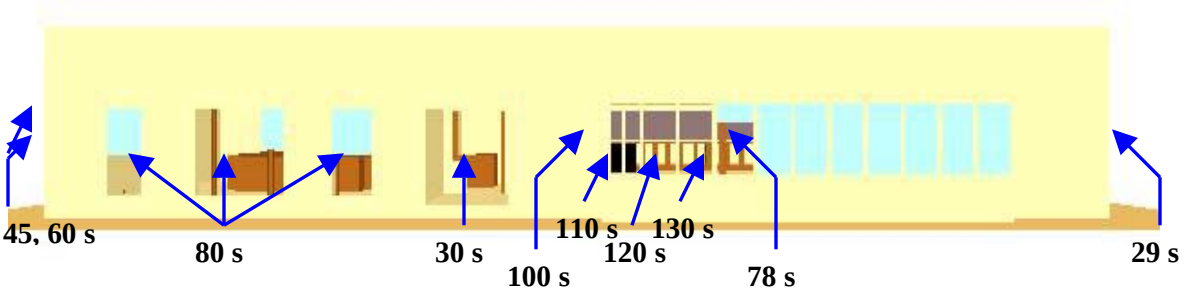

Figure 5-41. Visualization of Opening Times

5.3.3 FDS Simulation Results

The focus of this simulation was the examination of the conditions that may have been present in The Station night club during the early stages of the fire. Results from the bench-scale experiments and existing data were used to develop the input properties for the interior finish materials. The full-scale mockup results were used to compare against the FDS simulations to validate the implementation of the data in the model, and to determine the model's capabilities for this fire incident. Further, the sprinklered mock-up results were used to develop a means to model the sprinkler in the full nightclub simulation. Images from the WPRI video were utilized to develop model input to establish the location of the different interior finishes within The Station night club as well as being used as a general resource for confirming the physical arrangement of the nightclub. The simulation was run for 300 seconds to examine the time period from ignition to the approximate time of application of water by the fire department. The computation included simulated fire and smoke spread, potential temperatures, oxygen concentrations and visibility that may have existed in the actual incident. Each of these were compared to published tenability criteria.

In order to gauge the accuracy of the full night club simulation results, they were compared with the WPRI video record of the incident. In addition, analysis of the simulation considered published tenability criteria and the location of the victims within the night club.

(i) Heat Release Rate

The total heat released in the fire is plotted in Figure 5-42. The graph shows that after the alcove became fully involved with fire, at approximately 50 to 60 seconds, the heat release rate increased from approximately 2 MW to 54 MW in less than 50 seconds. Hence the rate of increase was more than 1 MW per second. As the fire spread throughout the structure and the fire became oxygen limited the heat release rate became steady at approximately 45 MW for approximately 150 seconds. After that time, the simulation began to deplete the fuel contained in the interior finish materials. The fire in the actual night club had spread into the structure and burned in and through areas of the roof and walls by this time. The simulation only provided fuel based on the interior finish and did not account for fuel being provided by structural elements and materials in building outer envelope.

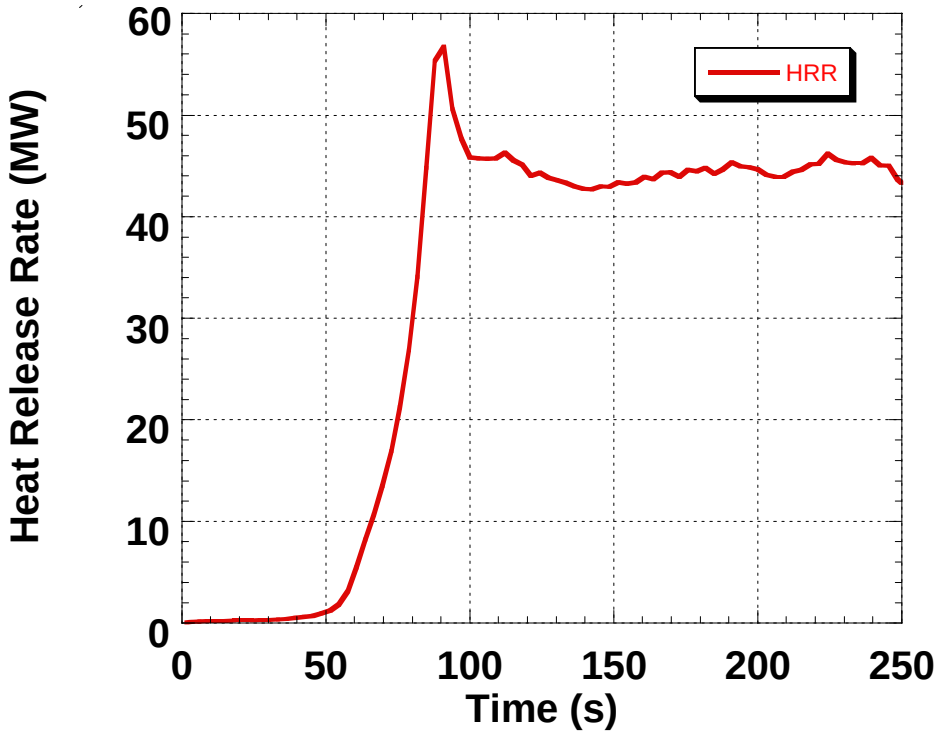

Figure 5-42. Total Heat Released in Building Fire Simulation as a Function of Time

(ii) Fire Growth and Smoke Spread

Images were selected from the WPRI video to compare with the FDS simulation results. Iso-surfaces of the heat release rate per unit volume and three dimensional smoke density parameters are displayed in the Figures 5-43 through 5-53. It should be noted that the orange color in Smokeview tracked the location of stoichiometric fuel and air mixture. If the temperature were high, then the orange surface could be thought of as a flame; if the temperature were below a threshold value, then no flame was actually present, just a non-burning mixture of fuel and air. Qualitative agreement can be seen between the pairs of images from the video and the simulation for both the initial growth prior to the videographer leaving the structure, and the outside view as the videographer walked around the structure. This similarity helped the investigation draw conclusions as to the conditions inside the structure even though the video was no longer recording inside.

Time "0" refers to the instant of ignition of the foam by the gerbs as documented in the WPRI video. All of the times that accompany the figures below are times after ignition. The times were chosen based on the image availability from the WPRI video. The images were chosen based on the visibility of the fire or the smoke from the fire. The last image set does not reflect the same time. The simulation stops at 300 s while the image from the video showing flames from the front of the night club was not recorded until 337 seconds after ignition. At this point in the fire, conditions were not changing as rapidly as during the fire development, so the comparison between the two images is reasonable.

The images from the video in Figures 5-43 and 5-44 capture the initial state of the fires on each side of the platform shortly after the gerb discharge had stopped. At 10 seconds after ignition, the fire can be seen burning on two surfaces at each of the corners; this is also considered in the simulation with the

Figure 5-43. Initial growth of fire on foam at corner of the alcove (10 seconds)

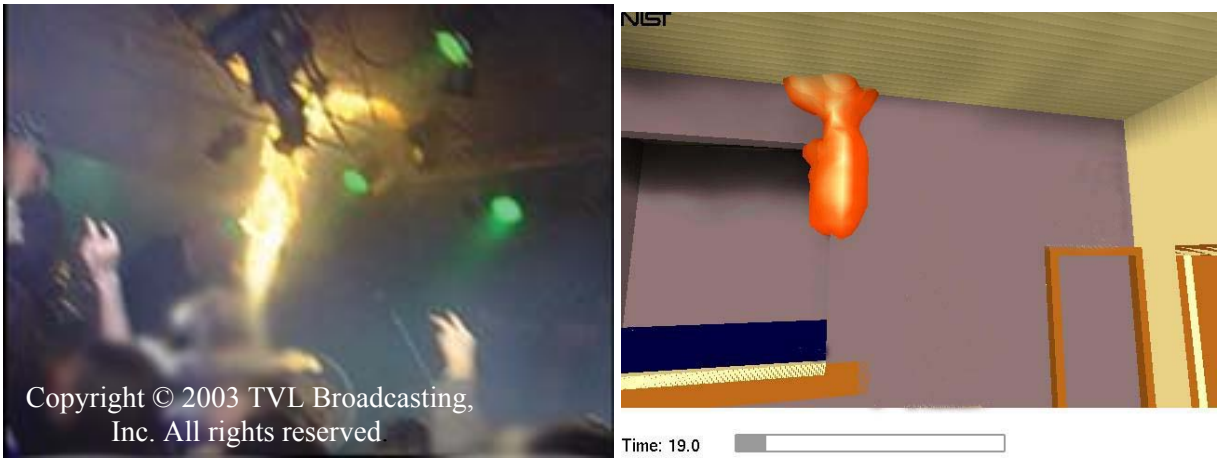

Figure 5-44. Flames impinging on ceiling (19 seconds)

placement of the ignition vents on both sides of the corner. In both the simulation and the actual incident the flames impinge on the ceiling within 20 seconds after ignition.

At 23 seconds after ignition, Figure 5-45, the videographer has begun to move toward the exit as have many in the crowd. Notice that many people are still facing the platform. The fire continued to grow and smoke has collected in the raised ceiling area over the dance floor. The smoke filling can be seen in the image from the simulation. (Note the black rectangular image on the floor is representative of the speaker cabinet, whereas the boundaries of the smoke layer are irregular.) At 53 s after ignition, the flames have grown and spread along the platform wall and into the alcove as shown in video image in Figure 5-46. In addition, the smoke is spreading across the lower level ceiling area toward the main exit. The flames have spread in the simulation as well and smoke is beginning to spill over from the dance floor area towards the exits and the main bar room, although it takes a few more seconds into the simulation for this to occur. Again the black rectangular objects on the floor are representative of speaker cabinets (near the platform) and the sound and lighting board (left side).

The videographer had exited the night club at approximately 70 seconds and headed toward the stage door. He then returns toward the main entrance and attempts to pass between the nightclub and the bus when he encounters a plume of black smoke pushing out of one of the window vents in the sunroom. The

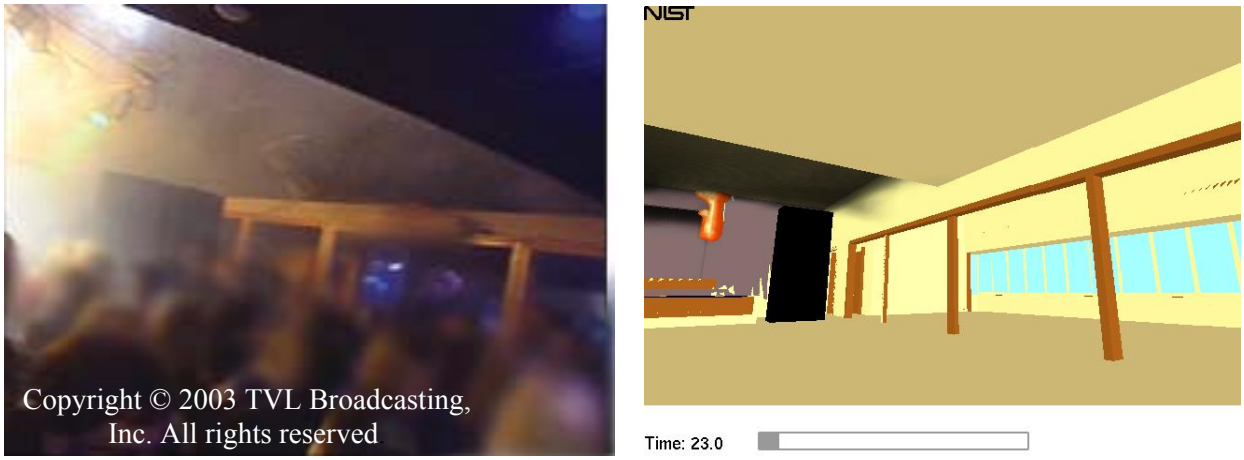

Figure 5-45. Videographer backing away from platform (23 seconds)

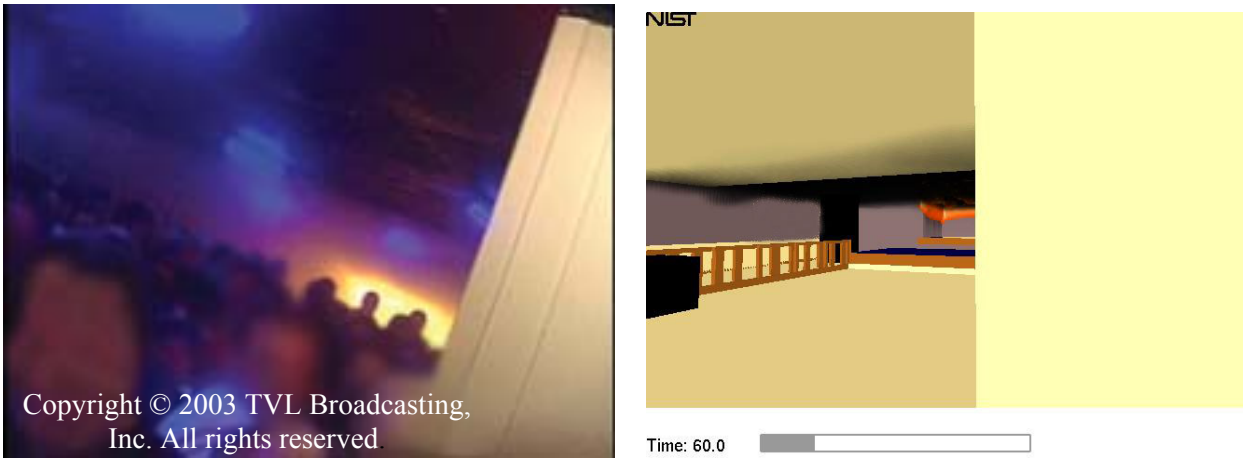

Figure 5-46. Smoke beginning to roll across ceiling (video 53 seconds, simulation 60 seconds)

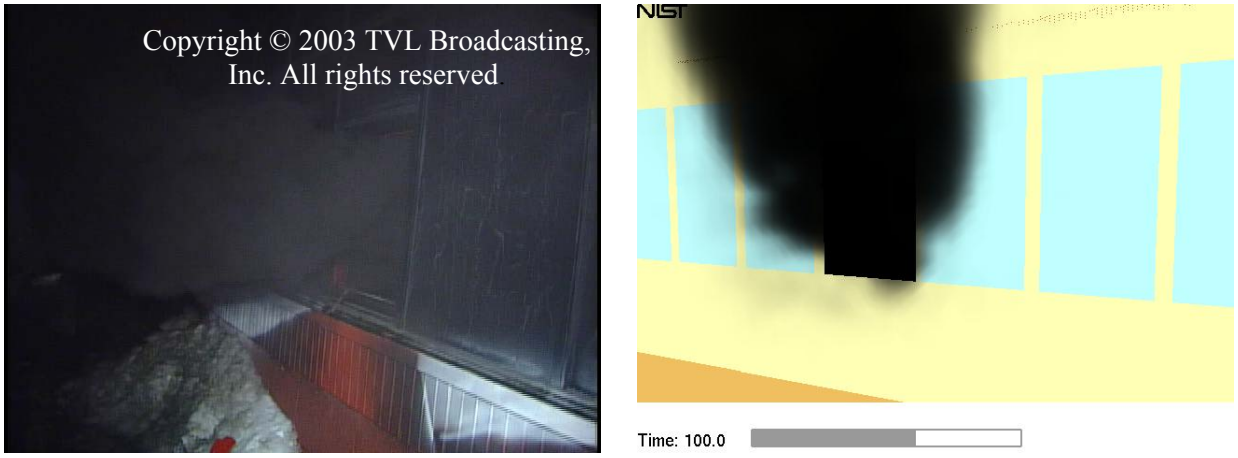

Figure 5-47. Smoke billowing outside from broken sunroom window (100 s)

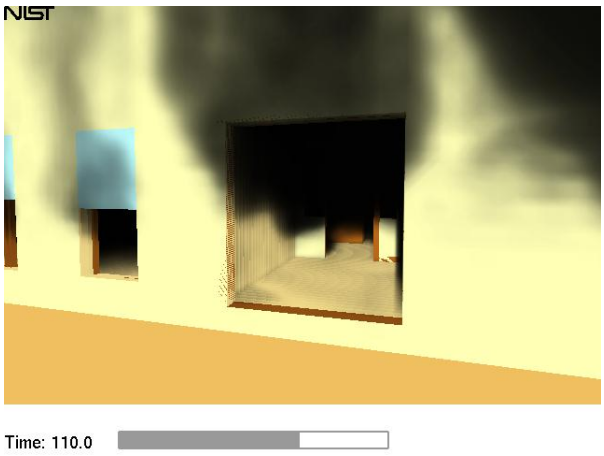

Figure 5-48. Light smoke emanating from front door of nightclub (110 seconds)

image from the simulation also shows a similar view. At approximately 110 s after ignition, smoke is flowing from the main entrance, the image from the simulation is given in Figure 5-48. The model did not account for people blocking the air flow into the doorway.

The Smokeview image in Figure 5-49 shows the smoke flow from the front door at 160 seconds after ignition in the simulation. In Figure 5-50, the simulated smoke flow from the main bar room windows is shown. More smoke is coming from the center window than the two side windows because the upper and lower portions of the center window have been removed while only the lower portion of the side windows are open in the simulation.

Figure 5-49. Heavy smoke leaving front door and open main bar window (160 seconds)

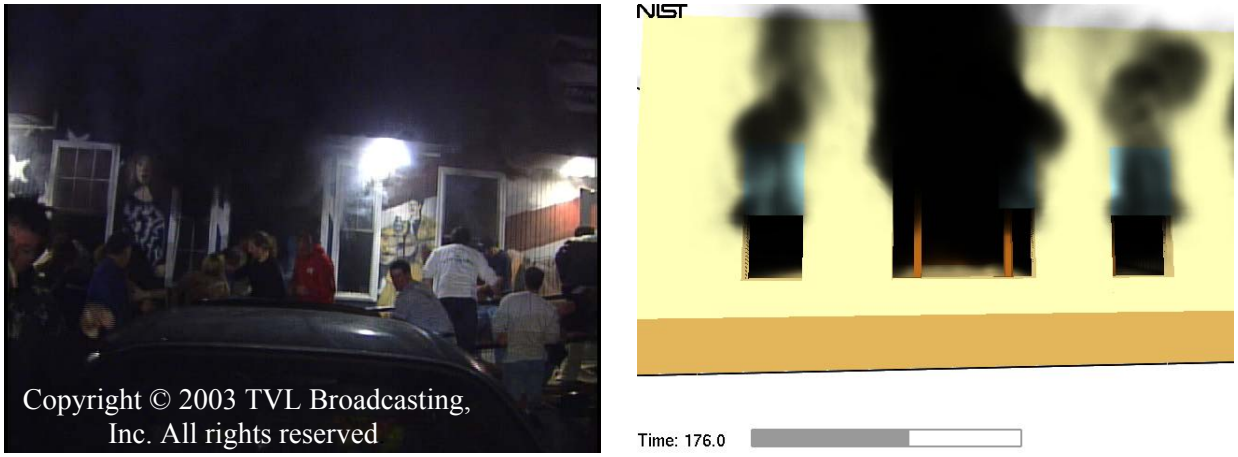

Figure 5-50. View of smoke plumes from front windows of horseshoe bar area (176 seconds)

The videographer moves around to the stage door again. The view inside the open door at approximately 289 seconds after ignition is shown in Figure 5-51 The image from the simulation agrees with the video image on the level of combustion products in the doorway. However without a comparison to the temperature in the doorway, the mixture fraction alone would indicate that more flames are in the area of the stage doorway than can be seen in the video image. The videographer continues around to the backside of the nightclub, at 300 s after ignition flames are coming through a small portion of the back wall (south wall) of the dance floor area and smoke is leaking from the bathroom hallway wall. The videographer moved toward the front of the night club again, at 309 seconds flames can be seen in the area of the front door. It takes another 25 seconds before he is in a position to record the images of the flames coming from the sunroom windows and the main door. The simulation stops at 300 s after ignition, short of the time that the entire night club reaches flashover conditions.

Figure 5-51. Looking into stage door exit (289 seconds)

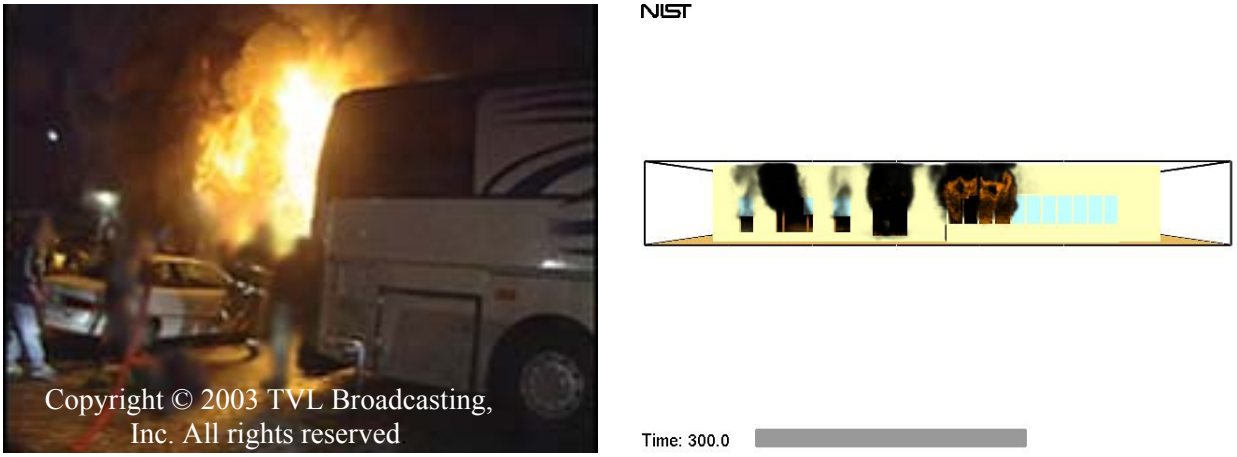

Figure 5-52. Flames breaking through front door and sunroom windows (337 seconds, video, 300 seconds simulation)

Smokeview images were rendered at certain time intervals from the view looking through the far side of the main bar to the platform area. (See Figures 5-53a,b.) This allowed for the conditions to be observed at several key locations: the platform area, the entrance to the main exit way and the main bar area. Many of the occupants traveled this path as either they were able to exit or were overcome by the conditions prior to being able to do so.

The fire developed quickly in the platform area as the foam burned and resulting in the alcove become fully developed with fire. Once that occurred the flames involved the entire rear wall and spread toward the main entrance, generating large amounts of smoke. At 70 s after ignition, the smoke can be seen in the area of the main entrance to the nightclub. This is consistent with the WPRI video. As the videographer leaves the nightclub, at approximately 70 s after ignition, smoke is flowing over the heads of people in the main entry foyer. However, even 80 seconds after ignition visibility remained high in the main bar room. This changed suddenly as the smoke and hot gases that were spilling out of the now-filled raised ceiling above the dance floor quickly spread to the main bar room. Based on the FDS simulation, within another 20 seconds, 100 s after ignition visibility was impaired, and remained so throughout the rest of the 300 second simulation. Flames can be seen in the last three images of Figure 5-53b as the surfaces in the main bar area began to burn.

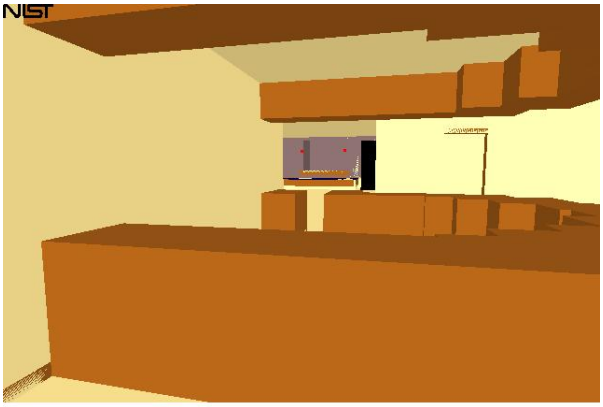

ignition (0 seconds)

20 seconds

40 seconds

60 seconds

70 seconds

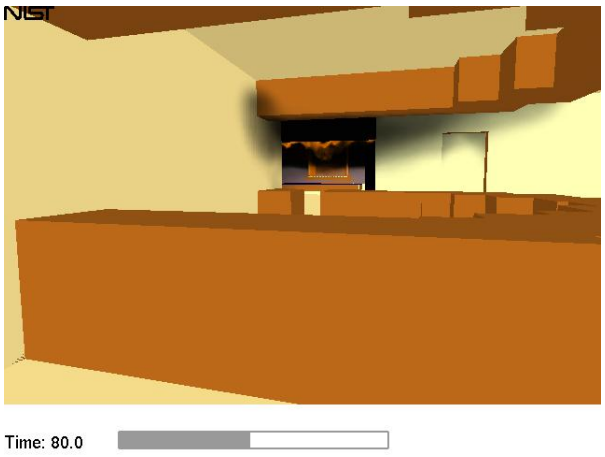

80 seconds

Figure 5-53a. View of fire from beyond horseshoe bar, looking at platform (0 s - 80 s)

85 seconds

100 seconds

200 seconds

250 seconds

Figure 5-53b. View of fire from beyond horseshoe bar, looking at platform (85 s - 250 s)

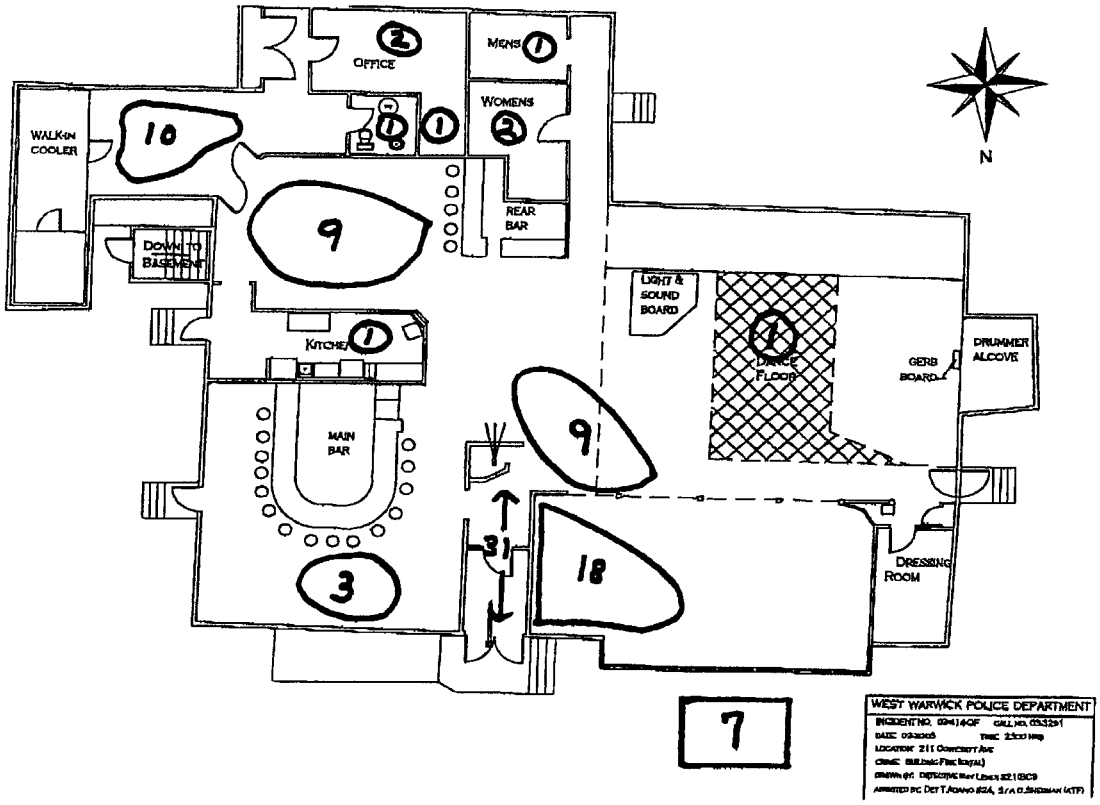

Figure 5-54. West Warwick Police Department Victim location diagram

(iii) Temperature

Temperature slices were examined to assess the tenability conditions that existed during the evolution of the fire. Horizontal slices were taken at both the 1.5 m (5 ft) and 0.6 m (2 ft) levels above the floor with the ceiling rendered transparent to examine the temperature distribution throughout structure as a whole. Vertical slices were used to analyze certain locations where groups of victims were located (See Figure 5-54). These locations included the main entrance as seen through the front door, the area leading into the exit area from the dance floor, and the left side of the sunroom and the open area adjacent to the side bar and kitchen. This analysis utilized 120 ºC (248 ºF) as the temperature tenability threshold [6]

Temperatures increase dramatically shortly after the alcove area reaches flashover conditions at approximately 65 seconds and then the platform area becomes fully involved in flames. The first two images in Figure 5-55a show the temperatures at 1.5 m (5 ft) above the floor at 80 and 85 seconds. Within that 5 second time interval the simulation predicts that dance floor area of the nightclub would have become untenable due to temperature. By 100 seconds after ignition, the simulation shows a large portion of the structure had become untenable due to temperature at the 1.5 m (5 ft) level. Figure 5-55b continues with the presentation of simulation temperature results from 160 second to 250 seconds after ignition. During this time interval temperatures continue to remain in the untenable range throughout the simulated night club, with the exception of areas that are considered closed off from the hot gas flow such

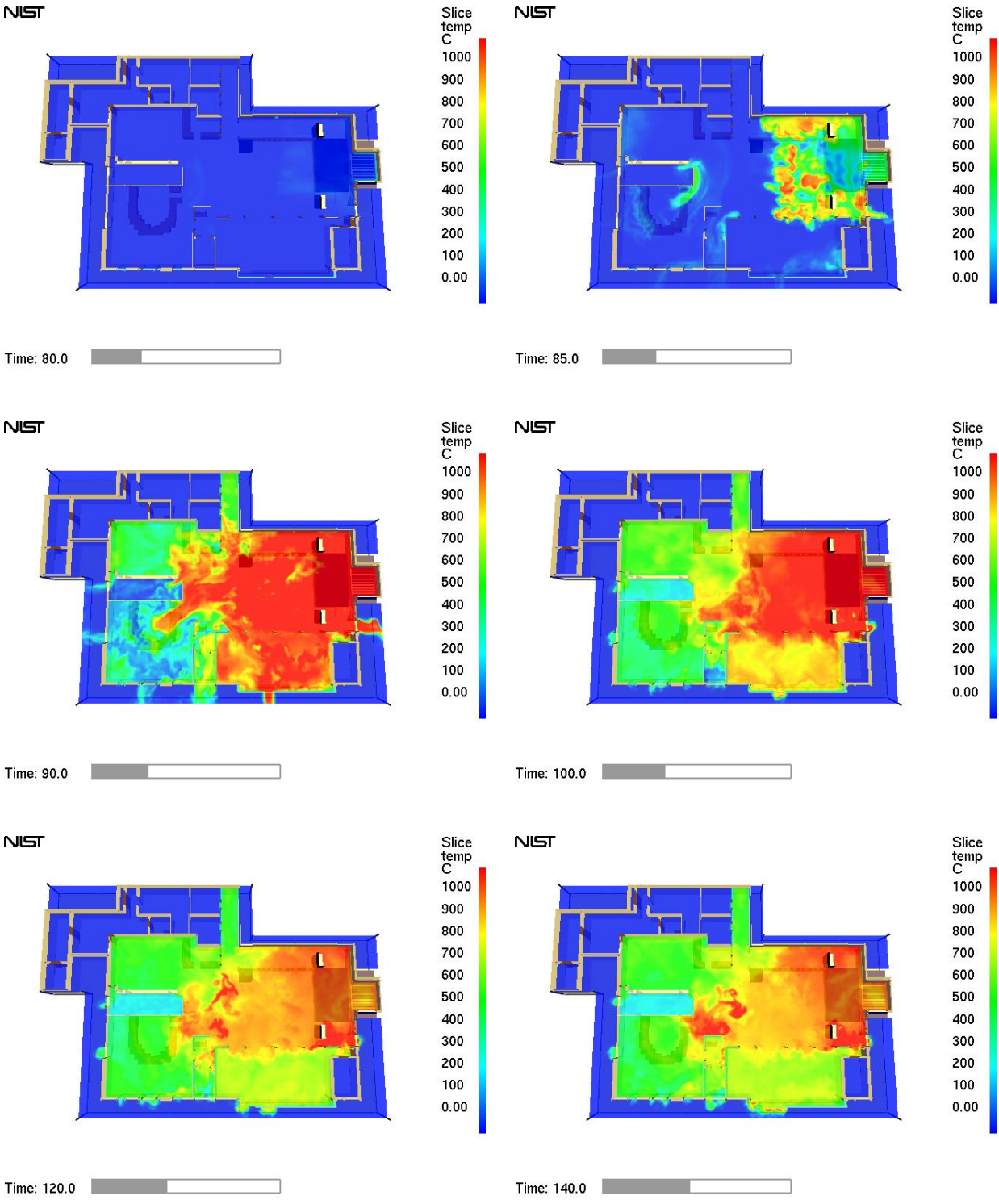

Figure 5-55a. Temperatures at 1.5 m (5 ft) above the floor, 80 seconds to 140 seconds

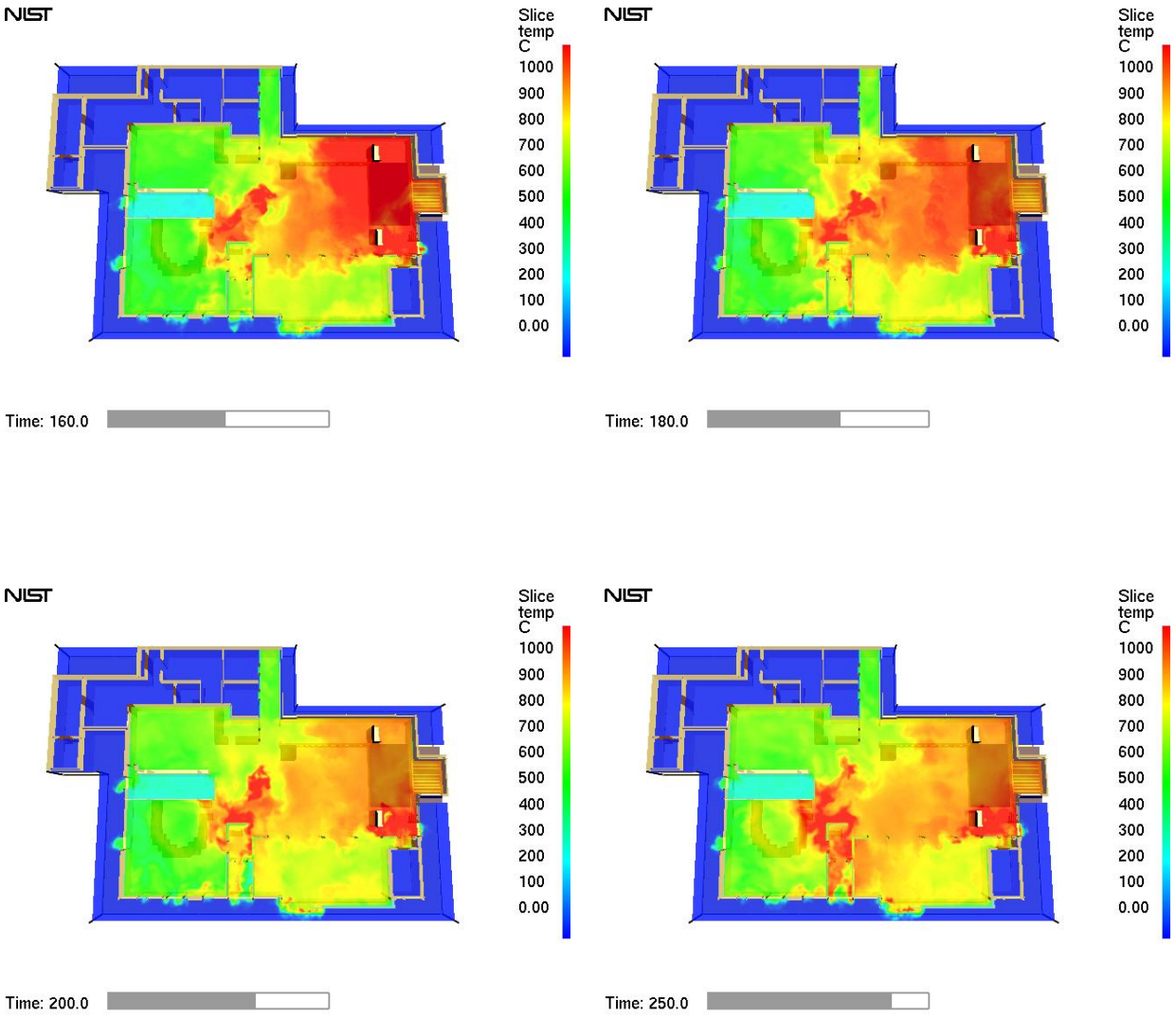

Figure 5-55b. Temperatures at 1.5 m (5 ft) above the floor, 160 seconds to 250 seconds

as the bathrooms, office and storage areas. These areas were assumed to be separated from the rest of the nightclub by closed doors, so they were modeled without a path for the gases to enter the spaces, hence they appear to remain in the tenable range. The kitchen area has an open door from the dart room and a open door that exits to the outside. The hot gas flow goes directly from the dart room to the exit doorway. This leaves the kitchen at a cooler temperature than the surrounding rooms.

At the 0.6 m (2 ft) height above the floor conditions remain tenable for a longer period of time than at the higher elevation. Figures 5-56a and 56b contain images captured at the same time intervals as in the previous figure. Figure 5-56a shows the dance floor and adjacent areas reach untenable temperatures in the simulation within 90 seconds after ignition. The sun room and dart room areas are predicted to reach untenable temperatures within another 10 seconds.

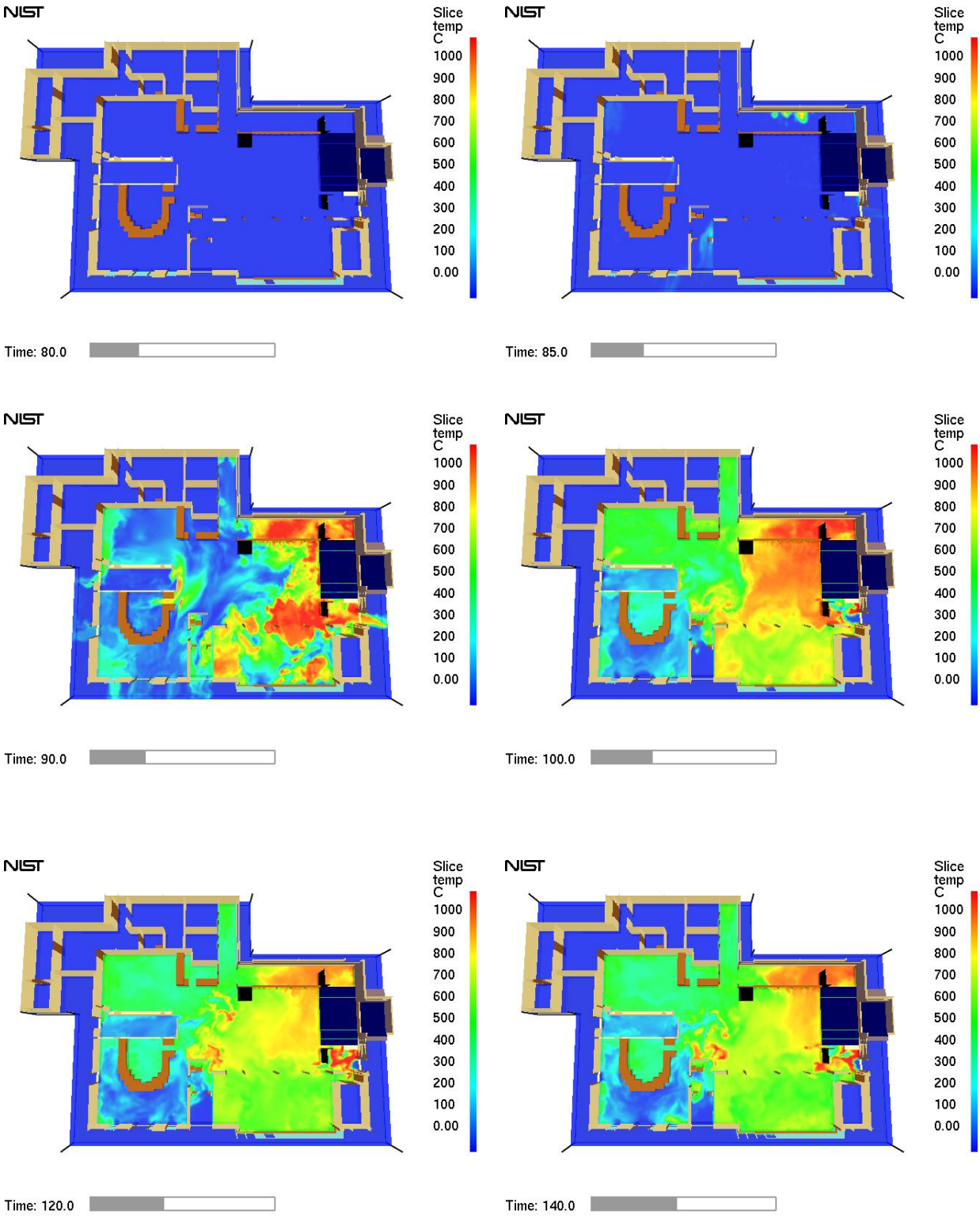

Figure 5-56a. Temperatures at 0.6 m (2 ft) above the floor, 80 seconds to 140 seconds

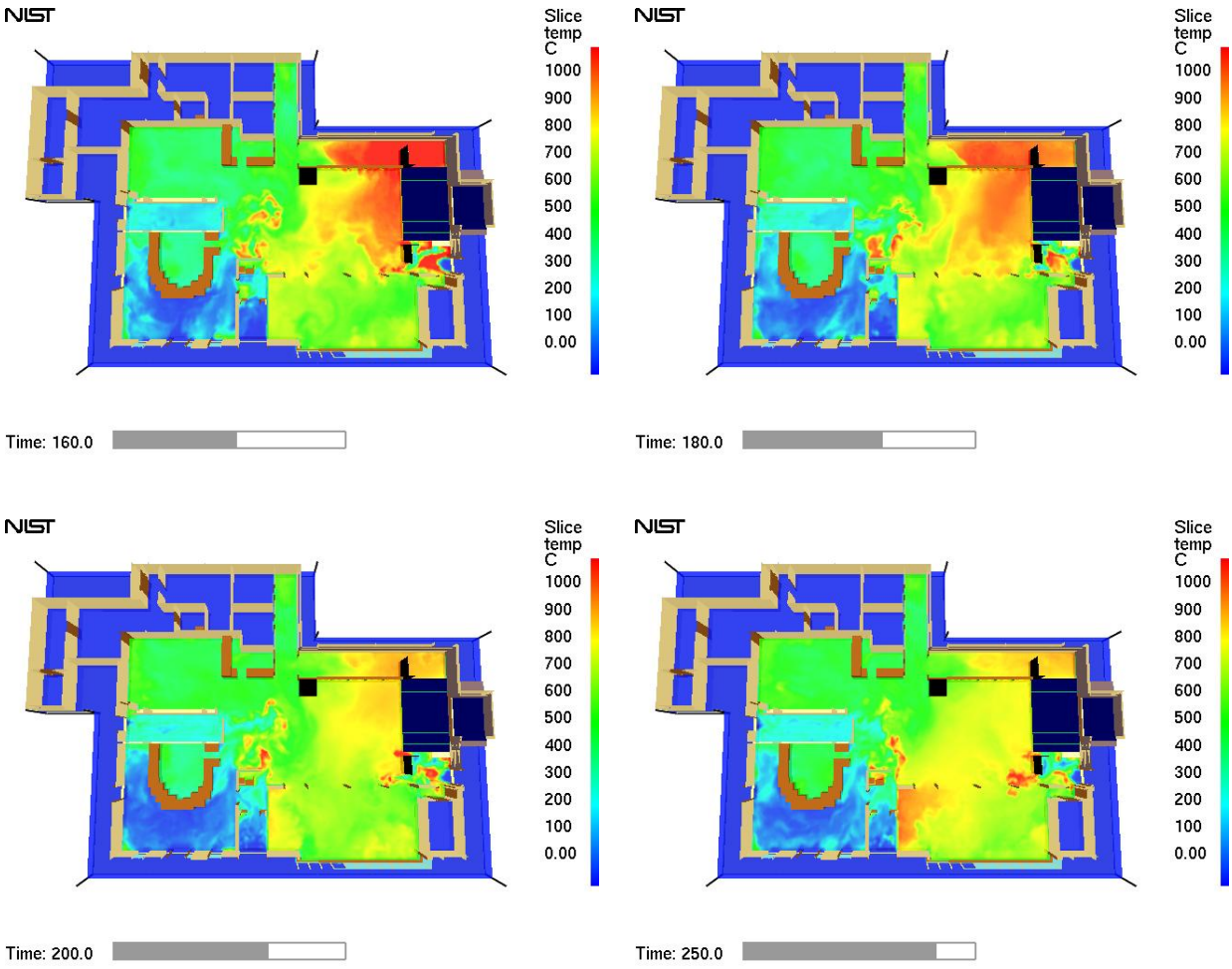

Figure 5-56b. Temperatures at 0.6 m (2 ft) above the floor, 160 seconds to 250 seconds

The significant differences in temperature between the 1.5 m (5 ft) elevation and 0.6 m (2 ft) occur in the main bar room and the main entrance. This area remains tenable at the lower level due to the inflow of fresh air through the open windows and open doorways. The cooler temperatures towards the floor at both the front door and main bar area explain why occupants were seen in the WPRI video escaping from the windows and doorway later into incident. The temperatures in Figure 5-56b do not change significantly regarding areas that have untenable conditions versus areas that remain tenable based on temperature only.

Figure 5-57a and 57b show the temperature predictions for the plane of data that is centered along the axis of the entry foyer. Temperatures just inside the front door, near the floor remain below the tenable limit because of the fresh air being drawn in through the doorway. This region of tenability decreases in a triangular orientation as the entranceway goes into the structure and gets smaller as the simulation continues. This simulation does not account for the occupants that accumulated in the doorway. Thirty-one victims were located in this area.

.

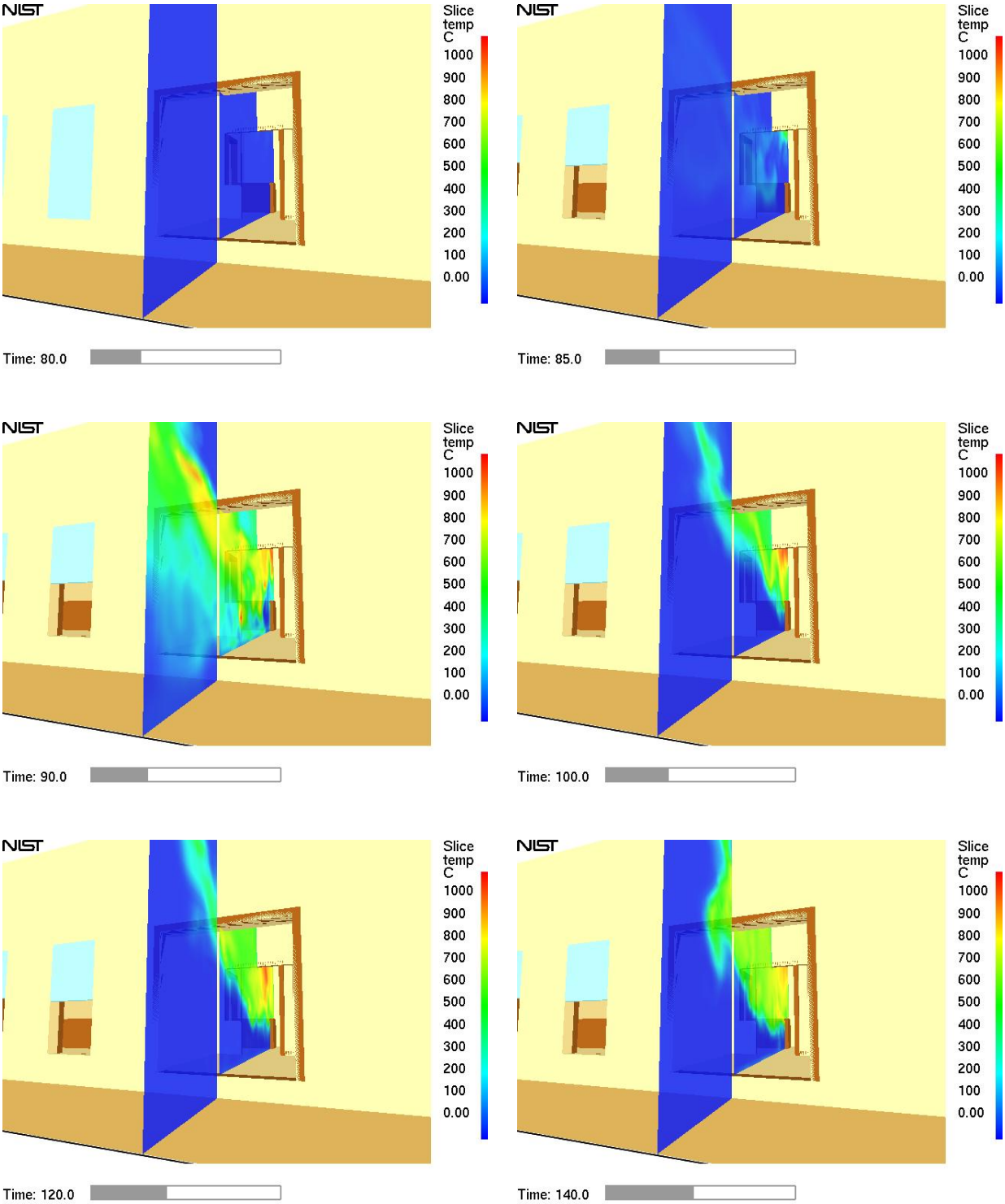

Figure 5-57a. Temperature profile through the center of the entry foyer, 80 seconds to 140 seconds

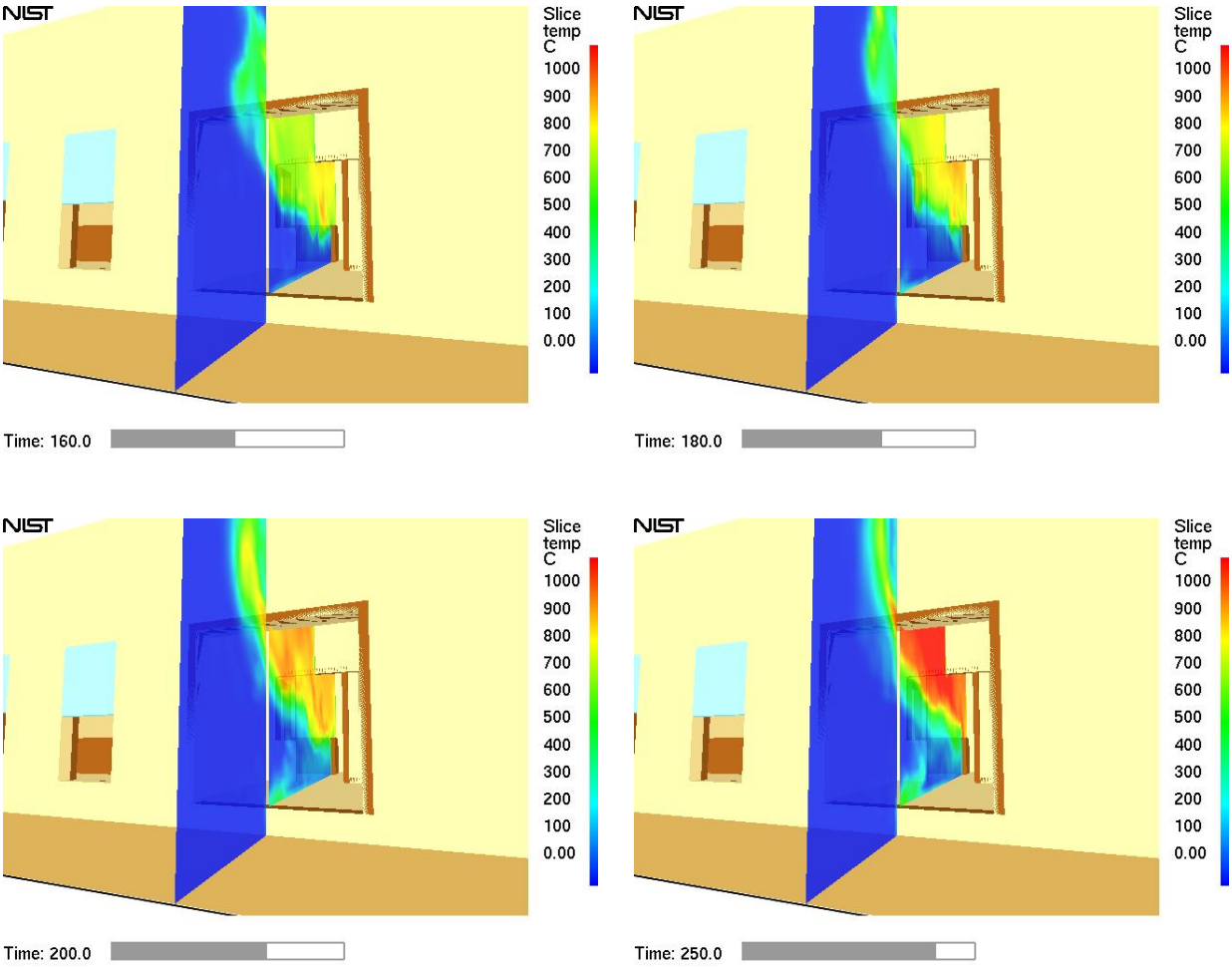

Figure 5-57b. Temperature profile through the center of the entry foyer, 160 seconds to 250 seconds

The area in the end of the sunroom adjacent to the entranceway was also a location that many victims were found. A vertical temperature slice through this area, shown Figures 5-58a and 5-58b, suggests that these victims did not have much time before the heat overcame them. Temperatures exceeded the 120 ºC (248 ºF) tenable threshold within 90 seconds after ignition. The simulation indicates that this change was rapid and extreme with temperatures in the upper portion of the space increasing from ambient conditions to flame temperatures on the order of 1000 ºC (1830 ºF) within 10 seconds. After the initial energy release due to the burning polyurethane foam (90 seconds), the predicted temperature decreased, but remained in the untenable range throughout the remainder of the simulation. Figure 5-58b shows that the temperatures increased again to 900 ºC (1650 ºF) at 250 s after ignition. The opening of portions of the bay windows between 78 seconds and 120 seconds after ignition had a minimal impact on reducing the temperatures in this part of the building. Eighteen victims were located in this area.

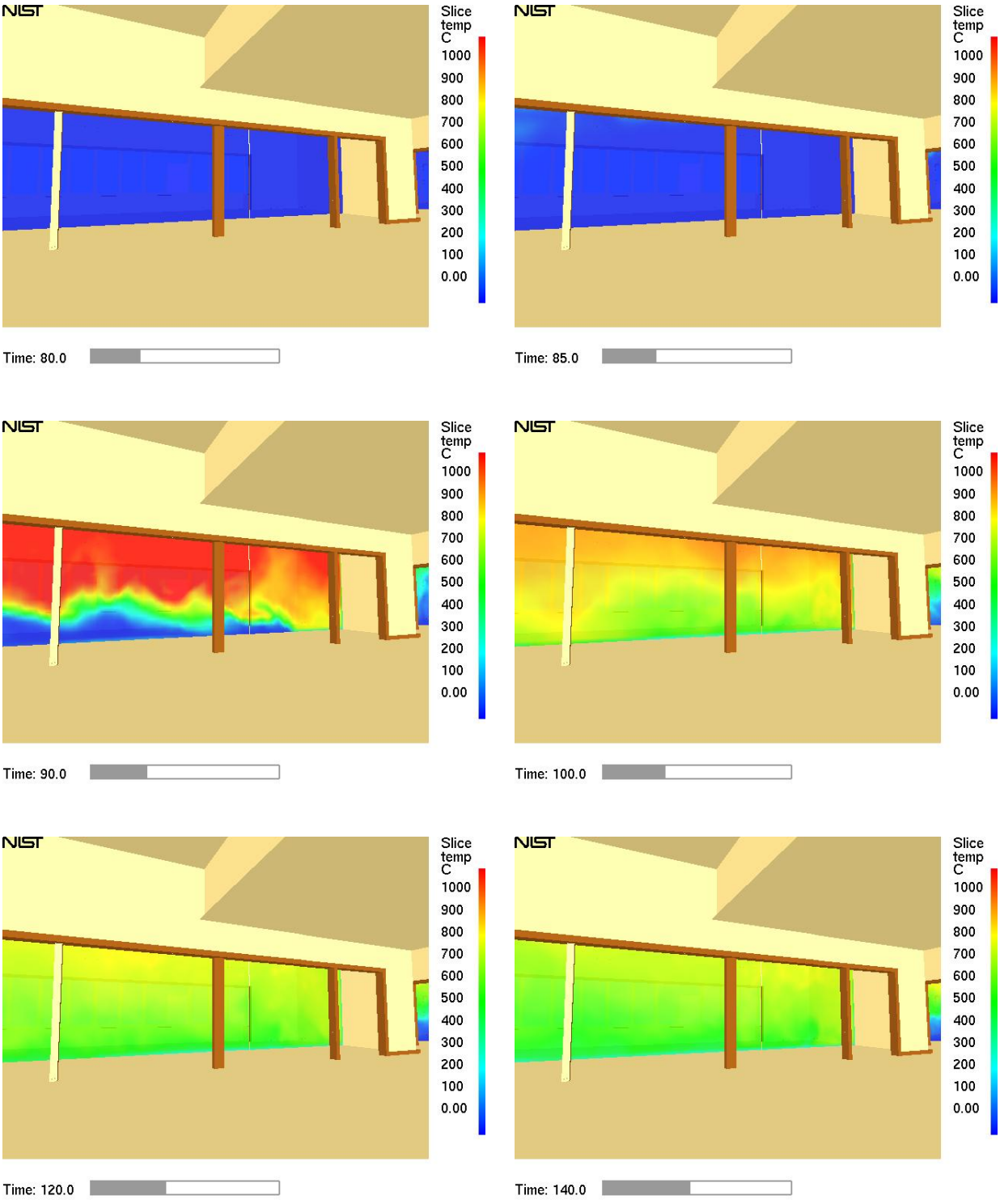

Figure 5-58a Temperature profile through the center of the sunroom, 80 seconds to 140 seconds

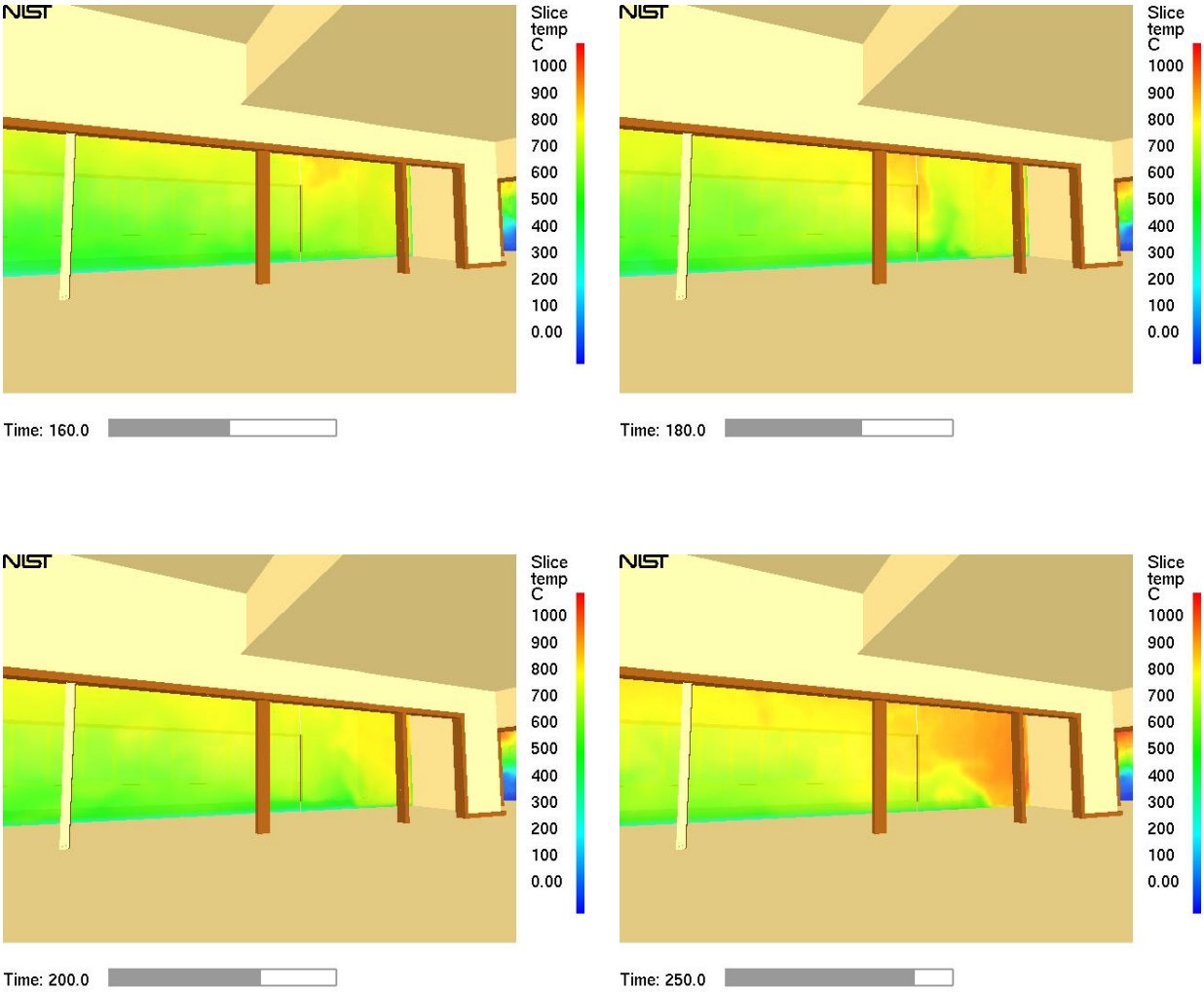

Figure 5-58b. Temperature profile through the center of the sunroom, 160 seconds to 250 seconds

Figures 5-59a and 5-59b depict the temperatures in the approaches to the main entry foyer. The vertical temperature slices cover the area at the end of the entrance foyer and next to the ticket booth. The view is from the dance floor area looking toward the main entrance (front door). What appears to be a pillar in between the intersection of the two vertical slices is a portion of the wall that separates the sunroom from the main entry foyer. The images demonstrate that temperatures were untenable outside of the entranceway and that if the occupants were not able to make it into the area of cool air coming in from the front doorway, they did not have a chance of survival. Temperatures near the floor exceeded 400 ºC (750 ºF) within 100 seconds of ignition. Nine victims were located in this area.

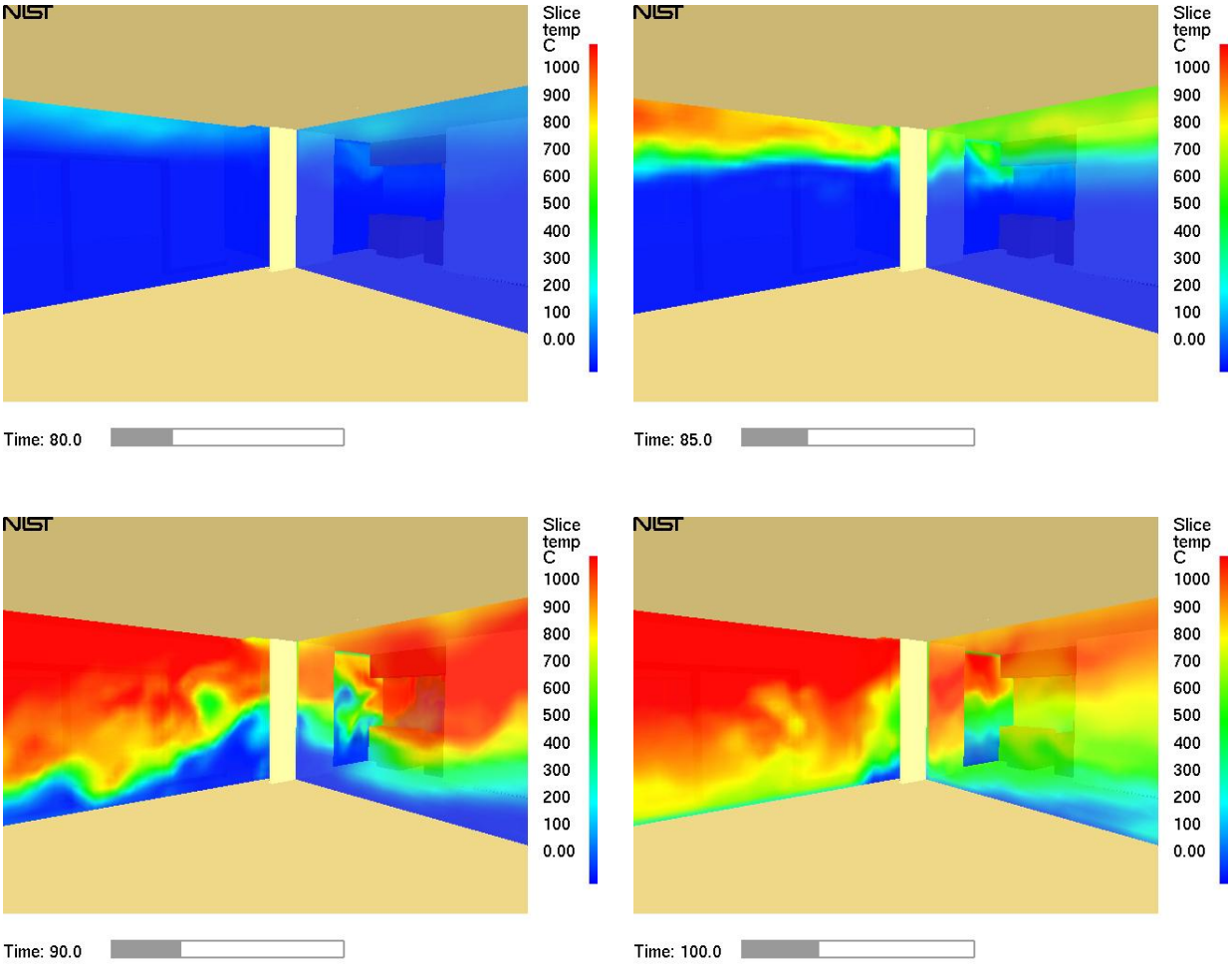

Figure 5-59a. Temperature profiles approaching main entry foyer, 80 seconds to 100 seconds

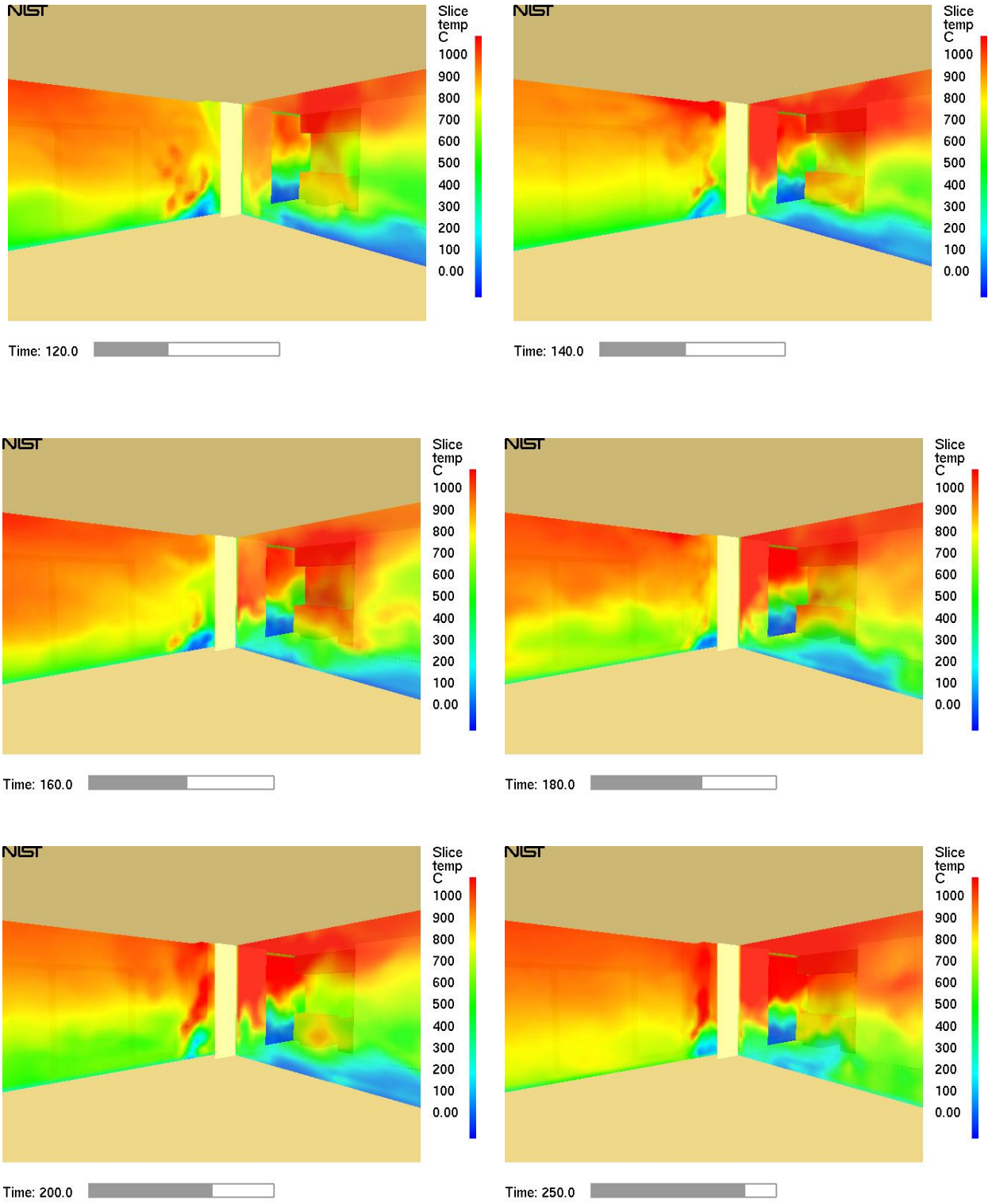

Figure 5-59b. Temperature profiles approaching main entry foyer, 120 seconds to 250 seconds

The area of the night club with the side bar and the dart room is shown in the simulated images with vertical temperature slices bounding the area to the north (toward the main entrance) and to the east (toward the storage/office area entrance). Figures 5-60a and 5-60b show the rapid change in thermal conditions between 80 seconds and 90 seconds after ignition. As in other parts of the night club simulation this significant increase in temperature was due to the burning of the polyurethane foam. Temperatures near the floor ranged from 200 ºC (390 ºF) to 600 ºC (1110 ºF) at 100 seconds. Figure 5-60b indicates that the temperatures remained in the untenable range throughout the rest of the simulation. In the incident, nine victims were found in this area.

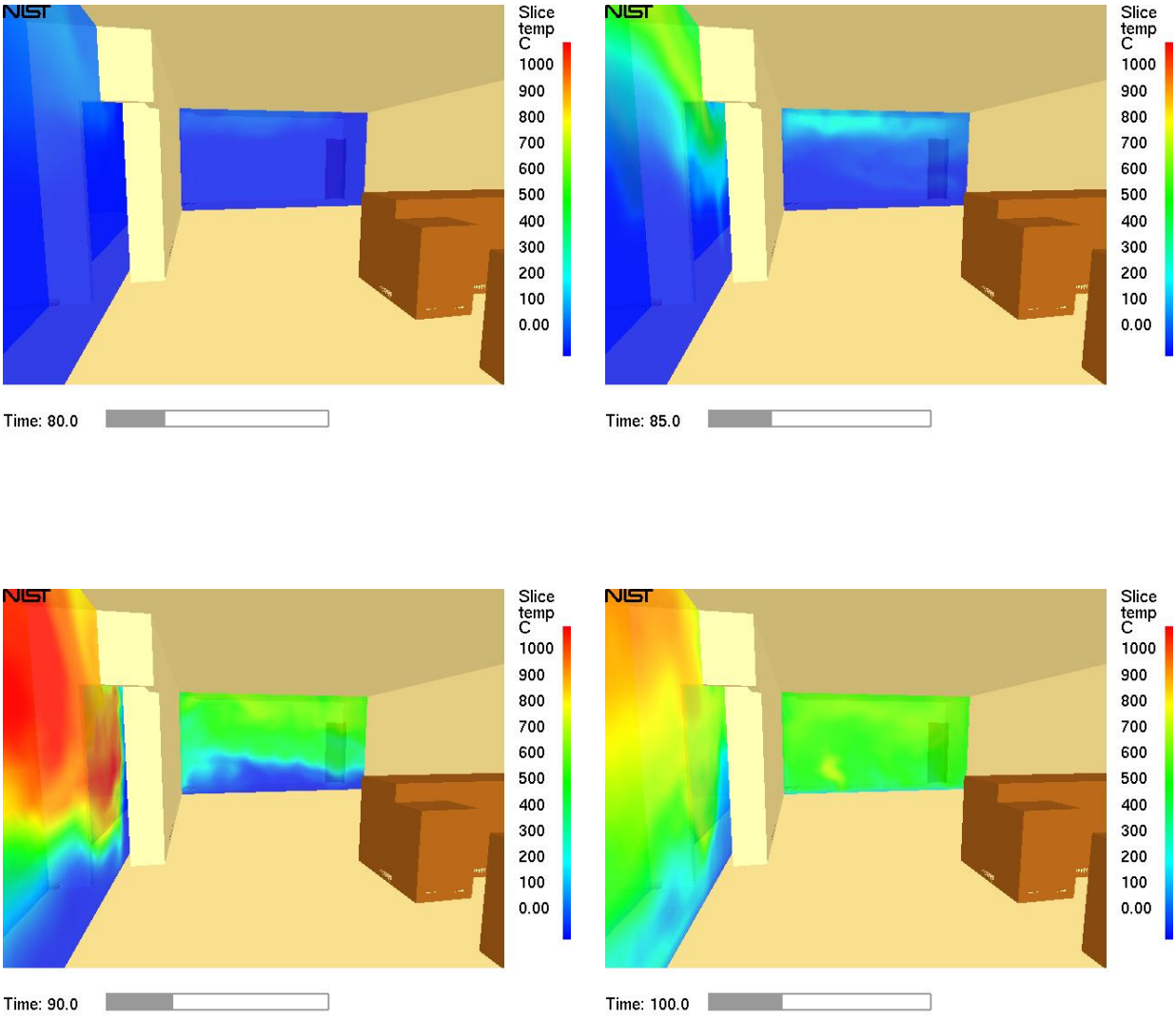

Figure 5-60a. Temperature profiles in the dart room, 80 seconds to 100 seconds

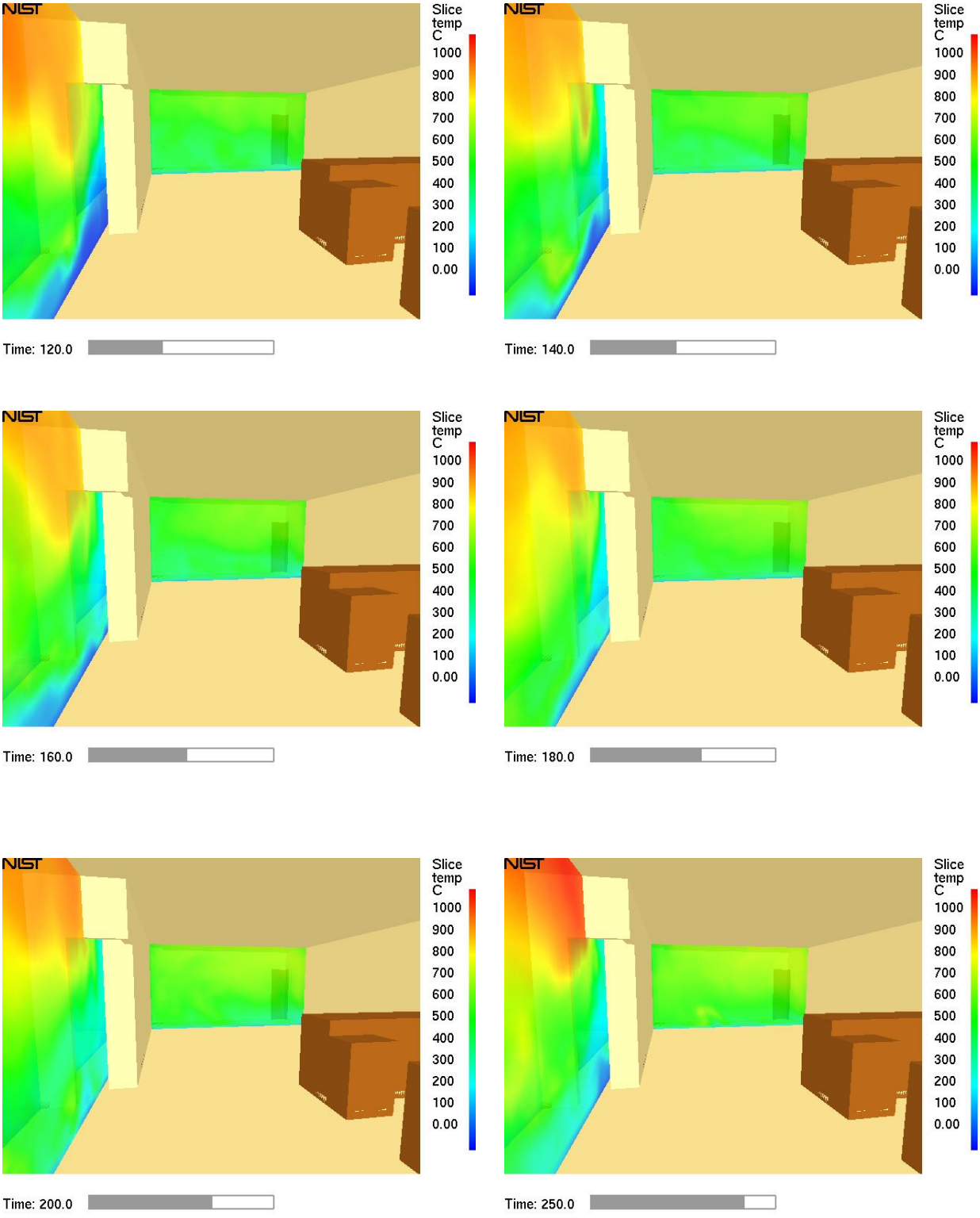

Figure 5-60b. Temperature profiles in the dart room, 120 seconds to 250 seconds

(iv) Oxygen

Oxygen volume fraction concentrations were also examined in the simulation to assess the tenability conditions that existed during the evolution of the fire. Horizontal slices were taken at both the 1.5 m (5 ft) and 0.6 m (2 ft) levels with the roof removed to examine the structure as a whole. This analysis will utilize a volume fraction of 12 % as the oxygen tenability threshold [6]. Based on that oxygen limit the following figures show that occupants would have had less than 100 seconds of tenable conditions.

Just as the temperature levels rose rapidly after the platform area became fully involved in flames, the oxygen levels drop proportionally. As shown by the three dimensional smoke output in the previous section, the smoke spreads quickly through the structure. Figure 5-61a contains four images ranging from 80 seconds after ignition to 100 seconds after ignition. This sequence has the most dramatic changes in oxygen concentration. Beyond 100 seconds the entire structure is untenable at the 1.5 m (5 ft) height. Tenability exists for the longest duration in the main bar area. Figure 5-61b shows the progression of the oxygen levels through the end of the simulation at 250 seconds. Most of the building, including the platform and dance floor areas, the dart room, the main entry foyer and the main bar room, is shown by the simulation to be significantly depleted of oxygen to less than 2 %.

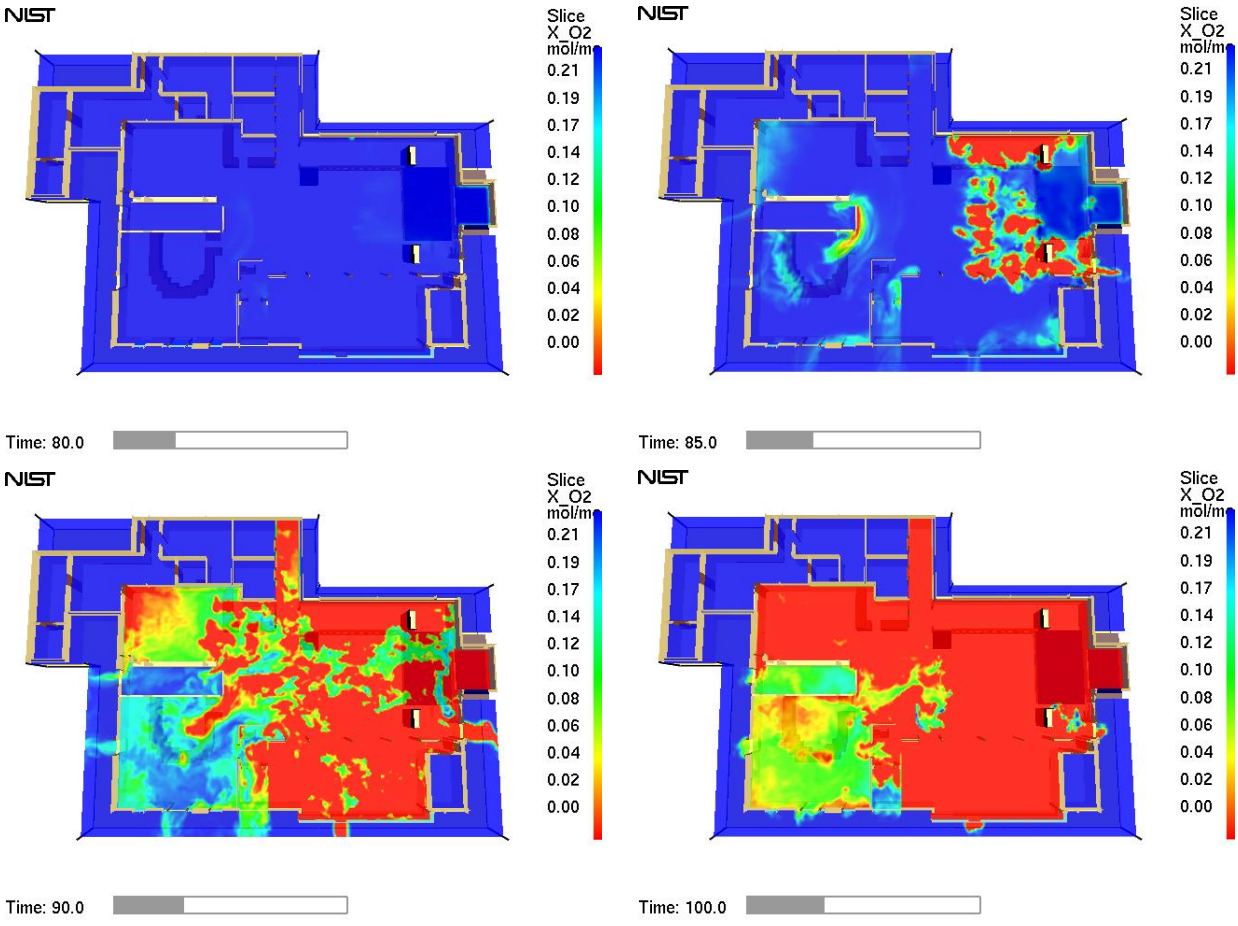

Figure 5-61a. Oxygen volume fractions at 1.5 m (5 ft) above the floor, 80 seconds to 140 seconds

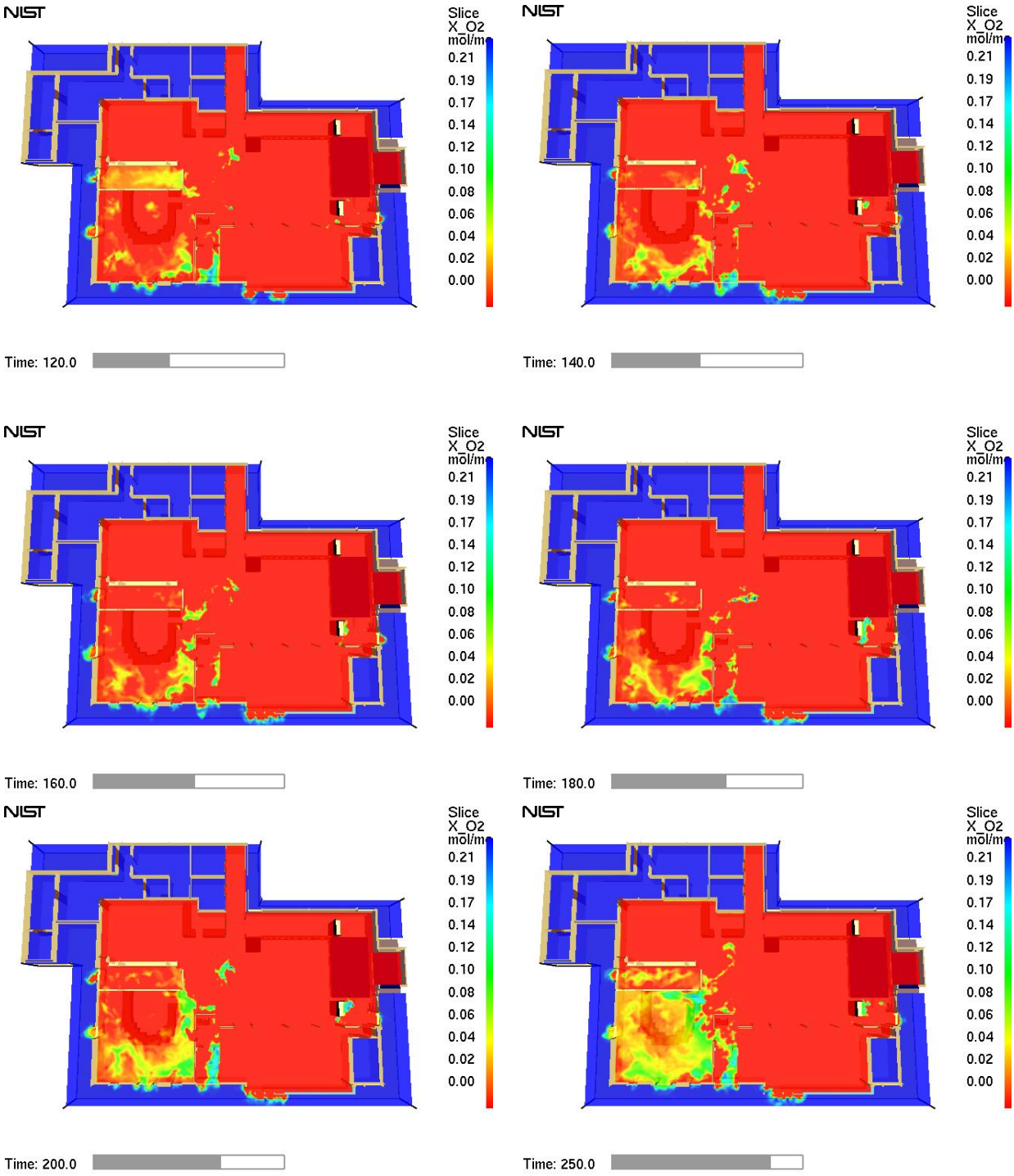

Figure 5-61b Oxygen volume fractions at 1.5 m (5 ft) above the floor, 120 seconds to 250 seconds

Figures 5-62a and 5-62b show the predicted oxygen volume fraction 0.6 m (2 ft) above the floor, beginning at 80 seconds after ignition through 250 seconds after ignition. At this lower level it is apparent that tenability is also not likely in any area other that the main bar area and the entranceway right inside the front door. The opening of the windows at the front of the main bar room creates a more tenable atmosphere, probably saving the lives of occupants as they can be seen being pulled from the windows in the WPRI video. Occupants that stayed low in the main bar area had a better chance of survival.

The images in Figure 5-62b, once again show a rapid decrease in tenable conditions due to oxygen depletion throughout most of the simulated nightclub with the exception of the main bar room and the main entry foyer. Due to the open doors and windows in these areas, the simulation indicates that sufficient fresh air was drawn in to maintain a level of tenability with respect to oxygen in the areas adjacent to the open windows and the main entry way. This trend is shown to continue through the end of the simulation. In the WPRI video, the last person recorded being assisted through a window from the main bar room occurs at 250 s seconds after ignition. This is consistent with the predicted oxygen concentrations near the windows.

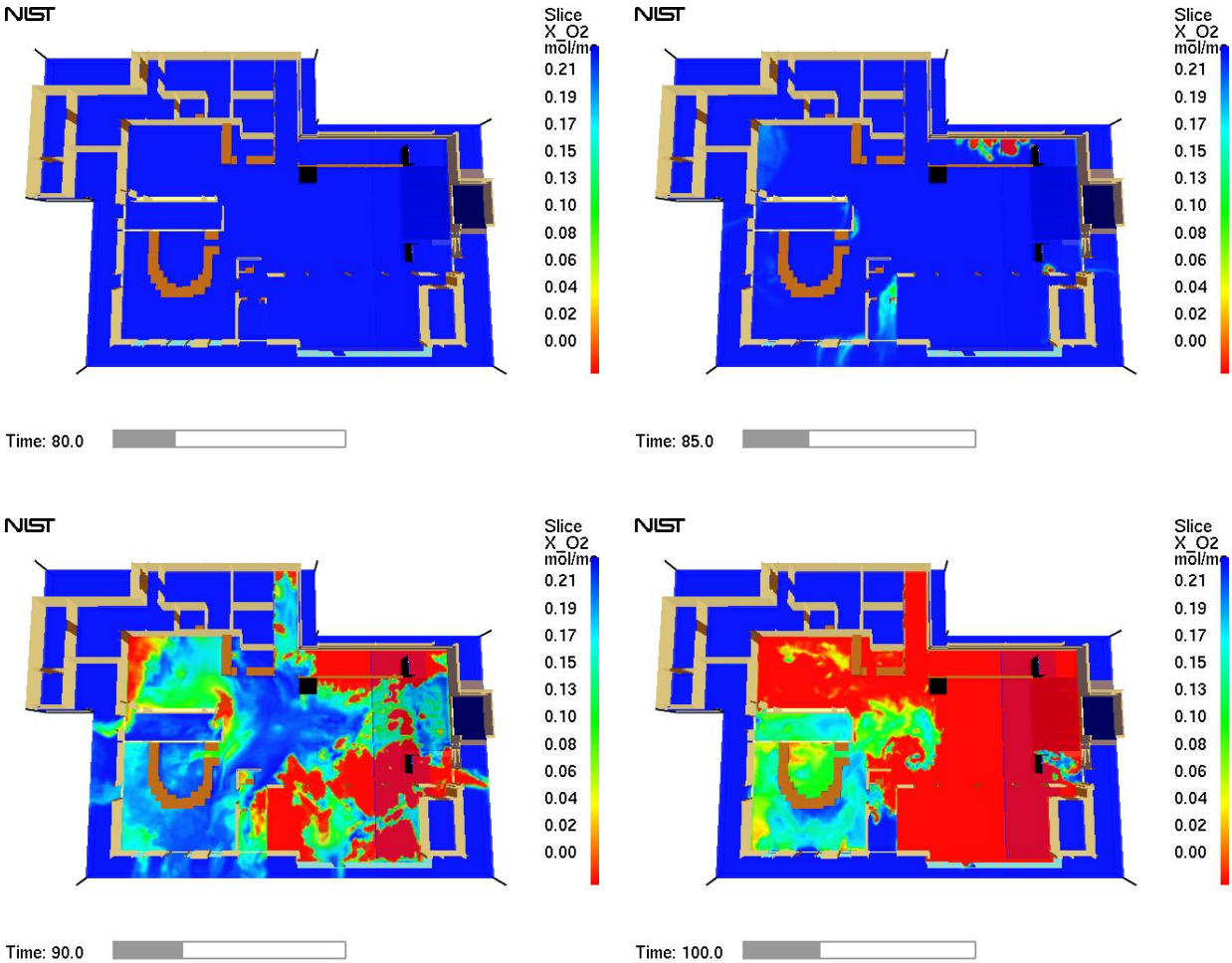

Figure 5-62a Oxygen volume fractions at 0.6 m (2 ft) above the floor, 80 seconds to 100 seconds

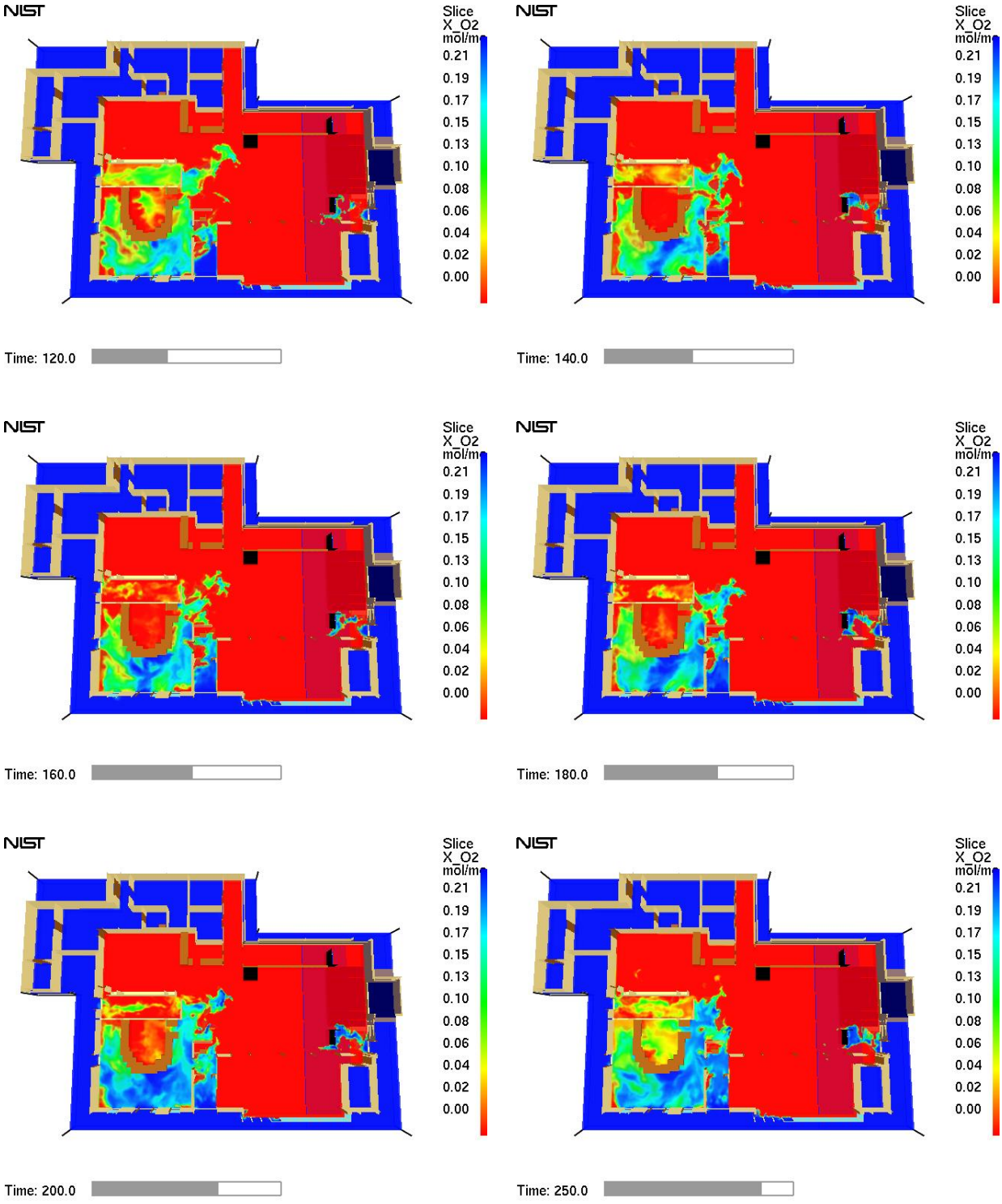

Figure 5-62b Oxygen volume fractions at 0.6 m (2 ft) above the floor, 120 seconds to 250 seconds

5.3.4 Simulation of full nightclub equipped with sprinklers

Another simulation of the full night club was completed in order to examine the effects that sprinklers may have had on the fire and the environment. The input from the FDS incident simulation was combined with the sprinkler input from the FDS sprinklered full-scale mock-up simulation. Five sprinklers were placed in the simulation. One was located in the center of the alcove and the other four were placed using 3.6 m (12 ft) spacing. The west sprinklers were 1.8 m (6 ft) north and 1.8 m (6 ft) south of the alcove sprinkler and 1.8 m (6 ft) east of the platform wall. The east sprinklers were also 1.8 m (6 ft) north and 1.8 m (6 ft) south of the alcove sprinkler and 12 ft east of the west sprinklers.

The sprinkler activation times from the sprinklered FDS simulation are given in Table 5-7. The sprinklers used in the FDS simulation are identical to those used in the full-scale mock-up FDS simulation. The properties of each sprinkler can be found in Table 5-2.

Table 5-7. FDS Predicted Sprinkler Activation Times

Sprinkler Location	FDS Sprinkler Activation Times (seconds)
Southwest	20
Northwest	16
Alcove	29
Southeast	Did Not Activate
Northeast	Did Not Activate

(i) Visualization

Figures 5-63a and 5-63b are rendered from Smokeview to examine the flame and smoke spread and the effect of the sprinklers. The images begin at ignition or t = 0 seconds and continue until 100 seconds after ignition. The first image in Figure 5-63a shows the two sprinklers over the platform area and the two sprinklers over the dance floor as small red dots along the ceiling. The larger red areas on the platform walls represent the location of the ignition burners. The sprinkler located on the ceiling of the alcove is hidden from view. The second image rendered at 20 seconds shows smoke being pushed away at the first sprinkler, which activated at 16 seconds after ignition. By 30 seconds after ignition, three of the sprinklers had been activated. This caused some of the smoke to be pushed down to the floor. The two sprinklers over the dance floor area did not activate during the simulation. Figure 5-63b has images from 70 seconds to 150 seconds after ignition. During this period the fire was significantly suppressed. The series of images show the smoke disbursing. The fire was extinguished fully at approximately 114 seconds. The smoke continued to spread and is diluted by fresh air entering the area.

Figure 5-64 provides another means of looking at the simulation. This image, rendered at 2 seconds after the first sprinkler activated, includes the visualization of the sprinkler droplets but does not include the visualization of the smoke. Notice that the activated sprinkler has changed color from red to green.

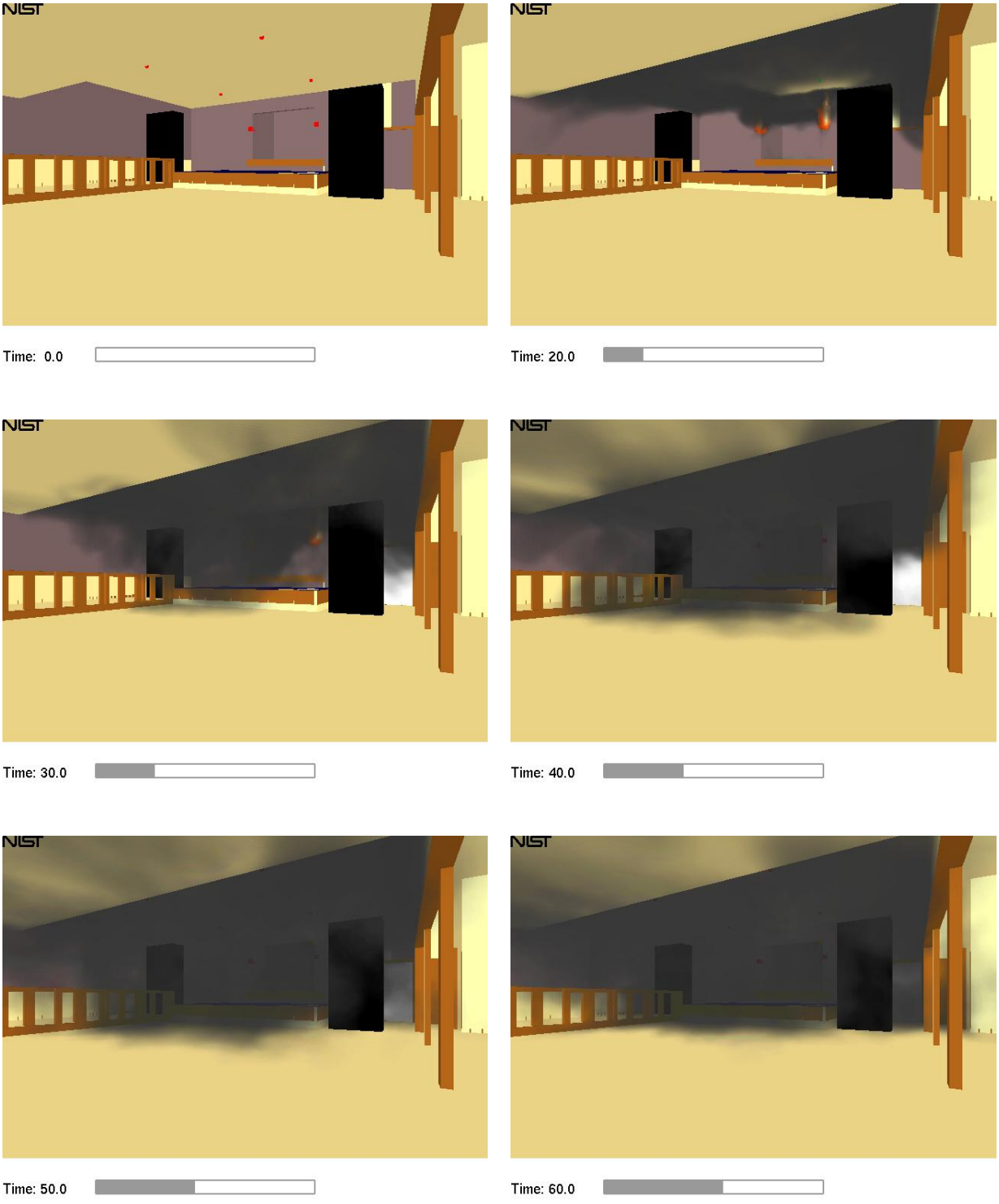

Figure 5-63a. Simulation of nightclub with sprinklers, 0 seconds to 60 seconds

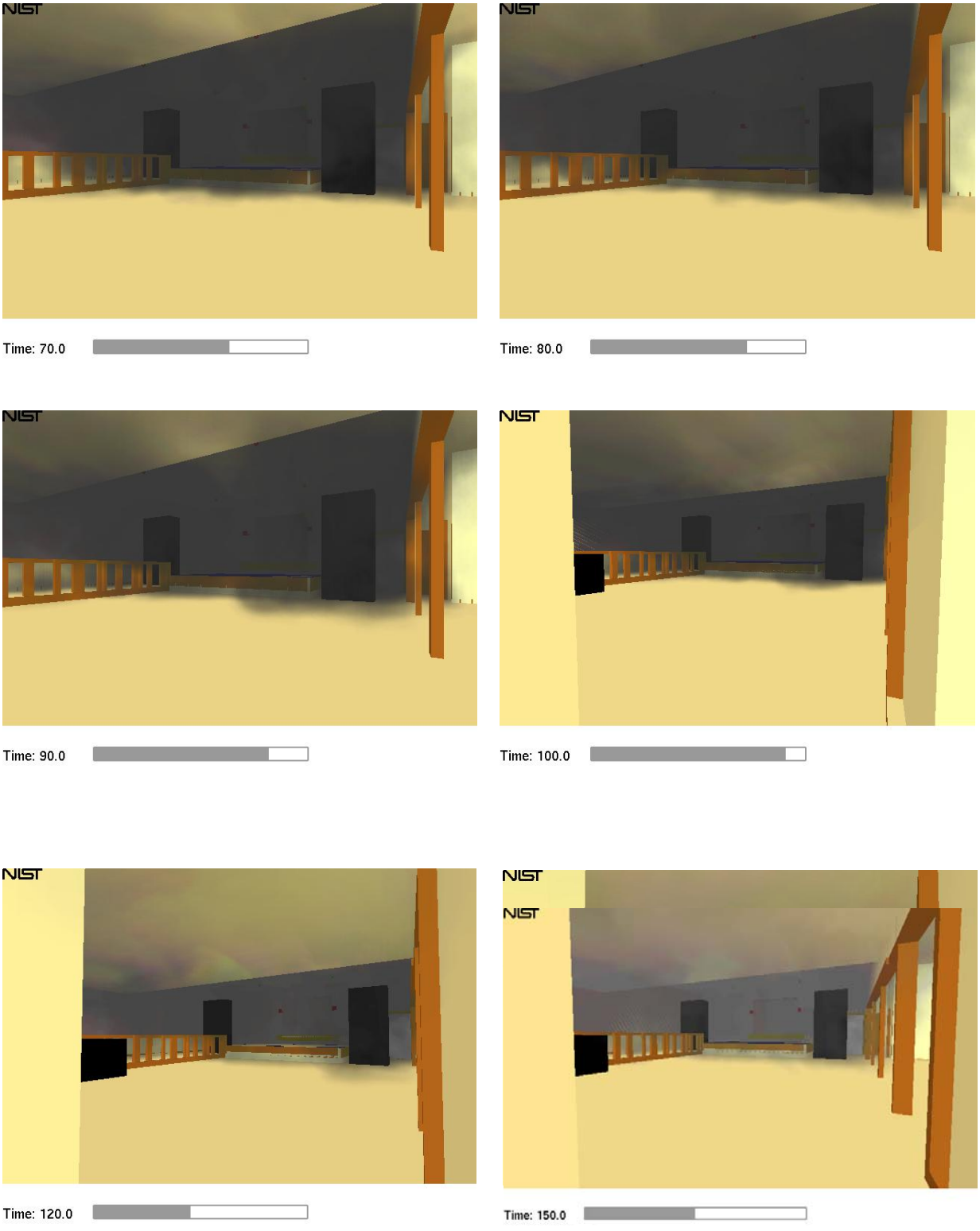

Figure 5-63b. Simulation of nightclub with sprinklers, 70 seconds to 150 seconds

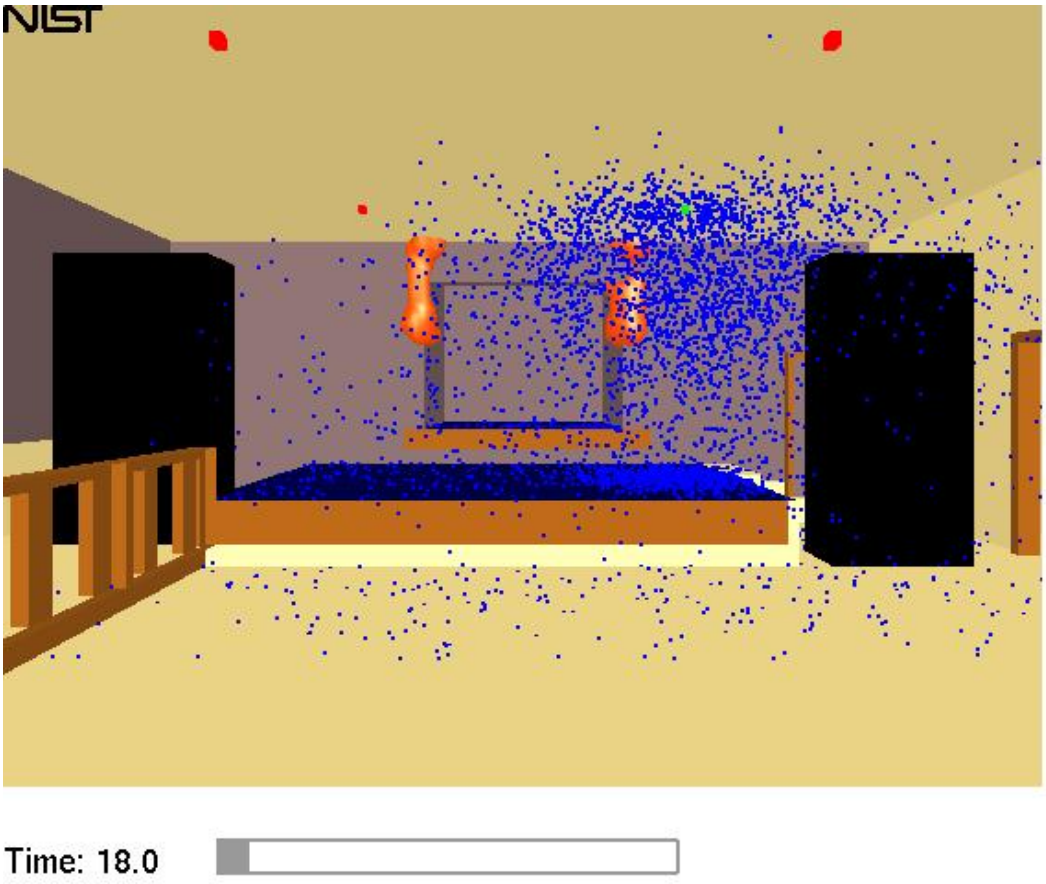

Figure 5-64. Simulation of northwest sprinkler activation 18 seconds after ignition, showing water flow with smoke "turned off."

(ii) Numerical Output

In this section, predictions of heat release rate, temperature, and oxygen volume fraction from the FDS sprinklered incident simulation are presented and compared to the non-sprinklered simulation and tenability criteria.

Figure 5-65 shows the FDS predicted heat release rate for the sprinklered simulation. The heat release rate reached its maximum of approximately 220 kW at 20 seconds. This heat release rate quickly declined as the three sprinklers activated and suppressed the fire.

Isothermal plots are shown in Figures 5-66a and 5-66b to assess the tenability conditions based on temperatures that were predicted during the simulation of the fire. The figures show horizontal isothermal images 1.5 m (5 ft) above the floor from the time of ignition (t = 0) to 100 seconds in 10 second intervals, and an image at 150 seconds. Due to the rapid activation of the sprinklers (three sprinklers were operating by 30 seconds after ignition), the temperatures at the 1.5 m (5 ft) level remain well below the temperature tenability threshold of 120 ºC (248 ºF) [6].

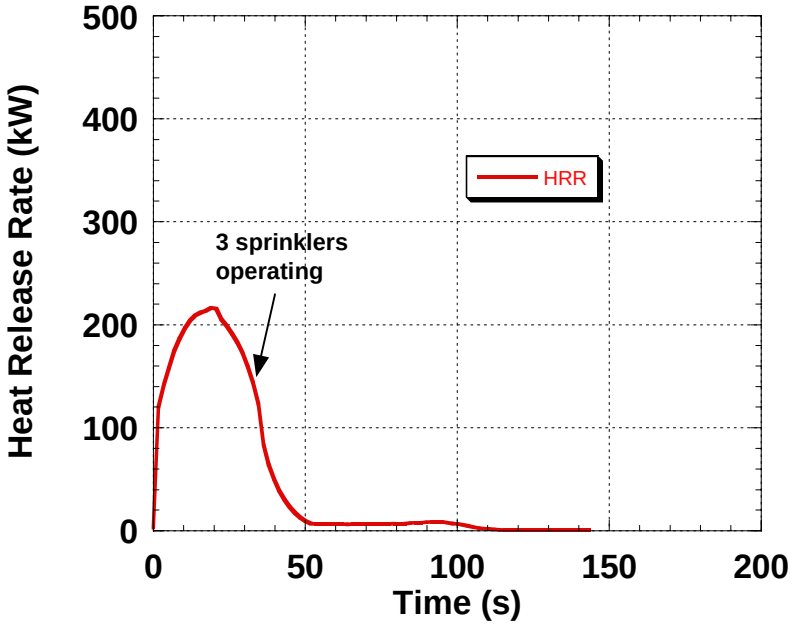

Figure 5-65. FDS predicted heat release rate for the sprinklered case.

The comparison between the temperatures 1.5 m (5 ft) above the floor in the non-sprinklered simulation (Figs. 5-55a and 5-55b) and in the sprinklered configuration (Figs. 5-66a and 5-66b) show dramatically different thermal conditions. (Note the large difference in color scales.) During the non-sprinklered simulation temperatures exceeded 1000 ºC (1830 ºF) in the platform and dance floor areas, and in the main bar room they exceeded 500 ºC (930 ºF) within 100 seconds. In the sprinklered simulation, the temperature exceeds 25 ºC at head height only near the platform; following sprinkler activation around 20 seconds, the thermal environment remains close to ambient up until the time the fire is fully extinguished at 120 seconds.

Given the limited fire spread and the resulting tenable gas temperatures, the heat flux tenability criteria was never exceeded in the sprinklered case.

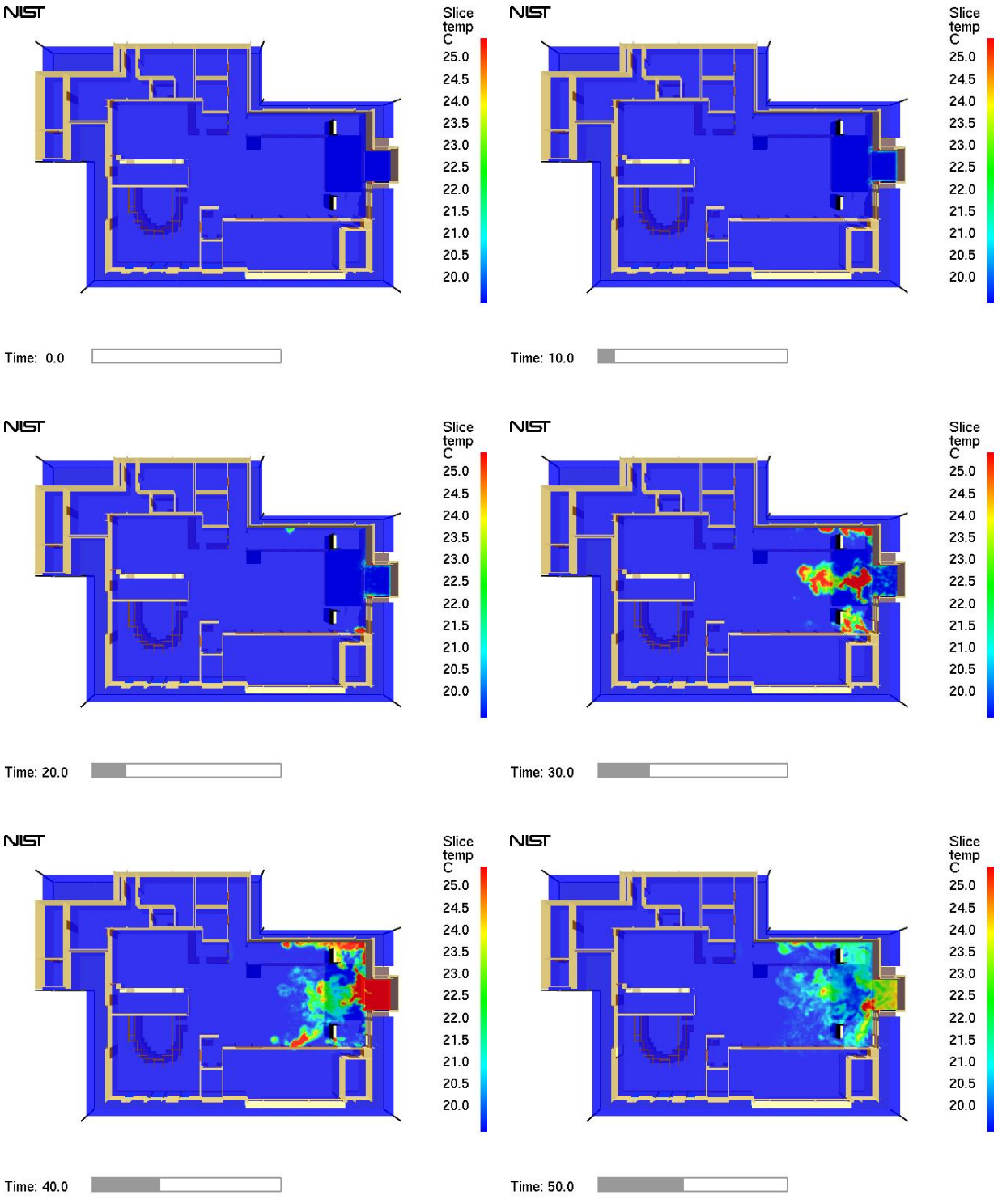

Figure 5-66a. Temperatures at 1.5 m (5 ft) above the floor, 0 seconds to 50 seconds

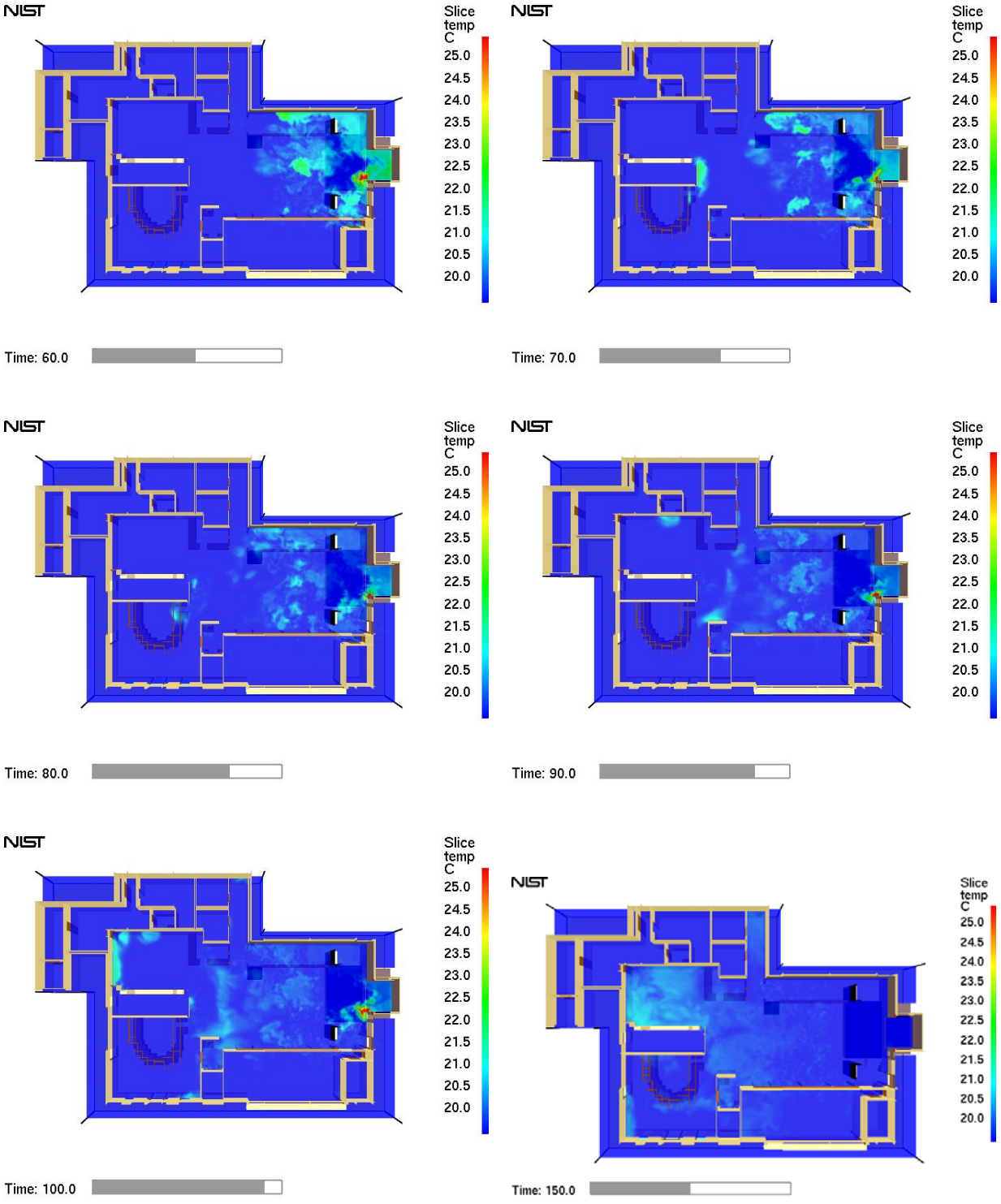

Figure 5-66b. Temperatures at 1.5 m (5 ft) above the floor, 60 seconds to 150 seconds

(iii) Oxygen

Oxygen volume fractions were also examined in the sprinklered simulation to assess the tenability conditions that existed during the evolution of the fire. Horizontal slices were taken at the 1.5 m (5 ft) level with the roof removed to examine the structure as a whole. This analysis will utilize a volume fraction of 0.12 as the oxygen tenability threshold [6]. Based on that oxygen limit, Figures 5-67a through 5-67c demonstrate that the atmosphere remained tenable during the entire duration of the simulation. In contrast, the non-sprinklered simulation predicted oxygen levels below 0.12 at the 1.5 m (5 ft) elevation throughout the building at 100 seconds after ignition and then continuing at untenable concentrations during the remainder of the simulation.

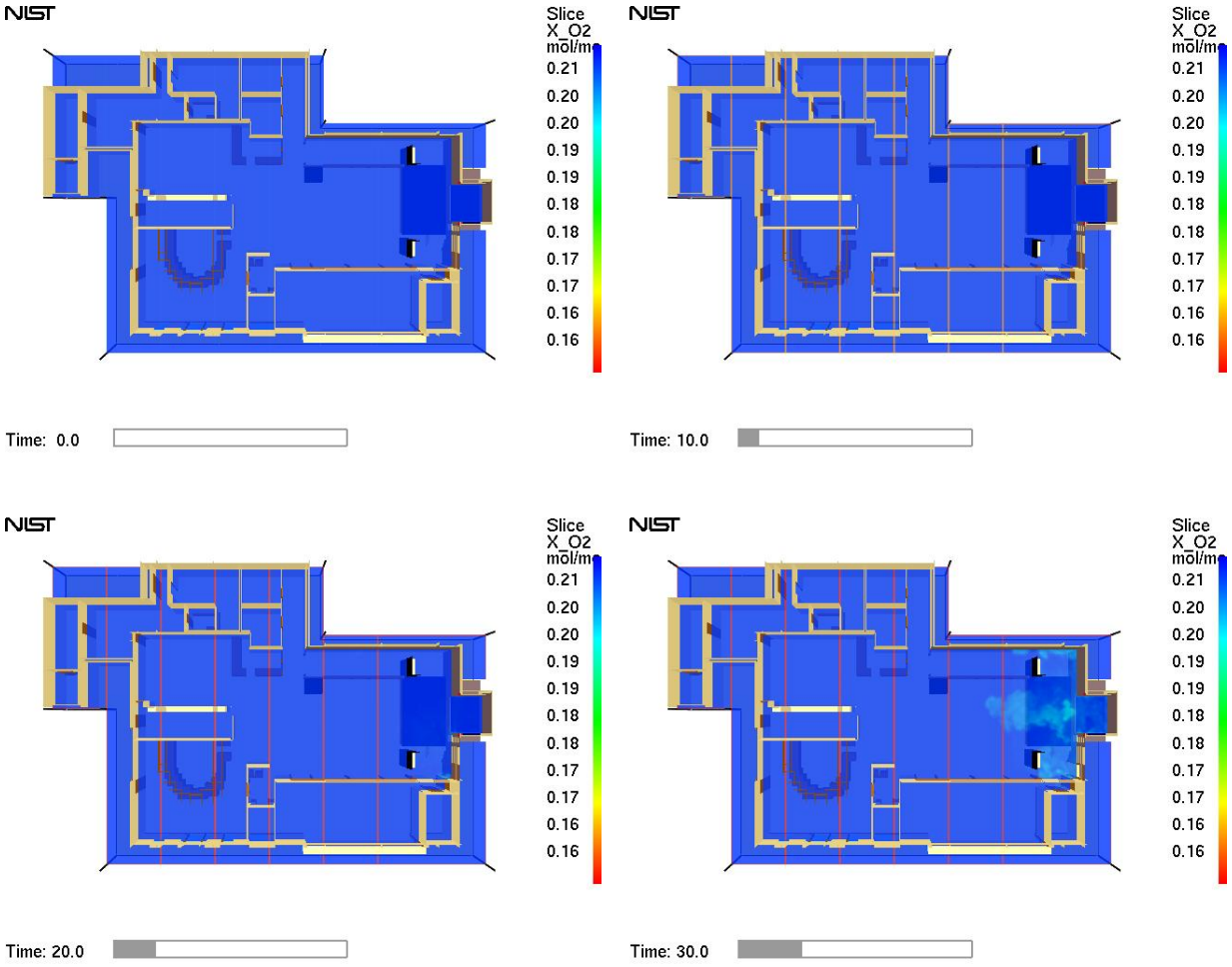

Figure 5.67a. Oxygen volume fractions at 1.5 m (5 ft) above the floor, 0 seconds to 30 seconds

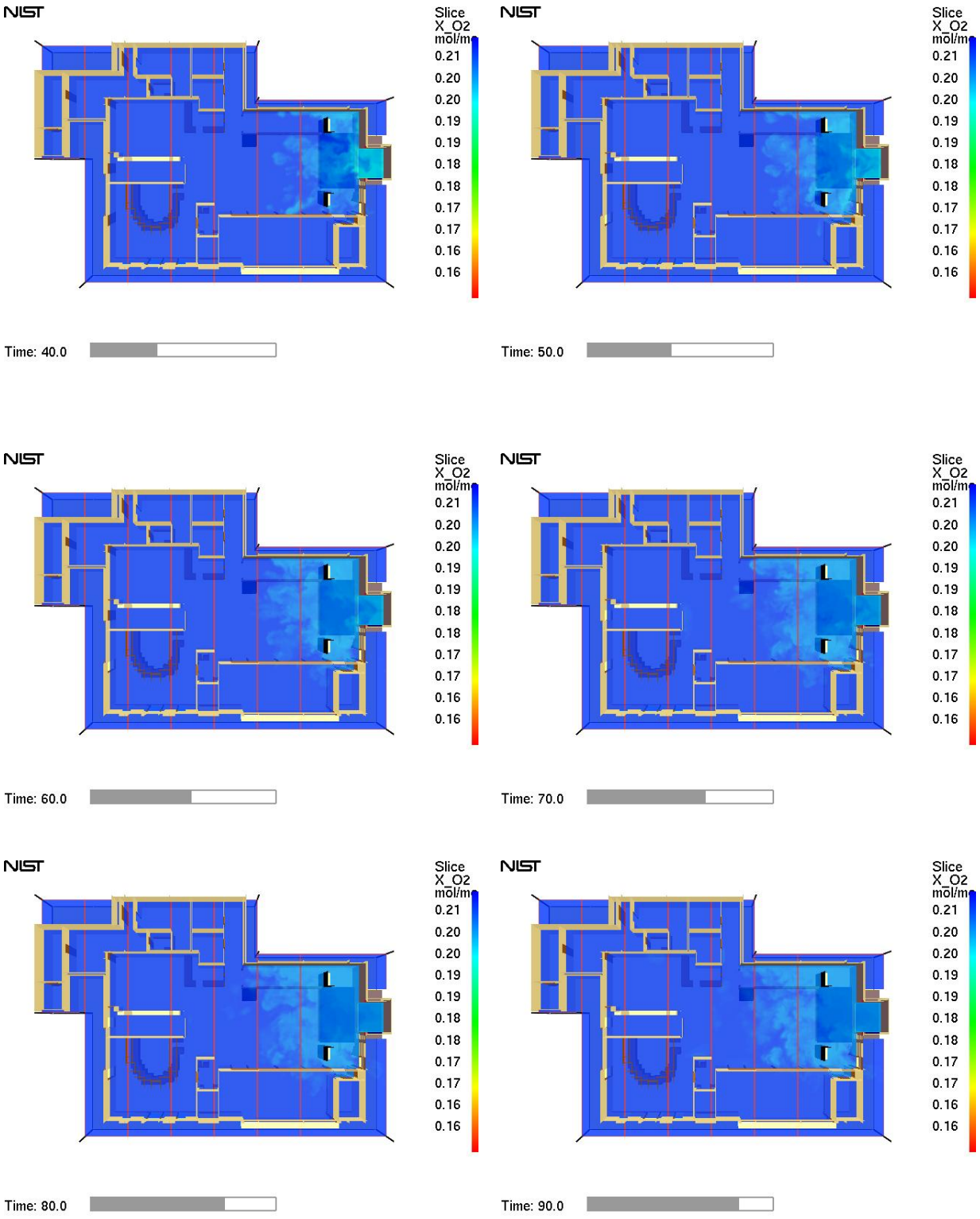

Figure 5.67b. Oxygen volume fractions at 1.5 m (5 ft) above the floor, 40 seconds to 90 seconds

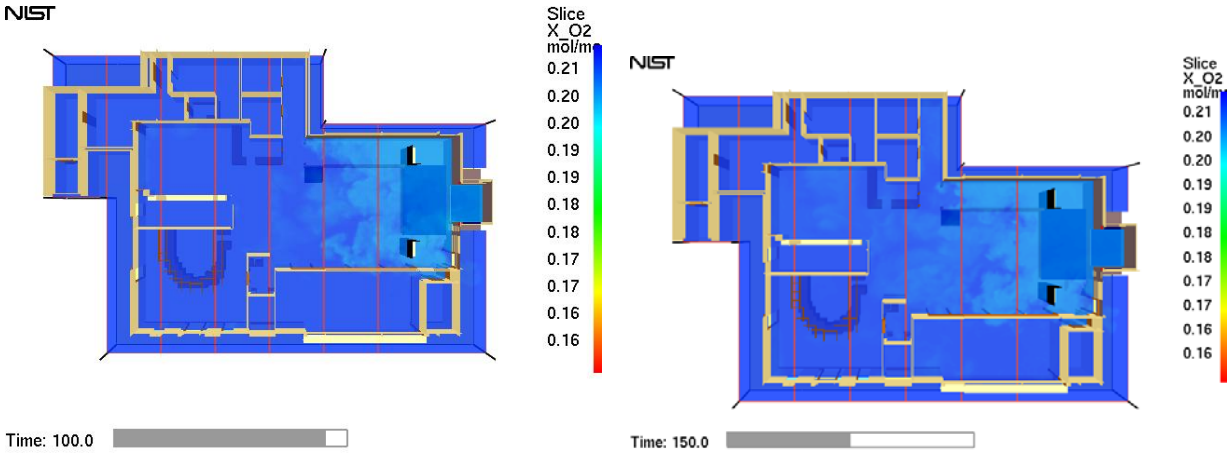

Figure 5-67c. Oxygen volume fractions at 1.5 m (5 ft) above the floor, 100 and 150 seconds

5.4 SUMMARY

Images from the WPRI video were utilized to develop model input to establish the location of the different interior finishes within The Station nightclub as well as used as a general resource for confirming the physical arrangement of the nightclub. The simulation was run for 300 seconds to examine the time period from ignition to the approximate time of flames throughout most of the nightclub as recorded by WPRI. The computation included simulated fire and smoke spread, and potential temperatures, heat flux and oxygen concentrations that may have existed in the actual incident. Each of these parameters were compared to published tenability criteria.

Results from some of the bench-scale experiments described in Chapter 4 and existing data were used to develop the input properties for the interior finish materials. The key parameters were the combustion properties of the foam/plywood wall: ignition temperature, heat of vaporization, and maximum burning rate. The results from the cone calorimeter tests of the polyurethane foam were not used directly in the simulation because of the composite nature of the foam-plus-plywood fuel on the wall and the limitations in grid resolution created by the sheer number of computational cells (of the order of 3 million) required to simulate the entire nightclub. As a consequence, the differences in heat release rate of the polyurethane foam measured by NIST and ATF had no impact on the simulation results.

The visual and numerical comparisons between the experiments and the FDS simulations of the experiments demonstrated reasonable agreement. The visual comparisons indicated a lag in fire development in the simulation relative to the experiments, but once the simulated fire grew large enough the growth rate and smoke development were consistent with the experiments. The temperature, heat flux, and the oxygen concentration comparisons show reasonable agreement between the experiments and the model in terms of both trends and range.

To gauge the accuracy of the full nightclub simulation results, they were compared with the WPRI video record of the incident and the map of victim locations. The FDS simulation predicted rapid fire growth due to the burning of the convoluted polyurethane foam. The simulation is consistent with the video record during the early stages of fire development. The conditions in the actual nightclub transitioned

from a fire within a compartment to a fully-involved wood structure fire burning in void spaces, the attic area, structural elements, and roofing materials. In the computer simulation, such regions and materials were not included, which led to a diminishing of the fire after 250 seconds as the fuel was consumed.

According to the computer predictions, many of the occupants had less than 90 seconds after ignition to exit the structure. The quickly spreading fire and rapid production of smoke led to high temperatures and low oxygen levels throughout most of the simulated nightclub. The exceptions were a few areas near the open windows of the main bar room and the open doorway to the main entry foyer. In these areas air from outside the structure was being drawn in providing a more tenable environment and more time for escape.

The effects of an automatic sprinkler system on a fire were modeled to a useful degree by FDS and visualized with Smokeview. Both the experiment and the FDS simulation demonstrate that the sprinklers would prevent flashover and considerably mitigate the hazard from the fire in the test enclosure. However, the degree to which the fire is controlled is different between the experiment and the model. The simulation has more flame spread along the edges of the alcove ceiling after activation of the sprinklers. While the ability of FDS to predict fire suppression is simplified and cannot capture all of the physics involved in the process, FDS is able to predict the trends in reasonable agreement with the measured temperatures, heat fluxes and oxygen volume fractions.

In the simulation of the full nightclub equipped with sprinklers, examination of the predicted temperature and the oxygen volume fractions shows tenable conditions would have existed over the duration of the simulation (300 seconds), as the fire was fully extinguished approximately 114 seconds after ignition.

5.5 REFERENCES FOR CHAPTER 5

1. McGrattan, Kevin; Forney, Glenn; "Fire Dynamics Simulator (Version 4) – User's Guide," National Institute of Standards and Technology, Gaithersburg, MD, NIST SP 1019, September 2004.

2. Forney, G. P. and McGrattan,K.B., "User's Guide for Smokeview Version 4 - A Tool for Visualizing Fire Dynamics Simulation Data," NIST SP 1017, National Institute of Standards and Technology, Gaithersburg, MD, August 2004.

3. McGrattan, K., ed., "Fire Dynamics Simulator (Version 4), Technical Reference Guide," NIST SP 1018, National Institute of Standards and Technology, Gaithersburg, MD, September 2004.

4. Heitaniemi, J., Hostikka, S., and Vaari, J. FDS Simulation of Fire Spread – Comparison of Model Results with Experimental Data. Technical Report VTT Working Paper 4, VTT Building and Transport, Espoo, Finland, 2004.

5.. Purser, D.A., "Toxicity Assessment of Combustion Products." *SFPE Handbook of Fire Protection Engineering, 3rd ed.* DiNenno, P.J., et. al. (eds). NFPA Quincy, MA, 2002.

6. Madrzykowski, D., and Vettori, R.L., "A Sprinkler Fire Suppression Algorithm," *Journal of Fire Protection Engineering, Vol. 4*, No. 4, 1992, pp 151-164.